THE UNIVERSITY OF MICHIGAN

INDUSTRY PROGRAM
OF THE
COLLEGE OF ENGINEERING

The Electrolysis of Some Liquid Alloys

JOHN C. ANGUS

January 1961
IP - 488

ANN ARBOR

THE UNIVERSITY OF MICHIGAN

INDUSTRY PROGRAM OF THE COLLEGE OF ENGINEERING

THE ELECTROLYSIS OF SOME LIQUID ALLOYS

John C. Angus

January, 1961

IP-488

UMR0105

ACKNOWLEDGMENTS

The author expresses his appreciation to the members of the doctoral committee, and especially to Professor Hucke who served as chairman. He would also like to thank the National Science Foundation, the Shell Oil Company, and the Jones and Laughlin Steel Company for providing the author with fellowships through part of his graduate work.

The United States Atomic Energy Commission provided the funds which made this work possible, under contract No. AT(11-1)-771.

The author would also like to thank the shop and laboratory personnel of the Department of Chemical and Metallurgical Engineering who aided in many portions of the work. The work of the chemists, especially Henry Iwata and James Gambell, who performed the analyses on the Bi systems is gratefully acknowledged. He expresses his thanks to Mrs. Marguerite Schaible who typed the first draft and to the Industry Program of the College of Engineering, which prepared the dissertation in its final form.

Special thanks go to Mr. John Verhoeven, whose aid in the experimental portions of the dissertation was invaluable.

Finally, the author expresses his gratitude for the patience and encouragement of his wife and parents throughout the course of this work.

TABLE OF CONTENTS

TABLE OF CONTENTS (CONT'D)

TABLE OF CONTENTS (CONT'D)

LIST OF TABLES

LIST OF FIGURES

ABSTRACT

Molten alloys can be electrolyzed with direct current. This effect is commonly called electrodiffusion. Data from electrodiffusion experiments can be used to make inferences about the structure of the molten alloys. The previous experimental data is limited and, in general, of very limited accuracy. The purpose of this research is fourfold: 1) to devise a technique whereby electrical mobilities in molten alloys at high temperatures can be determined, 2) to obtain accurate data on several Bi alloys, 3) to investigate a correlation that states that the component with the smallest atomic weight migrates to the cathode, and 4) investigate the possibility of the existence of intermetallic compounds in liquid Na-Hg alloys by means of electrodiffusion experiments.

In collaboration with another worker a method was devised for measuring electrical mobilities. The technique was tested by reproducing the value of the mobility reported by anpther investigator for Na in dilute Na amalgams. The earlier value is $+ 1.19 \times 10^{-4}$ cm^2/sec volt; the value obtained in this investigation is $+ 1.23 \pm 0.23 \times 10^{-4}$ cm^2/sec volt at the 95 percent confidence level. The technique was applied to the molten alloys Bi-Cu, Bi-Mg, Bi-Zr, and Bi-U. The following mobilities in $10^4 \times cm^2/sec$ volt were determined: Cu, at 0.5 wt.% and 500°C, $-1.85 \pm .25$; Mg, at 0.5 wt.% and 350°C, $-5.78 \pm .98$; Zr, at .0567 wt.% and 510°C, $+ 2.61 \pm 2.54$; U, at .0144-.310 wt.% and 445-500°C, $+2.57 \pm .67$. The mobilities are reported at the 95 percent confidence level. A positive mobility indicates the solute moves to the anode, a negative mobility means motion to the cathode. The sources of error were examined and suggestions given for increasing the accuracy of the technique.

Experiments on 0.5 wt. % Na amalgams show that the direction of transport of Na is to the anode when the temperature is below a certain value, and to the cathode when the temperature is above this value. The exact temperature of the reversal is uncertain since the experimental technique is not sufficiently sensitive to determine very low mobilities. It occurs in the range from 270 to 310°C. The reversal is interpreted as caused by the thermal decomposition of intermetallic compounds existing in the melt. This effect, which was predicted on the basis of the atomic mass correlation, has heretofore never been observed. It supplies additional evidence to that already available from thermodynamic, x-ray, and viscosity measurements for the existence of compounds in liquid alloys. In addition, a mechanism is presented as a possible explanation for the empirically observed correlation.

NOMENCLATURE

a	length of diffusion capillary, cm
A_o	Fourier coefficient
B_i	absolute mobility of the i-th species, cm/sec dyne
B_o	Fourier coefficient
C	dimensionless concentration, N/N_{res}
C_m	average dimensionless concentration
C_n	Fourier coefficient
D_i	self or intrinsic diffusion coefficient, cm^2/sec
D	ordinary diffusion coefficient, cm^2/sec
e	electronic charge,-esu
E	electric field strength, volts/cm
F	Faraday, 96,500 coulombs
I	current, amperes
j_2	current density, $amperes/cm^2$
J_i	flux, $moles/cm^2 sec$
k	Boltzmann's constant, erg/°K or proportionality constant in Equations (40) and (41)
L_{ij}	phenomenological coefficient from irreversible thermodynamics
m_e	mass of an electron, grams
m_i	mass of an atom of the i-th species, grams
Δm_1	change in mass of solute in capillary, grams
n	transport number, electrical equivalents of solute per Faraday
N_i	concentration of i-th species, $moles/cm^3$
N_o	molar density of solution, $moles/cm^3$

r	ionic radius, cm
r_i	friction coefficient between electrons and i-th species, dyne sec/cm
R	gas constant, ergs/°K mole
s	dimensionless constant, $U_l V/D$
t	dimensionless time, $D\Theta/a^2$
T	temperature, °K
u_e	mobility of an electron, cm^2/sec volt
u_i	intrinsic mobility of i-th species, cm^2/sec volt
U_l	observed solute mobility, cm^2/sec volt
v_e	velocity of an electron, cm/sec
v_i	ionic volume of the i-th species, cm^3, or ionic velocity of the i-th species, cm/sec
v	bulk convective velocity of fluid, cm/sec
V	voltage difference between ends of capillary, volts
W	work, ergs
x_i	mole fraction of i-th species
x	dimensionless distance, z/a
X_i	generalized "force" from irreversible thermodynamics
z_i	valence of i-th species
z	distance, cm

Greek Symbols

α	eigen value for first term of solution of partial differential equation when $s > 2$
β_n	eigen values for solution to partial differential equation
γ_i	activity coefficient of i-th species

η viscosity, g/cm sec

μ_i chemical potential of i-th species, ergs/mole

ν fundamental vibrational frequency of a metallic lattice, sec^{-1}

Π 3.14159265

ρ resistivity, ohm-cm

σ rate of entropy production, $ergs/cm^3$ °K sec

τ dimensionless time, $U_1 V\theta/a^2$, or relaxation time, sec

θ time, sec

Subscripts

r reversible

irr irreversible

res reservoir

Superscripts

' original concentration

" final concentration

CHAPTER I

INTRODUCTION

Electrodiffusion, or electroylsis, is observed when direct current is passed through molten alloys. In general, the electric field causes the components of a binary alloy to separate; one collects at the cathode and one at the anode. It is not an electrolysis in the normal sense since no oxidation or reduction takes place at the electrodes. Instead, the concentration changes until the ordinary diffusion flux, which is in a direction to remix the alloy, is equal to the electrodiffusion flux. At this point a steady state concentration distribution is obtained.

Electrodiffusion is one of the irreversible transport processes. It is analogous in many ways to the more well known thermal diffusion, or Soret effect. The driving "force" for thermal diffusion is the temperature gradient (°K/cm); in electrodiffusion it is the voltage gradient (volts/cm). The flux equation for electrodiffusion is simply

$$J_1 = U_1 N_1 E \qquad (1)$$

See page x for a complete list of symbols. The quantity U_1 is the electrical mobility of the solute atoms in cm^2/sec volt. The mobility is the average drift velocity in cm/sec imparted by an electric field strength of 1 volt/cm. Equation (1) is the defining relation for U_1. The mobilities are measured with respect to the container vessel. A positive mobility means the solute moves to the anode; negative, to the cathode.

Electrodiffusion, like thermal diffusion, is one of the "cross effects" that are described by the formalism of the theory of irreversible

thermodynamics. The corresponding cross effect for electrodiffusion is the diffusion potential. In other words, whereas electrodiffusion is the flow of mass caused by a voltage gradient, the diffusion potential is the generation of an electric potential by a concentration gradient. See Appendix V-B for a discussion of the theory of irreversible thermodynamics applied to electrodiffusion.

The commercial applications of the electrodiffusion process appear to be rather limited. In certain situations it might be feasible to purify metals through electrolysis. The limiting factor is the extreme irreversibility of the process. The efficiency of the electrolysis of liquid metals is on the order of .01 to .0001 percent (see Appendix V). Most of the electrical energy is lost as joule heat. For a constant electric field, E, the power requirements per unit volume of material are inversely porportional to the resistivity. Therefore, because of their high resistivity and high cost per pound, semiconductor materials may present the most fruitful area for this type of purification. It is theoretically possible to use electrodiffusion in conjunction with the normal zone refining purification technique to enhance the purification[1]. Besides the purification of metals other potential uses include separation of isotopes and the modification of the concentration distribution within metal samples.

Electrodiffusion may prove most useful in providing another method of examining the nature of liquid metals. From the results of electrodiffusion experiments inferences can be made about the structure of molten alloys. The experiments conducted for this dissertation were performed with this purpose in mind. Before describing the experiments (Chapter IV) it will be necessary to review the previous experimental and theoretical works on electrodiffusion (Chapter II) and then to examine in some detail a new correlation which predicts the direction of transport in molten alloys (Chapter III).

CHAPTER II

LITERATURE REVIEW

A. Experimental

The normal procedure for conducting electrodiffusion experiments is to fill a thin capillary with a molten alloy. High density direct current, of the order of 500 to 1500 amps/cm^2 is then passed through the tube. The experiment is continued until measurable separations are obtained. This requires times ranging from 5 to 100 hours depending on the system. Typical capillary lengths range from 3 to 50 cm. The principal experimental refinements over the years have been in the reduction of convective remixing and the method of analysis of the alloy. A complete discussion of the techniques used in this work is given in Chapter IV. A summary of all the systems that have been studied is given in Appendix I. A review of the previous experiments follows.

The American chemist, G. N. Lewis[2], was the first to successfully electrolyze a liquid metal alloy. His experiments were performed on Na and K amalgams at low temperatures. His data is semiquantitative at best. From then, until very recently, all of the work was carried on in Germany. Kremman conducted a lengthy series of experiments on many alloy systems. His work is summarized in a review by Schwarz[3]. Unfortunately, because of convection, Kremman's experiments can only be used to determine the direction of transport and not the magnitude. Kremman's experiments were performed in straight horizontal tubes. It is evident that this will lead to drastic convection currents as soon as there is an appreciable density difference between the two ends of the tube. This was

pointed out by Schwarz in his review. At the conclusion of an experiment, Kremman broke the diffusion tube into segments and chemically analyzed them in order to determine the direction of transport.

Schwarz[3] developed a technique for the direct meansurement of electrical mobilities. He measured the resistivity changes associated with the changes of concentration in the tube while the electrodiffusion was taking place. The measurements were made with electrical probes placed along the diffusion channel. This technique eliminates the necessity of chemical analysis, but it normally requires a knowledge of the resistivity of the alloy as a function of composition. In addition, the method is very insensitive if the resitivity is not a strong function of composition. Schwarz measured the mobilities of a number of amalgams at room temperature using this technique. Mangelsdorf[4] succeeding in reproducing some of Schwarz's work with a much more sophisticated apparatus. He also extended the experiments to other amalgams at or near room temperature. His measurements are undoubtedly the most accurate now available. Drakin and Maltsev[5] determined the steady state concentration distribution for a number of Na-K alloys with this method.

Despite the slow migration rates, experiments can be devised that give remarkable separations. Even with convection, Kremann obtained separations of 75 percent, i.e., the difference in the weight percentage of a component at the two ends of the tube was 75 percent. Mangelsdorf succeeded in obtaining almost completely pure mercury from amalgams containing 3.5 atomic percent Cd.

Drakin[6] performed a very interesting experiment in which he electrolyzed tubes of alloys of eutectic composition that were held just

over the eutectic temperature (Sn-Bi and Cd-Bi). He obtained almost complete separations in both cases. Normally the components of a eutectic freeze out alternately in thin laminar layers. After there has been a freezing out of one component, the remaining liquid is locally enriched in the other component, which in turn freezes out. This continues until there is no more liquid left. In Drakin's experiment, however, electrodiffusion caused a net drift velocity of the components towards opposite ends of the tube. This insured that supersaturation occurred only at the ends of the diffusion tube. For example, pure Sn would come out at the cathode and pure Bi at the anode. In theory this could continue until the tube was filled with solid Sn at one end and solid Bi at the other. The separation was not that good, needless to say, but still quite remarkable. Drakin purposely picked systems in which there is limited solid solubility. He proposed this technique as a method for separation of otherwise hard to purify elements.

Schwarz also utilized an indirect method for determining mobilities. By measuring the diffusion potential and applying the principles of the theory of irreversible thermodynamics, one can calculate the electrical mobility of the species in question. This work is summarized in Reference 3. Later, Mangelsdorf[4] checked Schwarz's results for the Cd-Hg system by a direct measurements of the mobility. The two experiments check within the experimental error of the measurements. This is another proof of the validity of the Onsager reciprocity relations. The relationship between the mobility and the diffusion potential is developed in Appendix V-B.

One of the most interesting observations that has come out of the older work is that some systems show a reversal of migration direction. Below a certain concentration an element will concentrate at the anode; above this concentration it goes to the cathode. This phenomenon will be discussed in detail in part III of the dissertation.

Recently, Haeffner[7] demonstrated that isotopic separation of Hg can be achieved by electrolysis. Since that time the "Haeffner Effect" has been observed in liquid Ga[8] and liquid K[9]. The isotopic separations are much smaller than the chemical separations in alloys.

B. Theoretical

The nature of the liquid state is still not fully understood. Since electrodiffusion in molten metals is a rather obscure branch of this field, its nature is even more of a mystery. The theory as it stands today is essentially qualitative in nature. Of the theories that have been proposed, several of them quite obviously have elements of truth in them. None can explain all of the data however.

Skaupy's Theory. The first theory was developed by Skaupy in a series of papers[10,11,12,13]. He argued that when a small amount of an element is added to a metal, it either increases or decreases the resistivity. If it increases the resistivity, it does it for one of two reasons: 1) either it increases the resistance to the flow of electrons, or 2) it contributes fewer electrons per atom to the "electron gas" than does the solvent metal. In the first case, the solute material must have a higher frictional resistance to the electron flow than does the solvent. This means the solute atoms should be "dragged" towards the anode with respect to the solvent. In the second case, the solute atoms will have a

smaller net positive charge than the solvent atoms. Therefore the solvent atoms should experience a greater force towards the cathode from the action of the electric field. In either case it is seen that a solute atom that increases the resistivity should have a net motion towards the anode with respect to the solvent. Next consider a solute that decreases the resistivity of the melt. Skaupy argued that this is also caused by one of two reasons: a) it either increases the number of free electrons per atom, or b) it decreases the net electron friction on the moving electrons. Reasoning as before, he said that in both of these cases the solute should concentrate at the cathode relative to the solvent.

Early work seemed to bear out Skaupy's hypothesis. Lewis[2] found that Na and K, which both increase the resistivity of Hg, collected at the anode. Agreement was also found in later work with the amalgams of Zn, Cd, Sn, Au, Ag, and Li. Serious discrepancies turned up when Bi-Hg, Pb-Hg, and Th-Hg were investigated. In the first system Bi goes to anode even though it decreases the resistivity. No movement is observed in the latter two systems although there is an appreciable decrease in resistivity of the amalgams compared to pure Hg. Still later work by Rabkin[14] shows that carbon goes to the cathode in liquid Fe, in opposition to the direction predicted by Skaupy.

Another difficulty arose when the Na-Hg and K-Hg systems were investigated at higher concentrations of solute. The direction of transport was found to reverse, i.e., above two percent Na, the Na goes to the cathode; above 2.5 percent K, the K goes to the cathode. This cannot be explained by Skaupy's theory unless the resistivity isotherm passes through a maximum at these compositions. It does not do this. Despite the failure of the theory in these systems, there is still considerable correlation between the change in resistivity and the direction of transport.

Kremman's Theory. R. Kremman noticed that the elements could be arranged in a series of increasing tendency to go to the cathode. In other words, for any two elements the one farthest down the series would concentrate at the cathode when a binary alloy of the two elements was electrolyzed. It had been observed that when an electric discharge was passed through a mixture of rare gases, the gas with the lowest ionization potential usually collected at the cathode. For this reason Kremman compared the series derived empirically from experimental observations with the series of decreasing ionization potentials. There is some correlation, but the empirical series can be arranged many different ways and still fit the data.

Wagner's Theory. Wagner[15,16] neglected the frictional effects of the electrons. He attempted to use the mobilities derived from self diffusion experiments to calculate the electric mobilities. To do this he used the Einstein relation for each species in the binary alloy

$$D_1 = B_1 kT$$
$$D_2 = B_2 kT \qquad (2)$$

In order to convert from the absolute mobilities, B_i, in cm/sec dyne, to electrical mobilities, u_i in cm^2/sec volt he used the relation

$$u_i = \frac{B_i z_i e}{300} \qquad (3)$$

It can be shown (Chapter III-B) that the observed mobility U_1 defined by Equation (1) is simply the difference of the two "intrinsic mobilities" u_1 and u_2. Combining Equations (2) and (3) one obtains Wagner's equation

for the observed mobility of the solute.

$$U_1 = \frac{e}{300\ kT}\left[D_1 z_1 - D_2 z_2\right] \qquad (4)$$

The sign of U_1, and thus the direction of transport, depends on the sign of the term $D_1 z_1 - D_2 z_2$. Since the self diffusion coefficients are in general unknown it is not possible to test Equation (4). If one assumes typical values for the diffusion coefficients one does obtain numbers of the correct order of magnitude. An additional weakness of Wagner's theory is the neglect of the effect of the electrons.

Schwarz's Theory. Schwarz[17] approached the problem from a completely different point of view. He drew an analogy between bouyant forces in a liquid in a gravitational field and the process of electro-diffusion. He also neglected the electron friction. The criteria that determines whether a solid sinks or floats in a fluid is simply whether the gravitational field exerts a greater force per unit volume on the solid or on the liquid. In other words, if the body has a greater mass density than the liquid it will sink; if not, it will float. Schwarz assumed the liquid metal could be treated as mixture of two types of positively charged species. When an electric field is applied the particles with the greatest charge per unit volume will "sink", i.e., move to the cathode. The criteria for the direction of motion is thus,

$$\frac{z_1 e}{v_1} - \frac{z_2 e}{v_2} \qquad (5)$$

Here v_i is ionic volume of the species. When Relation 5 is multiplied by the electric field strength one obtains the difference in force per

unit volume on each of the species. Combining this with the Einstein relation in the same manner as Wagner and using the solvent as a reference frame, Schwarz obtained the following equation for the observed solute mobility.

$$U_1 = \frac{v_2 \left(\frac{z_1}{v_1} - \frac{z_2}{v_2} \right) e D}{300\ kT} \qquad (6)$$

Here subscript 1 stands for the solute and subscript 2 for the solvent.

Schwarz claimed great accuracy for this equation. Upon examination of the data it is apparent that he made an arbitrary choice of valences. For the Na-Hg and K-Hg systems he compared his calculated mobilities to the observed values at the concentrations where they happened to agree. Since at higher concentrations the magnitude, and even the sign, of the mobility change, this comparison is meaningless. He failed to mention this in his paper. In addition, his theory implies fantastically high pressure gradients. These are of course not observed.

Drakin's Theory. Drakin[18] attempted to use classical thermodynamics to calculate the "equilibrium" concentration distribution of an alloy under the influence of an electric field. The essence of his development is very simple. First he claimed that the work required to transport a mole of material from concentration N' to N'' is given by

$$W = RT \ln \frac{N''}{N'} \qquad (7)$$

This, of course, assumes an ideal solution. Next, he said that the electrical work necessary transport a charged body in an electric field is

$$W = \sum z_i F \qquad (8)$$

Writing these equations for two components and combining he obtained

$$\ln \frac{N_1'}{N_2'} - \ln \frac{N_1''}{N_2''} = \frac{VF(z_1 - z_2)}{RT} \tag{9}$$

In a dilute solution of component 1 in component 2 one has

$$\ln \frac{N_1'}{N_1''} = \frac{VF(z_1 - z_2)}{RT} \tag{10}$$

Drakin tested this theory by plotting the $\ln \frac{N_1'}{N_1''}$ against V. According to Equation (10) this should give a straight line. For the Na-Hg and Ca-Hg systems he did indeed obtain this linear dependence. However, one can show that a plot of this type will in general give a straight line. First write the flux equation for one dimension, including the flux caused by ordinary diffusion.

$$J_1 = U_1 N_1 E - D \left(\frac{\partial N_1}{\partial z} \right) \tag{11}$$

When the steady state condition has been reached in the tube, the flux J_1 will be equal to zero. Using this fact and rearranging one has

$$\frac{dN_1}{N_1} = \left(\frac{U_1}{D} \right) E \, d \, z \tag{12}$$

Now assume that the term U_1E/D is constant along the length of this diffusion tube. This is a good assumption for dilute solutions. Upon integrating and using the fact that $Ea = V$ one obtains

$$\ln \frac{N_1'}{N_1''} = \left(\frac{U_1}{D} \right) V \tag{13}$$

Equation (13) is of the same form as Equation (10). Drakin's test is therefore invalid. Baranovski[19] criticized Drakin's theory on the grounds

that it is erroneous to assume equilibrium for such an irreversible phenomenon as electrodiffusion. He also pointed out that it is not possible to explain the reversal of migration direction with this theory.

Mangelsdorf's Theory. Mangelsdorf[20] has recently revived Skaupy's theory. However, he maintains that the net force on the solute atom is not solely due to the effects stated by Skaupy, but also includes interactions between the solute atom and the surrounding shell of solvent ions. He claims that the erroneous predictions of the simple theory of Skaupy may be explained by these interactions. Quantitative predictions of mobilities are not possible with this theory.

CHAPTER III

CORRELATION OF ELECTRODIFFUSION DATA

A. Empirical Observations

Correlation. Considerable time was spent during the course of the study in investigating the reasons that cause a solute atom to move in the direction that it does. During this work it was noticed that a very simple criterion could be used to predict the direction of motion in liquid metal systems. Almost without exception, the metal with the smallest atomic mass goes to the cathode. This is true not only for binary systems, but also for ternaries. The previous data are summarized in Appendix I. The systems that do not follow the correlation are marked with an asterisk. The direction of isotopic separation is not predicted; in the systems studied the light isotope goes to the anode. Despite its failure with isotopes the correlation is still quite remarkable and unexpected.

Reversal of Transference Direction. It is of particular interest to examine the systems in which the direction of transport reverses in the light of the atomic mass correlation. Four of these systems are known: Na-Hg, K-Hg, Ba-Hg, and Na-K. Results of experiments on the first three systems are discussed in Reference 3; Drakin[5] studied the Na-K system. The results are summarized in Table I. Upon close examination of Table I two significant observations may be made. First, the point of reversal (the concentration at which no transference takes place) is at, or very close to, a concentration corresponding to compound formation in the solid state. In the Na-Hg system there is an incongruently melting compound, $NaHg_4$, at 2.8 weight percent Na and a congruently melting compound $NaHg_2$

at 5.4 weight percent Na. For the Ba-Hg system the incongruently melting compound $BaHg_{11}$ is at 5.9 weight percent Ba. In the K-Hg system there are the compounds KHg_{11}, KHg_8, and KHg_4 at 1.9, 2.3, and 4.7 weight percent K respectively. The compound Na_2K is formed at 54 weight percent sodium in the Na-K system. All of the phase diagrams were taken from Hansen(21). The second observation that one may make is that in each case the component in stoichiometric excess of the compound composition migrates to the cathode.

Compound Formation. In order to interpret these observations in terms of the atomic mass correlation, one first postulates the existence of the intermetallic compounds in the liquid state. Consider the Na-Hg system for an example. Suppose the compound $NaHg_2$ persists in the liquid state with no decomposition into Na and Hg. On the high Hg side of the $NaHg_2$ composition one would have the species $NaHg_2$ and Hg; on the high Na side, $NaHg_2$ and Na. The mass correlation thus predicts that the Na should go to the cathode for high Na concentrations and to the anode when its concentration is low. This is indeed the case. Similar arguments hold for the other three systems. Schwarz(3,p.55) observed that the reversal took place at points where compounds were formed. He also proposed that the species exist in the liquid state as discussed above.

It will now be useful to discuss other work which indicates the existence of compounds or quasi-compound associations in liquid alloys. First of all it should be pointed out that compound formation in the true chemical sense of the word is not necessary to explain the electrodiffusion experiments cited above. All that is required is a solvation or association that ties up the atoms a good share of the time. The "compound" in the liquid may be continually breaking up and reforming. Indeed, since the

TABLE I

REVERSAL OF MIGRATION DIRECTION

System	Weight Percent	Component Moving to Cathode
Na-Hg	0.0 to 2.0 % Na	Hg
	2.0 to 100.0 % Na	Na
K-Hg	0.0 to 2.5 % K	Hg
	2.5 to 100.0 %K	K
Ba-Hg	0.0 to 2.7 % Ba	Hg
	2.7 to 100.0 % Ba	Ba
Na-K	0.0 to 48.0 % Na	K
	48.0 to 100.0 % Na	Na

compounds in most of the cases mentioned in Table I melt incongruently, one would not expect them to remain as permanent entities in the melt. The inference is clear, however, that if the chemical bonding forces are strong enough to form a stable compound at one temperature, they will still be active at higher temperatures, above the decomposition point. The association in the liquid alloy may or may not have a composition corresponding to integral numbers of atoms as in solid alloys. One would, however, expect the composition of the liquid association to lie in the general area where strong compound forming tendencies are present in the solid state.

Perhaps the most direct evidence for compounds present in liquid metallic alloys comes from thermodynamic measurements. Kubaschewski and Catterall[22] summarize the data available for the Na-Hg, K-Hg, and K-Na systems. For the first two systems the entropy of mixing is available; these entropies are negative. They draw the following conclusion (p.22). "The (data) clearly shows that ΔS_{298} is negative. This is due partly to the fact that the solid alloys are formed at room temperature from solid

potassium and liquid mercury. However even considering the entropy of fusion of mercury, the entropies of formation still seem to be negative, indicating the presence of fairly strong ionic bonds in the amalgams which obviously persist in the liquid state" (emphasis mine). Entropies of formation are not available for the Na-K system. The integral heats of solution of Na-K alloys are slightly positive[23]. This in itself would tend to indicate little or no association.

Another direct test for compound formation is given by X-ray studies. Sauerwald and Teske[24] find that for the K and Tl amalgams the compounds KHg_2 and Hg_5Tl_2 probably persist in the liquid state. The Na-K system has been extensively examined. The evidence for the compound Na_2K is conflicting. The first work was done by Banerjee[25]. Banerjee plotted the radial distance to the first peak versus the composition of the alloys. His data showed a "plateau" at the Na_2K composition. He took this to be evidence for the existence of Na_2K in the liquid. More recently Gingrich and Henderson[26] re-examined the system. By determining the radial distribution function they determined conclusively that there are no permanent molecules of Na_2K. They state that this does not rule out the possibility of clustering. They also constructed a plot of the radial distance to the first peak versus percent composition. Their curve is considerably different than Banerjee's but it has a discontinuity of slope right at the Na_2K composition. They say, however, that this in itself cannot be used as unambiguous proof for the existence of Na_2K. Orton, Shaw, and Williams[27] have obtained still another version of this same plot. Their data indicates no discontinuities at Na_2K.

Resistivity data shows that there is ordering in the alkali metal amalgams. Müller[28] has studied the resistivity of the Na-Hg, K-Hg, and Na-K systems as a function of composition. In the two amalgams he found discontinuities in the curves at the compositions corresponding to $NaHg_2$ and KHg_2. He attributed the discontinuities to the presence of the compounds. Bornemann[29,30] attributes a high degree of stability to these compounds on the basis of his resistivity studies. Müller's work on the Na-K system showed that the resistivity continuously increases from both ends of the phase diagram, reaching a maximum at approximately 75 weight percent K. This behaviour is commonly observed in solid alloys. It indicates a lack of association or ordering.

The viscosity of the liquid Na-K system has also been determined. Kremann[31] noticed a sharp discontinuity in the viscosity at a composition corresponding to the compound NaK_2. Ewing, Grand, and Miller[32] were unable to duplicate the earlier work. Their experiments were considerably more precise than Kremann's. They found no discontinuities; however they noticed that near the liquidus the viscosity could not be correlated with Andrade's equation. The measured viscosities at low temperatures were too low. They attributed this to compound formation or association.

Further evidence may be cited for the alkali metal amalgams. The ordinary diffusion coefficients of Na, K, Li, and Rb are a half or a third as great as elements of comparable size[33]. It has been known for some time that ordinary diffusion coefficients can be correlated using the Einstein equation (Equation (2)) and the Stokes equation

$$B = \frac{1}{6\Pi r\eta} \qquad (14)$$

Combining the two one has

$$D = \frac{kT}{6\pi r\eta} \qquad (15)$$

From the data one may infer that the effective radius of the diffusing ion is considerably greater than the ionic radius. The most logical explanation is that each alkali metal ion has several solvent (Hg) ions associated with it.

Other, rather indirect, evidence may be cited. Studies of the species present in the vapor in equilibrium with the liquid alloys have been made. Barrat[34] and Roder[35] found evidence for the HgK and HgNa species in the vapor phase.

In summary, one can say that the hypothesis of compound formation in the systems showing reversal of transference has considerable support from other fields. The evidence appears much more conclusive for the amalgams than it does for the Na-K system.

The amalgams and the Na-K system were the only alloys discussed above. Other systems show the same effects. Knappwost[36] discussed the structure of molten Mg-Pb alloys in terms of thermodynamic and resistivity data. He concludes that there are "residual aggregates" (electron binding groups) present in the liquid with the Mg_2Pb composition. Roll and Motz[37] found evidence for intermetallics in liquid Cu-Sn from resistivity measurements.

B. Interpretation of the Correlation

The correlation was expressed in terms of atomic mass. Since the atomic mass is proportional to the atomic number, and for most alloy

pairs is also proportional to the atomic size, one could equally well state the correlation in terms of these parameters. In fact, if one uses atomic size one can immediately postulate a reason for the correlation. The larger atoms will in general present a greater resistance to the flow of electrons than the smaller atoms (Reference 38, pages 289-91). If this is the case, one might expect the large atoms to be dragged towards the anode with respect to the smaller atoms by the electron stream. This interpretation is quite plausible physically and fits most of the observed data. In the following pages a development will be presented which uses the above argument in combination with assumptions about the nature of the atomic motion in order to arrive at an approximate equation for the electron mobility that agrees with the correlation.

Darken's Equation. First it will be instructive to review one of the recent treatments of diffusion in liquids and solids. This is the work done by Darken(39). Darken says there are two "intrinsic diffusion coefficients" D_1 and D_2. Because D_1 and D_2 may have different magnitudes there will be, in general, a bulk convective motion of the liquid. Darken writes the flux equation for each of the components including the convection.

$$J_1 = -D_1\left(\frac{\partial N_1}{\partial z}\right) + vN_1 \tag{16}$$

$$J_2 = -D_2\left(\frac{\partial N_2}{\partial z}\right) + vN_2 \tag{17}$$

Here v is the bulk velocity of convection as would be measured by an inert marker. From the assumption that the atomic volume of the mixture

is constant throughout the experiments one has for the velocity v.

$$v = \frac{1}{N_o}\left[D_1 \left(\frac{\partial N_1}{\partial z}\right) + D_2 \left(\frac{\partial N_2}{\partial z}\right)\right] \tag{18}$$

Substituting Equation (18) into Equation (16) one has for the total flux of component 1.

$$J_1 = - \left[D_1 x_2 + D_2 x_1 \right] \left(\frac{\partial N_1}{\partial z}\right) \tag{19}$$

Here x_1 and x_2 are the mole fractions of components 1 and 2. By comparison of Equation (19) with the Fick's law definition of the diffusion coefficient, i.e.,

$$J_1 = -D \frac{\partial N_1}{\partial z} \tag{20}$$

one has directly that

$$D = x_2 D_1 + x_1 D_2 \tag{21}$$

Darken also derived an expression to take into account nonideality of the binary mixture. Since this is not pertinent to our discussion it is not included here. Darken's equation has been verified experimentally in solid binary systems by Darken(39) and by Cohen(40). Grace(41) has shown that diffusion in liquid metals also follows Darken's equation. These experiments were primarily directed at testing Darken's thermodynamic correction term, but in the process necessarily tested the development given above.

Electron Mobility. Next it is necessary to review one of the oldest and simplest models for calculating the mobility of an electron

in a metallic lattice. This theory was developed by Riecke[42], Drude[43], and Lorentz[44]. The summary of their treatments given below was taken from Mott and Jones[38]. Suppose that the electrons in the metal lattice are free and can accelerate when an external electric field is applied. After a time 2τ the electron collides with an atom and its momentum is completely destroyed. The quantity τ is called the relaxation time. The equation of motion of the electron during acceleration is

$$\frac{dv_e}{d\theta} = - \frac{eE}{m_e} \tag{22}$$

Immediately after a collision, the velocity in the direction of the field is zero. After 2τ seconds the velocity is

$$v_e = - \frac{2\tau eE}{m_e} \tag{23}$$

The time average drift velocity is therefore

$$\overline{v}_e = - \frac{\tau eE}{m_e} \tag{24}$$

The mobility, in cm^2/sec volt is obtained by dividing through by the field strength E.

$$u_e = - \frac{\tau e}{m_e} \tag{25}$$

This early model of electrical conductivity succeeded in explaining the Wiedemann and Franz ratio, and gave correct order of magnitude predictions of the conductivity of most metals. It failed when applied to the temperature dependence of conductivity, or the observed heat capacity of the electrons.

Mobility of Atoms. We are now in a position to derive an equation for the mobility of species in a liquid metal alloy. First assume there are two "intrinsic mobilities" u_1 and u_2. As in Darken's treatment, if these mobilities are different one will in general have a bulk convective flow. The flux equations including the convective motion are thus

$$J_1 = u_1 N_1 E + v\, N_1 \tag{26}$$

$$J_2 = u_2 N_2 E + v\, N_2 \tag{27}$$

Assuming a constant molar density one has for the convective velocity v.

$$v = - \frac{E}{N_o}\left[u_1 N_1 + u_2 N_2\right] \tag{28}$$

Substituting Equation (28) into Equation (26) one obtains the flux expression for component 1.

$$J_1 = (u_1 - u_2)\, N_1 x_2 E \tag{29}$$

For dilute solution of component 1 in 2, Equation (29) reduces to

$$J_1 = (u_1 - u_2)\, N_1 E \tag{30}$$

By comparing Equation (30) with Equation (1), the definition of mobility one finds

$$U_1 = (u_1 - u_2) \tag{31}$$

The observed mobility is simply equal to the difference of the two "intrinsic mobilities".

In order to estimate the magnitude of the intrinsic mobilities a method analogous to that used for the mobility of an electron will be used. A highly idealized picture of the motion of the metallic ions will be postulated. It will be assumed that the only forces acting on the ions are those caused by the action of the electric field on the charge the ions carry and the frictional effect of the electron stream on the ions (electron scattering). The first force is simply $z_i eE$ and the second force $r_i \bar{v}_e$, where r_i is the frictional coefficient between the conduction electrons in dynes sec/cm and $\bar{v}_e$ the average drift velocity of the electrons in cm/sec. Next, consider the ions as free to move about, and free to accelerate when a net force is applied to them. As in the case of an electron, the ion loses all of its momentum when it undergoes a collision with another ion. The equations of motion for the ions are

$$\frac{dv_1}{d\theta} = \frac{z_1 eE + r_1 \bar{v}_e}{m_1} \tag{32}$$

$$\frac{dv_2}{d\theta} = \frac{z_2 eE + r_2 \bar{v}_e}{m_2} \tag{33}$$

After a collision the velocity is zero, after time θ the velocities are

$$v_1 = \frac{(z_1 eE + r_1 \bar{v}_e)\theta}{m_1} \tag{34}$$

$$v_2 = \frac{(z_2 eE + r_2 \bar{v}_e)\theta}{m_2} \tag{35}$$

The time average drift velocities over the period 2τ are thus

$$\bar{v}_1 = \frac{\int_0^{2\tau} v_1 d\theta}{2\tau} \tag{36}$$

$$\bar{v}_2 = \frac{\int_0^{2\tau} v_2 d\theta}{2\tau} \tag{37}$$

Evaluating the integrals one has

$$\bar{v}_1 = \frac{(z_1 eE + r_1 \bar{v}_e)\,\tau}{m_1} \tag{38}$$

$$\bar{v}_2 = \frac{(z_2 eE + r_2 \bar{v}_e)\,\tau}{m_2} \tag{39}$$

The following important assumption will now be made: namely, the frictional coefficient r_i is proportional to the mass of the ion m_i. The justification for this assumption will be presented later.

$$r_1 = km_1 \tag{40}$$

$$r_2 = km_2 \tag{41}$$

Substituting into Equation (38) and Equation (39) one has

$$v_1 = \frac{(z_1 eE + km_1 \bar{v}_e)\tau}{m_1} \tag{42}$$

$$v_2 = \frac{(z_2 eE + km_2 \bar{v}_e)\tau}{m_2} \tag{43}$$

Subtracting Equation (43) from Equation (42) and dividing through by E

one finds for the difference of the intrinsic mobilities

$$u_1 - u_2 = \left[\frac{z_1}{m_1} - \frac{z_2}{m_2}\right] e\tau \qquad (44)$$

Using Equation (31) one has finally

$$U_1 = \left[\frac{z_1}{m_1} - \frac{z_2}{m_2}\right] e\tau \qquad (45)$$

Equation (45) appears to show the reason for the mass correlation. Assuming that the charges on the ions are approximately the same, U_1 will be positive when $m_1 > m_2$. From Equation (1) it follows that Component 1 will go to the anode. Also, Equation (45) gives mobilities of the correct order of magnitude when representative values of the constants are used. For example, take m_1 = 100 AMU, m_2 = 50 AMU, $z_1 = z_2 = +1$, and $\nu = 10^{-13}$ sec. The mobility is then 9.6×10^{-4} cm^2/sec volt. The magnitude of τ was estimated by using the reciprocal of ν, the fundamental vibrational frequency of a typical lattice. The magnitudes of measured mobilities range from zero to 12×10^{-4} cm^2/sec volt. The intrinsic mobilities may be estimated by using the Stokes equation (for the terminal velocity a sphere moving through a viscous liquid) and Andrade's theory of viscosity. The result is almost identical in form with Equation (37) and gives quantitative predictions of the same accuracy[45].

The preceeding development leaves several questions unanswered. First, it has been stated by some that it is incorrect to postulate the existence of two intrinsic mobilities in fluids[46]. This criticism applies to the Darken equation as well as to the development presented above. The experiments of Schadler and Grade[41] indicate however that the Darken equation does agree with the observations, at least within the

presently obtainable experimental accuracy. In addition, McCarty and Mason[47] have shown that the Kirkendall effect occurs in gaseous diffusion. They made a direct measurement of the bulk convective motion, v. This is strong evidence for two intrinsic diffusion coefficients.

In order to derive Equation (44) it was necessary to assume that the drag force exerted on the ions by the electrons was proportional to the mass of the ion. According to Mott and Jones (Reference 38, pp. 289-91) the electron drag force will be proportional to the effective area presented by the atoms, all else being equal. The size of a metallic atom is, more often than not, proportional to its mass. In fact, 85 percent of the alloy systems that have been electrolyzed follow this generalization. Thus to a first approximation one can assume that the drag force exerted by the electrons on the metallic ions will be proportional to the ions' size and thus also to their mass.

The assumptions that are necessary to obtain the desired mass dependency given in Equation (45) should be reemphasized. First it was necessary to assume that the resistance of an atom to motion when a net force is applied is the inertia arising from its mass. This, of course, is a very idealized picture of atomic motion. Secondly, the effect of electronic friction on the atomic motion was handled by the assumption that the friction coefficient was proportional to the mass of the atom. This may be treated as an assumption per se, although there is the reason stated above that leads one to believe that in many cases this assumption will be valid.

The belief that Equation (45) is a good first approximation to the true state of affairs in the liquid alloy is substantiated by the correct predictions of both direction and magnitude of the electrical mobilities.

CHAPTER IV

EXPERIMENTAL

A. Purpose of Experiments

Cu-Sn Experiments. The Cu-Sn system is interesting because it gives a partial test of the atomic mass correlation versus the resistivity correlation of Skaupy and Mangelsdorf. The Cu-Sn system is one in which these two correlations give different predictions. There are few liquid metal systems for which there is both resistivity and electrolysis data available to test the two correlations. It was felt an additional test should be made. The Cu-Sn system had been studied at 50 weight percent by Kremann and Gruber-Rehenburg.[48] They showed that the Cu went to the cathode, in agreement with the atomic mass correlation. However, according to Mangelsdorf his correlation can only be applied to dilute solutions. Therefore, the experiments were conducted at 2.0, 1.5, and 0.44 weight percent Cu.

Na-Hg System. The Na-Hg system was studied in an attempt to verify the hypothesis of compound formation in the liquid metal alloy. If the reversal of transference direction (discussed in Chapter III) is due to association of the two types of atoms, at sufficiently high temperatures one would expect to find this reversal to vanish. Dilute Na amalgams were studied at temperatures up to the normal boiling point of mercury. At lower temperatures the sodium is transported to the anode.[49] At high temperatures, if the association is broken down by thermal agitation, one would expect the transport of sodium to be to the cathode. In addition, the mobility of Na at room temperature was determined. Schwarz[3]

has measured this mobility by two separate methods i.e. diffusion potential and resistivity probes. The present measurements serve as an excellent check on the absolute accuracy, as well as the precision, of the experimental technique developed in this dissertation.

Quantitative Determination of Mobilities in Non-Mercuric Systems. The only previous quantitative measurements of mobilities were on mercuric alloys at or near room temperature. The magnitude of mobilities in other systems at higher temperatures is thus of considerable interest. One of the purposes of this work was to develop a method that will give results of reasonable accuracy. This work was done with Mr. John Verhoeven. This method was applied to the following alloys: Bi-Cu, Bi-Mg, Bi-U, and Bi-Zr. The compositions and temperatures were severely limited by the shape of the liquidus line, the reactivity of the solute, and the quantities of solute necessary for an accurate analysis. The solute composition was chosen as low as possible so that the results would be applicable to testing any theory assuming dilute solutions.

B. General Remarks on Experimental Method

Acknowledgement. All of part B, Chapter IV, of this dissertation was developed in collaboration with Mr. John Verhoeven. The work has been published separately in a University of Michigan Research Institute Report (Reference 50). The results of the report are essential for explaining the experimental procedure and for the analysis of the data presented in the latter part of the dissertation. For this reason it is included with the notation that the work contained in it was only partially done by the author of the dissertation.

Calculation of Mobility from Data. The experimental method in brief simply involves passing high density direct current through a thin capillary of molten metal initially at uniform concentration. The concentration at one end of the capillary is maintained constant by keeping it in contact with a large reservoir of the molten alloy. (See Figure 1.) At the end of the experiment the tube and reservoir are chemically analyzed. The resistivity of the melt, the current, the time, and the increase (or decrease) of solute in the capillary are then known. All of the solute that enters (or leaves) the capillary must cross the boundary between the reservoir and capillary. Therefore by applying Equation (1) to the reservoir-capillary boundary, one can calculate the mobility directly by making a mass balance.

$$J_1 = U_1 N_1 E \tag{1}$$

Equation (1) may also be written in the following form.

$$U_1 = \frac{\Delta m_1}{N_1 I \rho \theta} \tag{46}$$

Here Δm_1 is the total change in the mass of solute in the capillary. Note that the cross sectional area of the capillary at the reservoir does not appear in Equation (46). Since one has determined the rate of transport of solute across the boundary between the capillary and the reservoir, the corresponding mobility is for the conditions prevailing at this boundary. In other words, the mobility that one calculates is the mobility of the solute atoms in an alloy of the reservoir composition.

Back Diffusion. Equation (46) was derived under the assumption that the concentration N_1, at the reservoir entrance remains constant throughout the experiment. This requirement is easily met in practice by

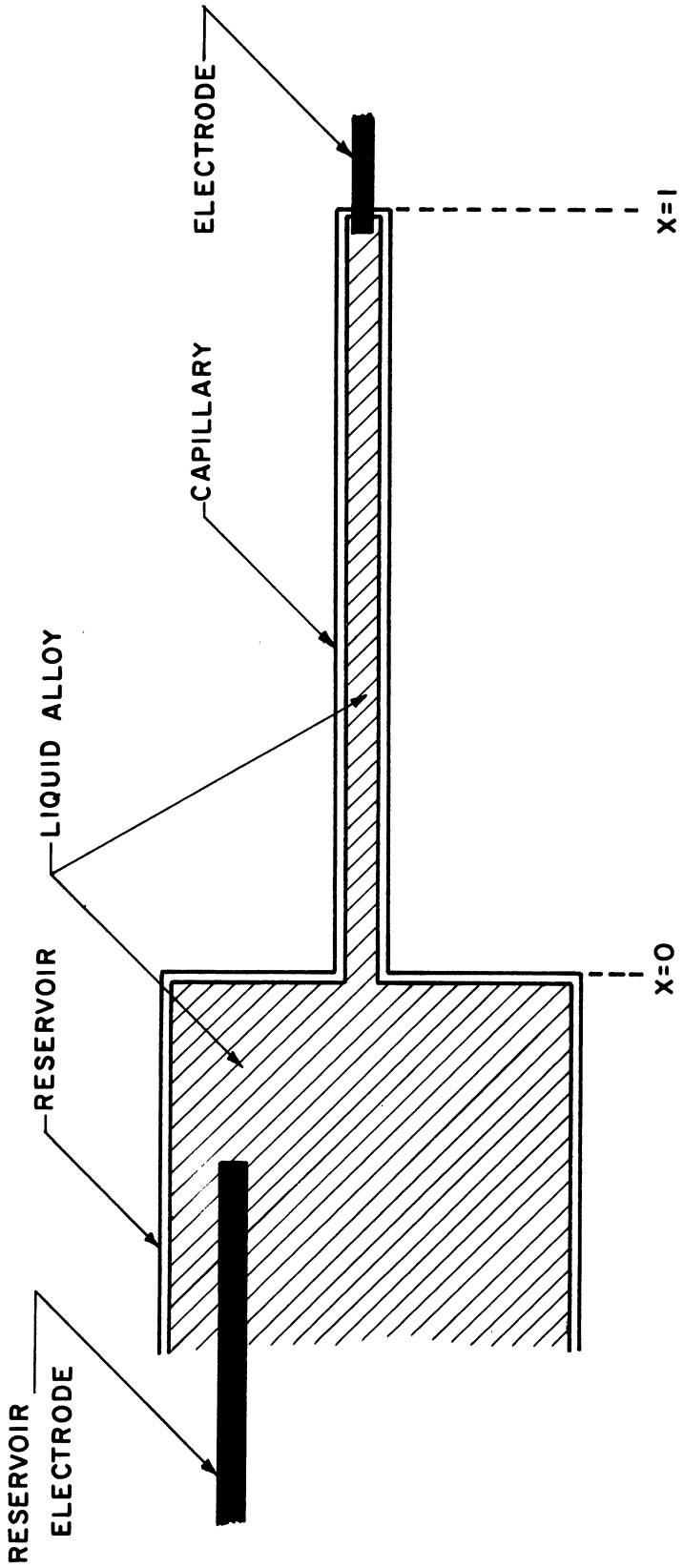

Figure 1. Schematic Diagram of Diffusion Cell.

using a sufficiently large reservoir. Also, it was assumed that the only flux of solute across the reservoir-capillary boundary was caused by electrodiffusion.

This requirement is more difficult and requires some analysis. Since the concentration of solute in the capillary is changing, concentration gradients will be formed within it. If a concentration gradient is formed at the mouth of the capillary, solute will be transported across the reservoir-capillary boundary by ordinary diffusion. Intuitively one would expect that as one moves solute into the capillary from the reservoir it will "pile up" at the far end of the capillary. As more and more solute enters the capillary, the concentration will gradually increase back down the tube towards the reservoir. If the solute is run out of the capillary, the concentration should first decrease at the far end of the tube. The concentration then decreases back down the tube towards the reservoir as the experiment proceeds. Initially, then, Equation (46) will be satisfied. However, as soon as a concentration gradient is formed at the capillary mouth, solute will be transported into (or out of) the capillary by ordinary diffusion. The ordinary diffusion flux will always oppose the electrodiffusion flux. This will make the calculated mobilities too low. If the experiment is continued for a very long time the steady state condition is reached. At this point the concentration gradient at the mouth of the capillary has increased to the point where the ordinary diffusion flux is equal and opposite to the electrodiffusion flux.

One can easily determine whether an experiment has proceeded to the point where back diffusion takes place. A series of otherwise identical runs are made for various lengths of time. For the runs at low times

one should find the same mobility, i.e., Δm_1 is directly proportional to θ. This is the true value of the mobility. After a certain time one will find the calculated mobilities become smaller. These runs have progressed to the point where the back diffusion is appreciable. The author has observed this effect in the Bi-Cu and Na-Hg systems.

Solution of Diffusion Equation. Even though one has a direct experimental check on the validity of the data, this is of limited help in designing experiments. The degree of back diffusion is determined by the interplay of a number of factors, e.g., the ordinary diffusion coefficient, D, the electrical mobility, U_1, the electric field strength, E, the length of the tube, a, and the time of the experiment, θ. In order to determine exactly how these parameters affect the changing concentration profile within the capillary tube, it is necessary to solve the diffusion equation for the boundary conditions of these experiments. The one dimensional flux equation for dilute solutions including ordinary diffusion is

$$J_1 = U_1 N_1 E - D\left(\frac{\partial N_1}{\partial z}\right) \tag{47}$$

Differentiating once with respect to distance one obtains the desired partial differential equation

$$\left(\frac{\partial N_1}{\partial \theta}\right) = D\left(\frac{\partial^2 N_1}{\partial z^2}\right) - \left(\frac{U_1 V}{a}\right)\left(\frac{\partial N_1}{\partial z}\right) \tag{48}$$

Here the approximation was introduced that the electric field strength E throughout the tube may be approximated by the total voltage drop, V, divided by the tube length "a" and that D is not a function of concentration. The boundary conditions are

$$N_1 = N_1(\text{res.}) \qquad \text{for} \quad z = 0, \ \theta > 0. \tag{49}$$

$$U_1 N_1 E - D\left(\frac{\partial N_1}{\partial z}\right) = 0 \qquad \text{for } z = a,\ \theta > 0. \tag{50}$$

The first is the constant concentration restriction at the reservoir end of the capillary. The second states that the flux is zero at the electrode end of the capillary. The initial condition is

$$N_1 = N_{1(\text{res.})} \qquad \text{for } 0 \leq z \leq a,\ \theta = 0\ . \tag{51}$$

This particular problem had not been solved. Mason,[51] Furth,[52,53] and DeGroot[54] integrated the same equation, but for boundary conditions corresponding to a capillary closed at both ends. The complete solution of the equation is given in Reference 50. Only the final result will be given here. The following dimensionless quantities are defined

$$x = \frac{z}{a}, \quad s = \frac{U_1 V}{D}, \quad C = \frac{N_1}{N_{1(\text{res.})}}, \quad t = \frac{D\theta}{a^2}$$

There are three separate solutions depending on the magnitude of the dimensionless quantity "s".

For $s = 2$

$$C_{(x,t)} = \exp sx + A_o\, x \exp(x-t) + \sum_{n=1}^{\infty} C_n \sin \beta_n x \exp\left[\frac{sx}{2} - \left(\beta_n^2 + \frac{s^2}{4}\right)t\right] \tag{52}$$

For $s > 2$

$$C_{(x,t)} = \exp sx + B_o \sinh \alpha x \exp\left[\frac{sx}{2} + \left(\alpha^2 - \frac{s^2}{4}\right)t\right] + \sum_{n=1}^{\infty} C_n \sin\beta_n x \exp\left[\frac{sx}{2} - \left(\beta_n + \frac{s^2}{4}\right)t\right] \tag{53}$$

For $s < 2$

$$C_{(x,t)} = \exp sx + \sum_{n=1}^{\infty} C_n \sin \beta_n x \exp\left[\frac{sx}{2} - \left(\beta_n^2 + \frac{s^2}{4}\right)t\right] \tag{54}$$

where

$$A_o = -\frac{6}{e} \tag{55}$$

$$B_o = \frac{16\,\alpha\, s \cosh\alpha \exp(-s/2)}{(s^2 - 4\alpha^2)(s - 2\cosh^2\alpha)} \tag{56}$$

$$C_n = -\frac{16\,\beta_n\, s \cos\beta_n \exp(-s/2)}{(s^2 + 4\,\beta_n^2)(s - 2\cos^2\beta_n)} \tag{57}$$

The eigen values α and β_n are determined by the roots of the following eigen functions

$$\alpha \coth\alpha = \frac{s}{2} \tag{58}$$

$$\beta \cot\beta = \frac{s}{2} \tag{59}$$

Equation (58) has only one root for each value of $s > 2$. It has no roots for $s < 2$. Equation (59) has an infinite number of roots for each value of s. Tables of these roots are given in Reference 50.

From the solution the concentration profile in the capillary was computed for various values of the dimensionless mobility "s" on the Bendix G-15 computer. The results are given in Figures 2 and 3. It is evident that the intuitive reasoning about the shape of the concentration profile was correct.

In order to accurately determine the effect of back diffusion the solutions were integrated over the length of the capillary. This then gives C_m the average dimensionless concentration in the tube, as a function of time alone. Figure 4 and 5 show how C_m varies with t, the dimensionless time, for parameters of "s", the dimensionless mobility. Here one can see the effect of back diffusion. The concentration initially

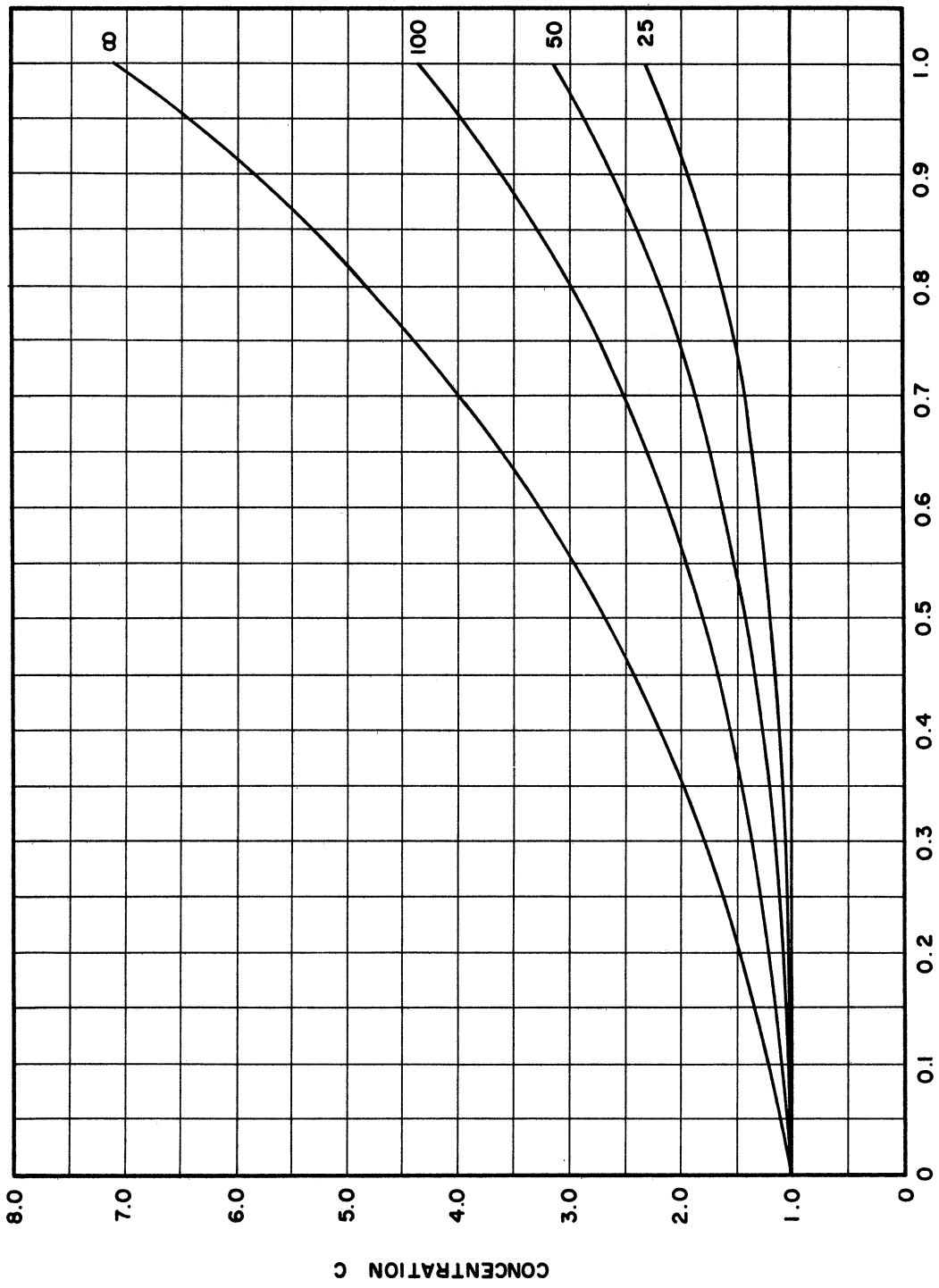

Figure 2. Concentration Distribution in Capillary, Parameters of Time in Hours, $s = +1.96$, $D/a^2 = .0072$ sec^{-1}.

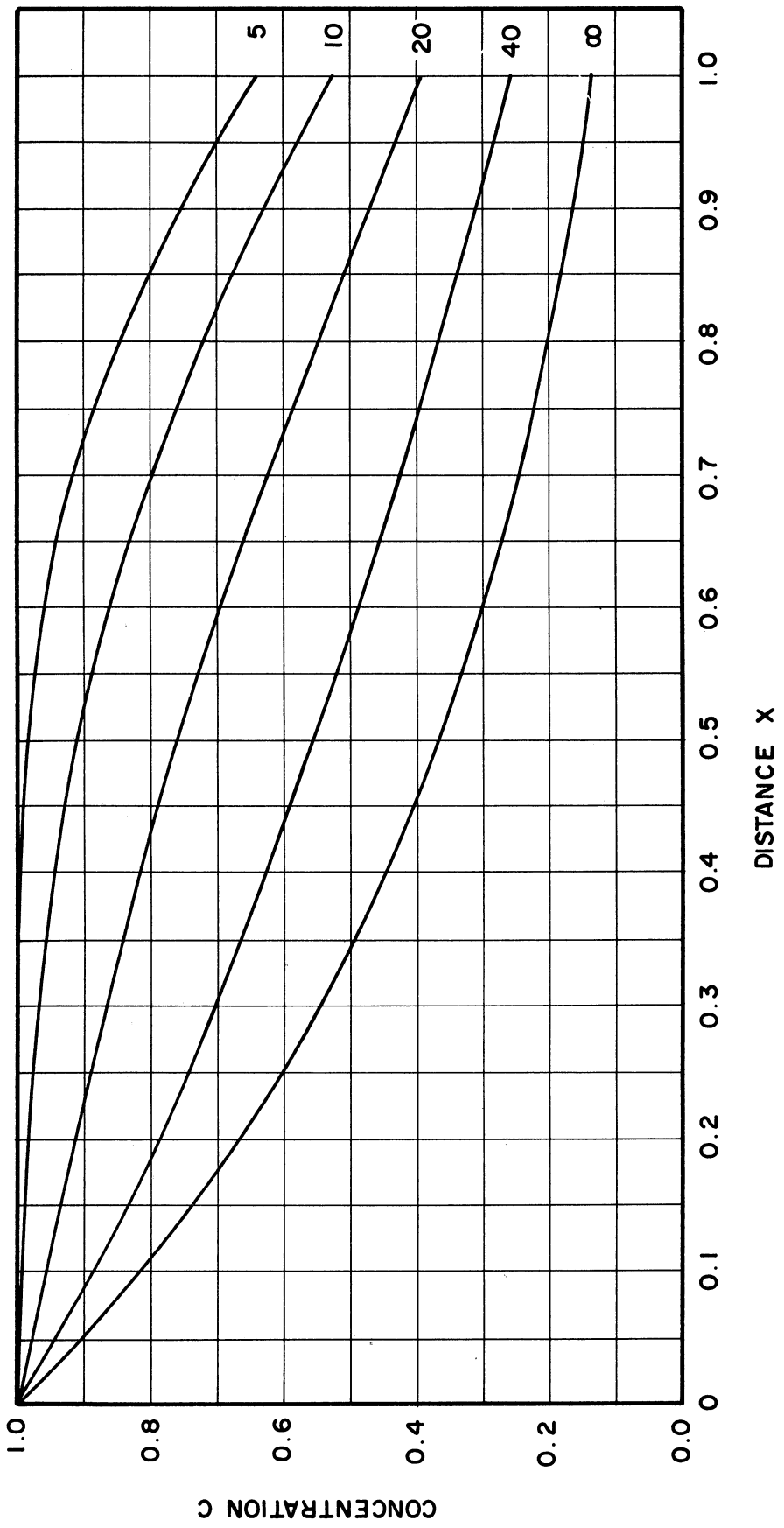

Figure 3. Concentration Distribution in Capill
in Hours, $s = -2.00$, $D/a^2 = .0072\ sec^{-1}$.

changes at a rate directly proportional to time. After a while the rate of change diminishes. At long enough times the curves become parallel to the abscissa, indicating that the steady state condition has been reached.

Figures 6 and 7 show the percent error caused by back diffusion versus the percent change in the average capillary concentration. From these figures one can see that it is much better to run the solute into the capillary rather than out of it. It is also evident that the larger the "s", the smaller the error. Since $s = \frac{U_1 V}{D}$ it becomes necessary to use as high a field strength as possible. The field strengths can normally be no higher than 0.1 volts/cm. The current densities necessary to go above this generate so much I^2R heat that the temperature rise in the capillary becomes intolerable. One has no control over the magnitude of D (assuming no convection is present). The only other possibility for increasing "s" is then to increase the length of the capillary "a". Since $V = Ea$ doubling "a" will double "s" at constant E. However, the dimensionless time is $D\theta/a^2$. From Figure 4 this means that one must run the experiment twice as long in order to obtain the same increase in concentration.

Examination of Equation (46) reveals a shortcoming of this method. In order to determine Δm_1 one must subtract the initial capillary concentration from the final capillary concentration. Unless there is a large concentration change the analytical errors will be greatly magnified. Large concentration changes, however, lead to back diffusion. One must therefore compromise in the choice of experimental conditions. The magnification of the analytical errors was rigorously determined in Reference 50. The

results are given in Figure 8. The numbers on the curves in Figure 8 signify the number of independent determinations of the initial capillary composition, i.e., reservoir composition. Obviously only one determination can be made of the final capillary composition.

Determination of Diffusion Coefficients. A very interesting sidelight on the mathematical treatment of the experiments is the possibility of determining the ordinary diffusion coefficient. By choosing the dimensionless time as $U_1 V\theta/a^2$ rather than $D\theta/a^2$ one can construct plots equivalent to Figures 4 and 5. This procedure leaves the diffusion coefficient D in only one of the dimensionless parameters. These plots are shown in Figures 9 and 10. One makes a series of identical experiments but at progressively longer times. As explained previously, the short time runs will give the true value of the mobility. One now knows U_1, V, a, and the results of an experiment that has gone to the point where back diffusion takes place. Therefore both the coordinates of Figure 9 (or 10) are specified. This determines the value of "s" from which the diffusion coefficient is calculated. This technique was applied to the Cu-Bi system. (The results will be discussed in Chapter IV-E.)

Other Precautions. Electrodiffusion is a very slow process. The normal migration velocities are only about 1×10^{-5} as great as the drift velocity of an electron. At very high field strengths the migration velocities may be as high as 0.5 cm/hr. The low viscosity of liquid metals makes it very difficult to avoid convection currents in the melt. This can destroy any separation that may have taken place. These items,

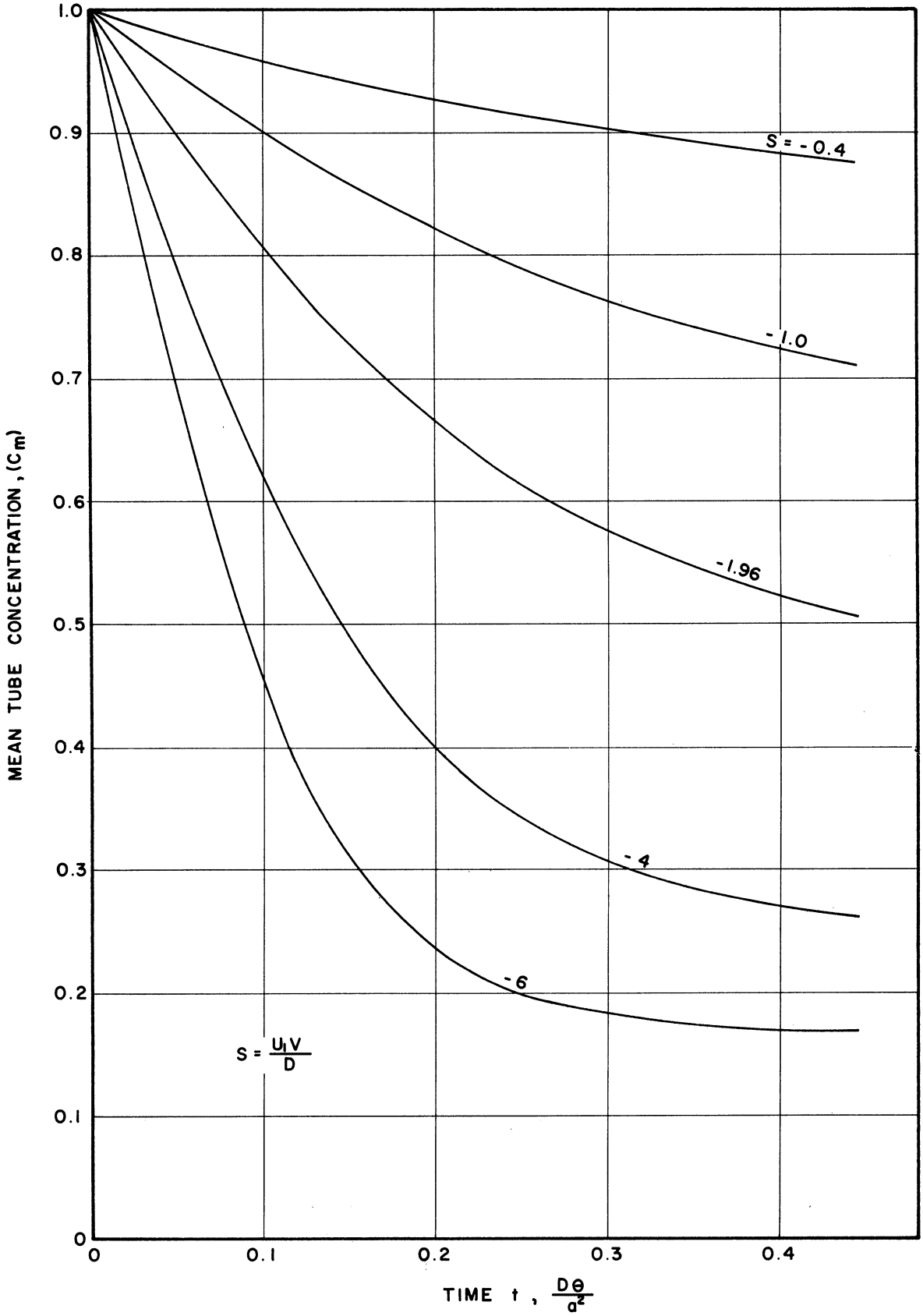

Figure 4. Mean Tube Concentration Versus Dimensionless Time

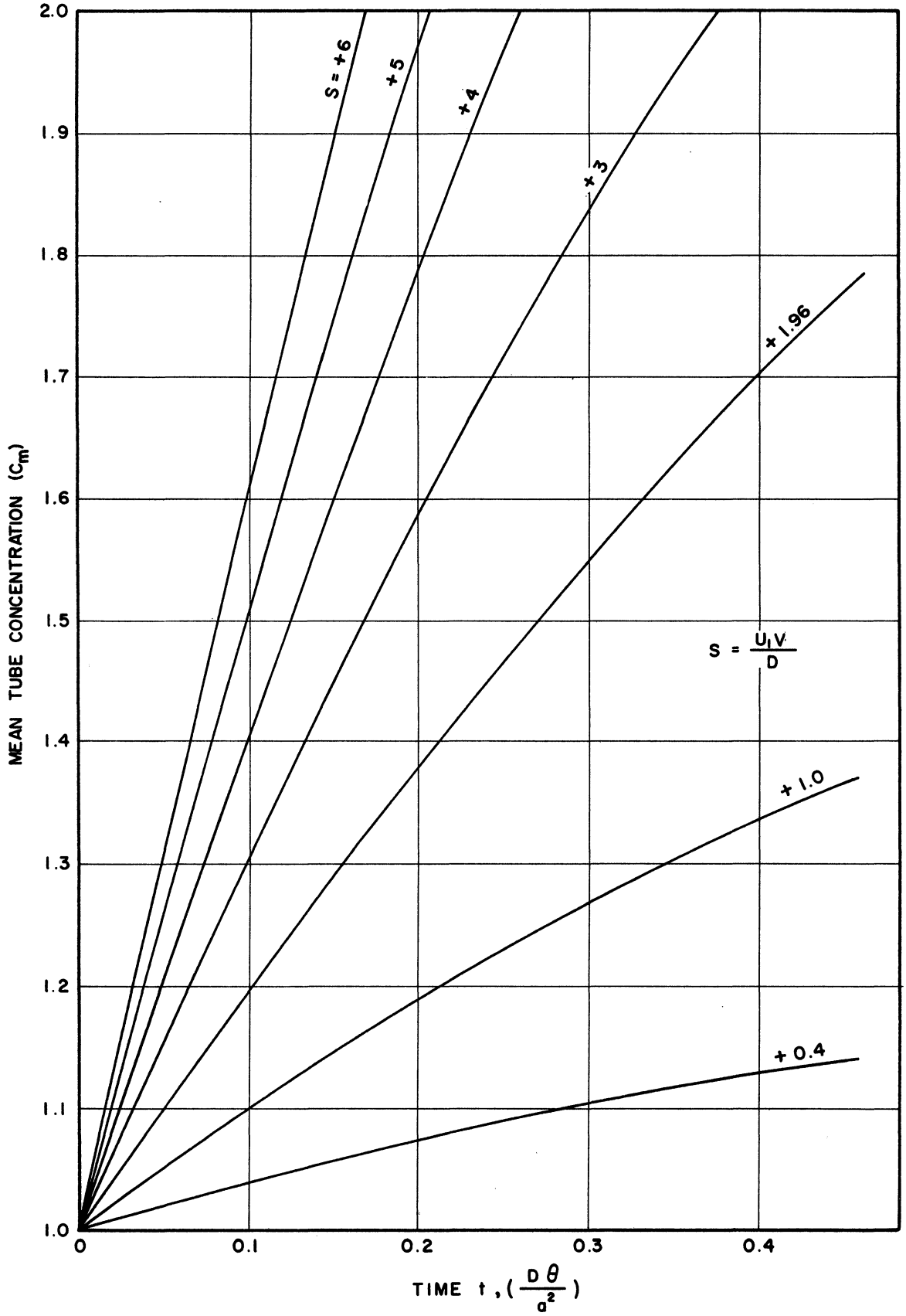

Figure 5. Mean Tube Concentration Versus Dimensionless Time

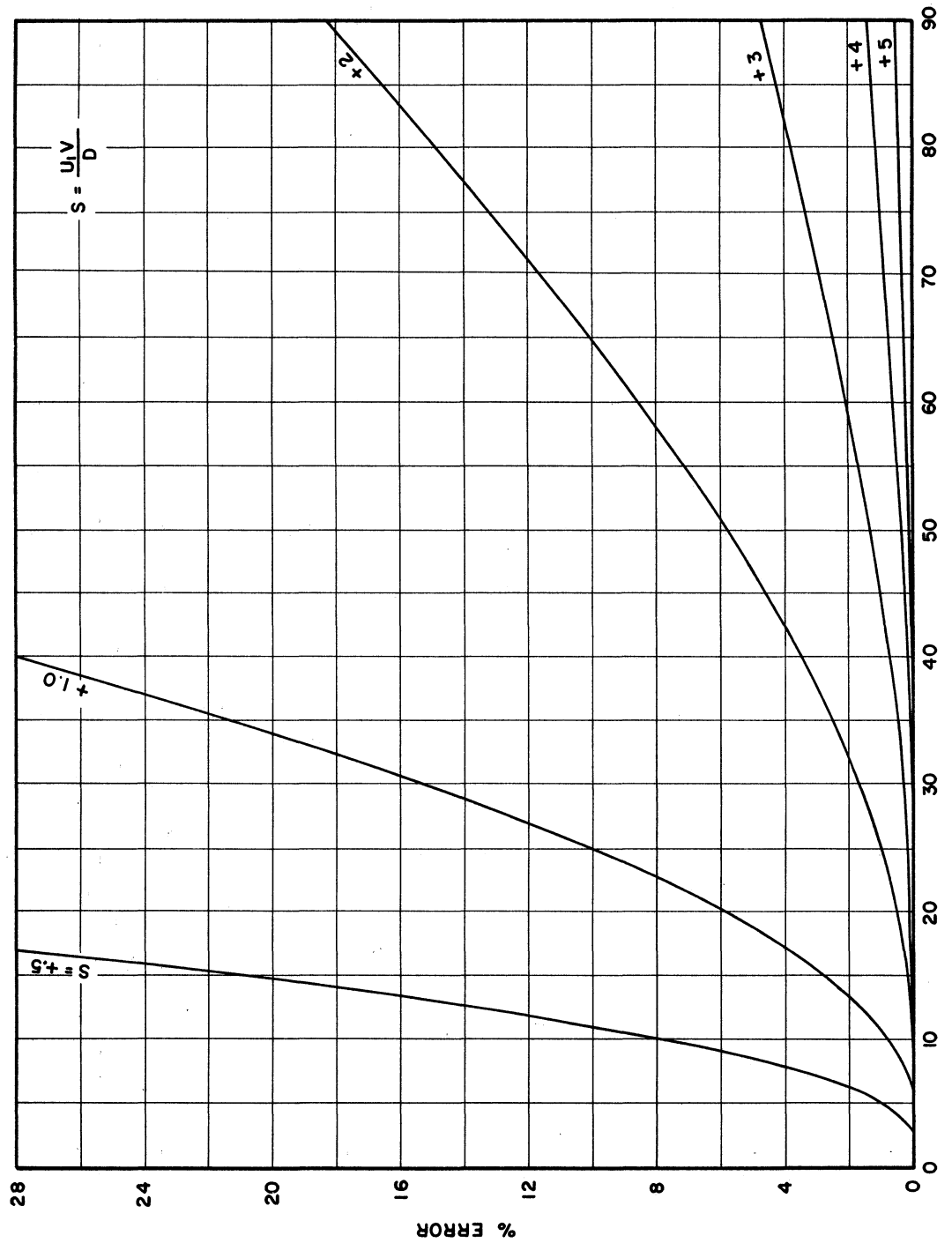

Figure 6. Percent Error in Mobility Versus Percent Change in Capillary Concentration

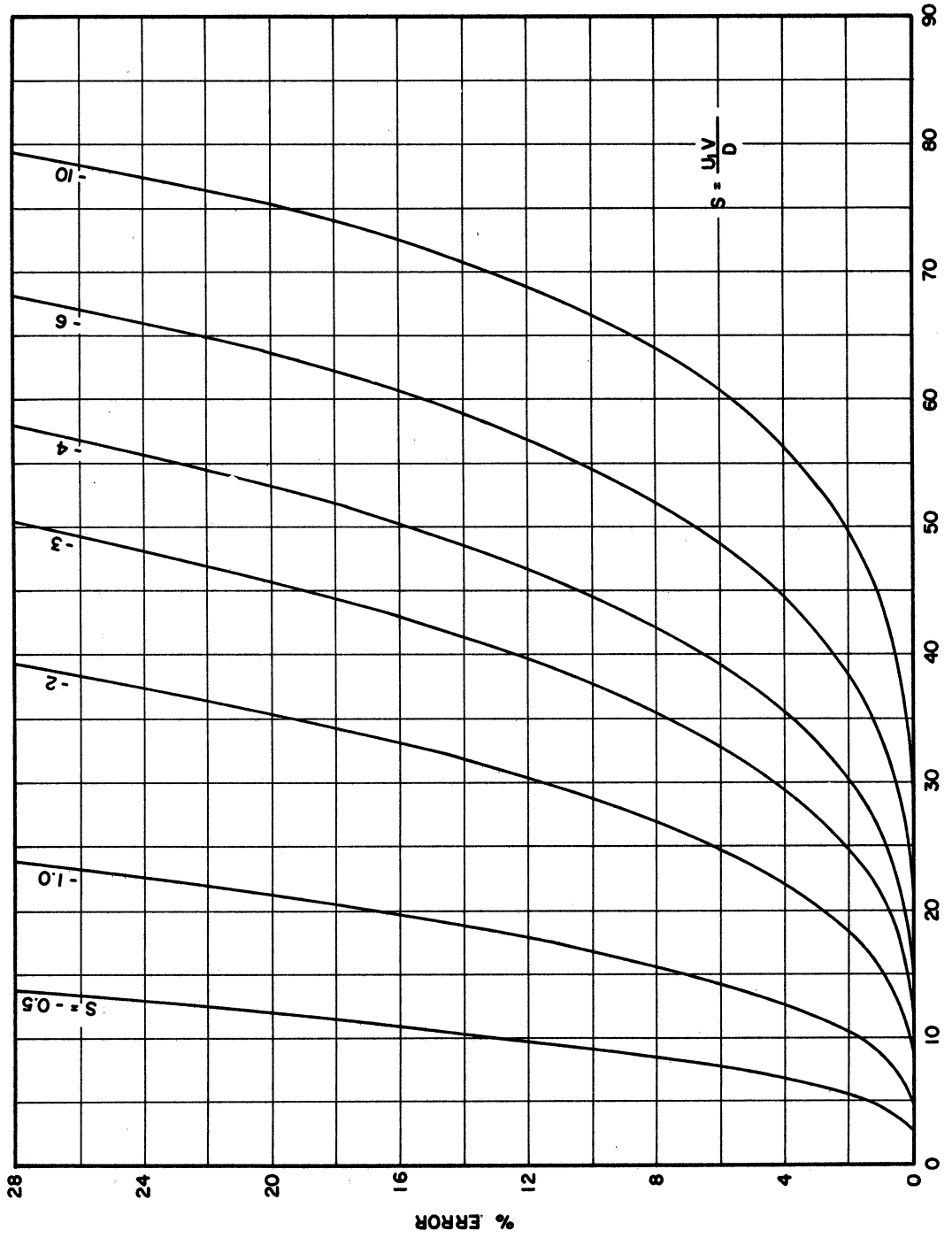

Figure 7. Percent Error in Mobility Versus Percent Change in Capillary Concentration

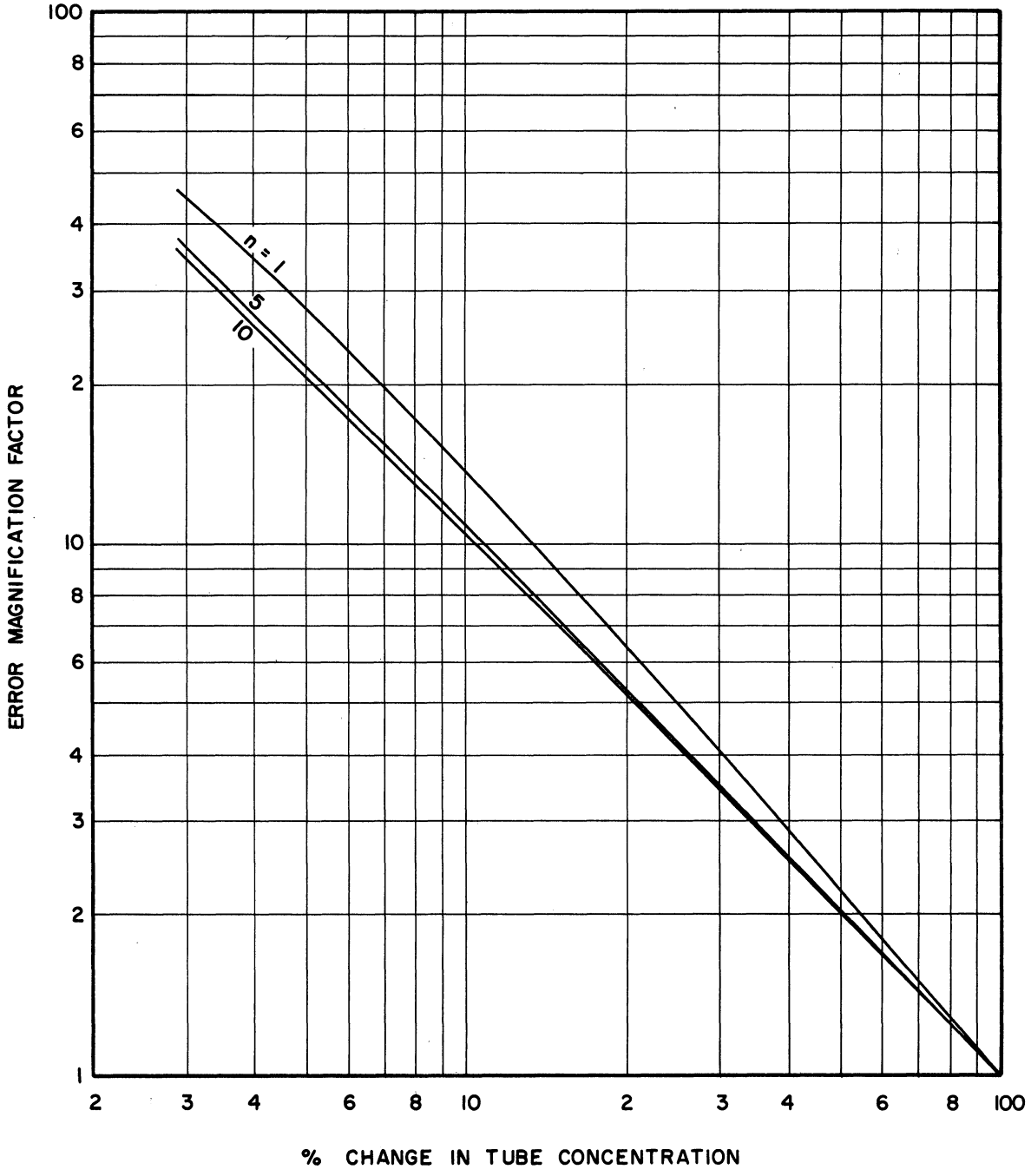

Figure 8. Error Magnification in Mobility Calculation

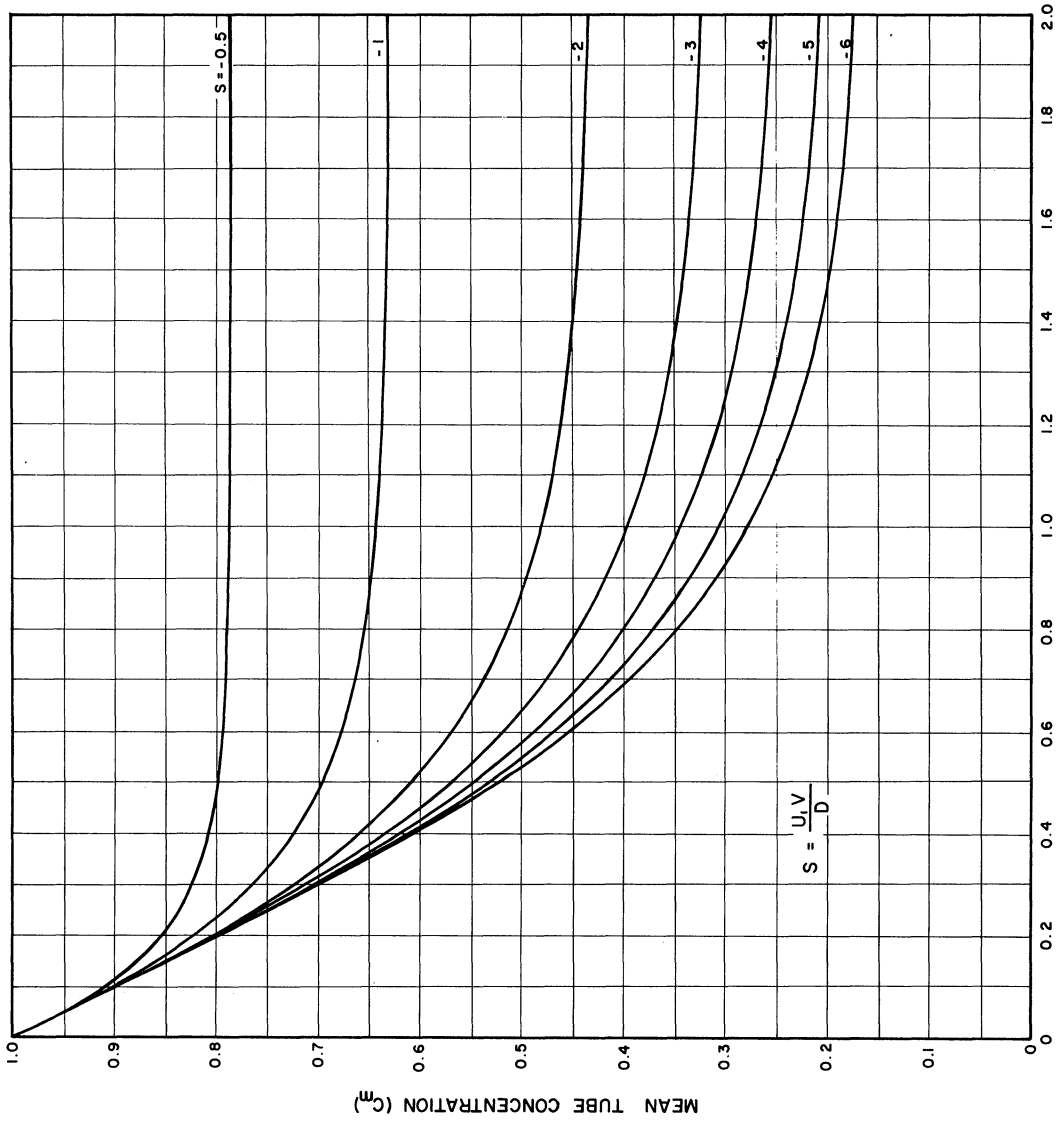

Figure 9. Mean Tube Concentration Versus Dimensionless Time

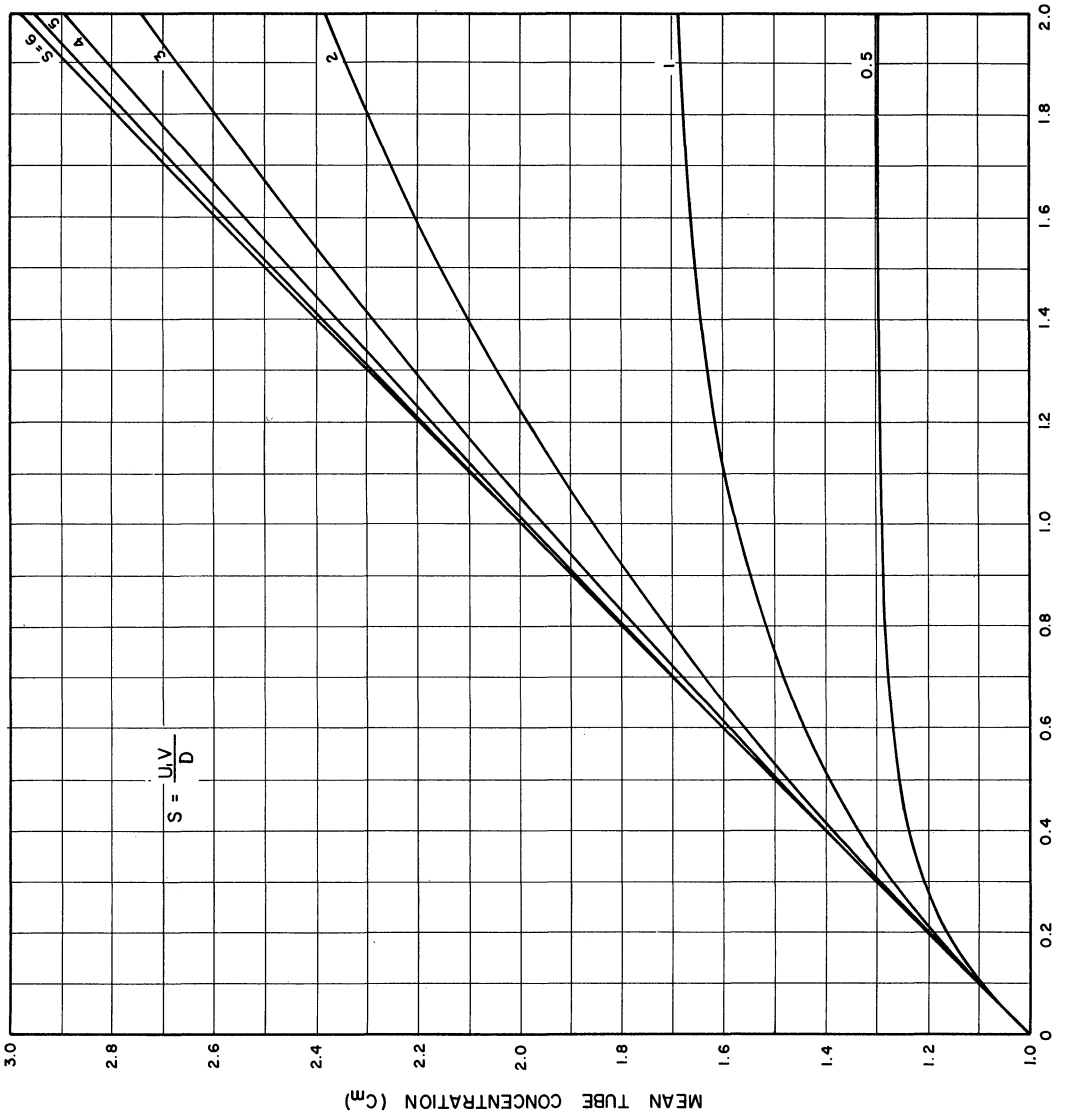

Figure 10. Mean Tube Concentration Versus Dimensionless Time

plus the difficulty of obtaining large electric field strengths in a highly conductive medium cause numerous experimental difficulties.

Mathematically, the effect of convection is to increase the apparent diffusion coefficient D. This lowers the magnitude of "s"; consequently, one must be content with smaller concentration changes in order to avoid back diffusion. This can easily be seen from Figures 6 and 7. To reduce convection one uses as small a capillary as possible. This gives a high surface to volume ratio. The viscous drag of the wall on the liquid metal reduces the convective mixing. The high surface to volume ratio also allows more efficient transfer of the I^2R heat generated within the capillary, which reduces the temperature rise in the tube. The total power generated is proportional to the square of the current while the field strength is only directly proportional. This means that the total I^2R heat developed is reduced by decreasing the capillary size while maintaining the same field strength. In addition, one should run the experiments so that when concentration gradients form, the least dense substance is on top. Any temperature gradients in the liquid metal must be such that the cooler metal is on the bottom. These procedures insure that all the density gradients in the liquid metal will be stable and will not cause convection.

C. Cu-Sn System

Experimental Procedure. The Cu-Sn system was the first system studied. The experimental apparatus is somewhat more primitive than in the later work. The diffusion cell is shown in Figure 11; the vacuum system in Figure 12. The constant temperature bath was a resistance

wound pot containing lead-bismuth eutectic alloy. The temperature in the bath was uniform within 1°C. The bath temperature was measured with an electrically insulated chromel-alumel thermocouple placed in the molten metal. The temperature of the alloy in the tube was a few degrees hotter than that of the bath due to the I^2R heating of the direct current. Heat transfer calculations show that this temperature rise will be no greater than 13°C. No attempt was made to measure the temperature in the tube directly. The temperature was maintained within $\pm$ 10°C during the time of the runs.

The first step in making a run was to place from 10 to 20 grams of a previously prepared Cu-Sn* alloy in the 10mm pyrex chamber of the diffusion cell. The diffusion cell was then evacuated to a pressure from 1 to 10 microns of mercury. This was sufficient to prevent oxidation of the alloy. The cell was then immersed in the liquid metal bath, which had previously been brought to the operating temperature. Evacuation was continued until outgassing had ceased and the pressure had returned to the above value. Helium gas was then bled into the cell until a positive absolute pressure of from 16 to 20 pounds per square inch was obtained. This procedure forced the liquid metal alloy into the capillary tubing. It made contact with the tungsten electrode at the lower end of the tube. The direct current was passed through the cell in such a manner that the lightest element, Cu, went up into the reservoir from the diffusion tube. This procedure insured that any density gradients that form are in a

* The Sn was Baker and Adamson 99.97% reagent grade shot. The Cu was Baker and Adamson 99.98% Cu shot.

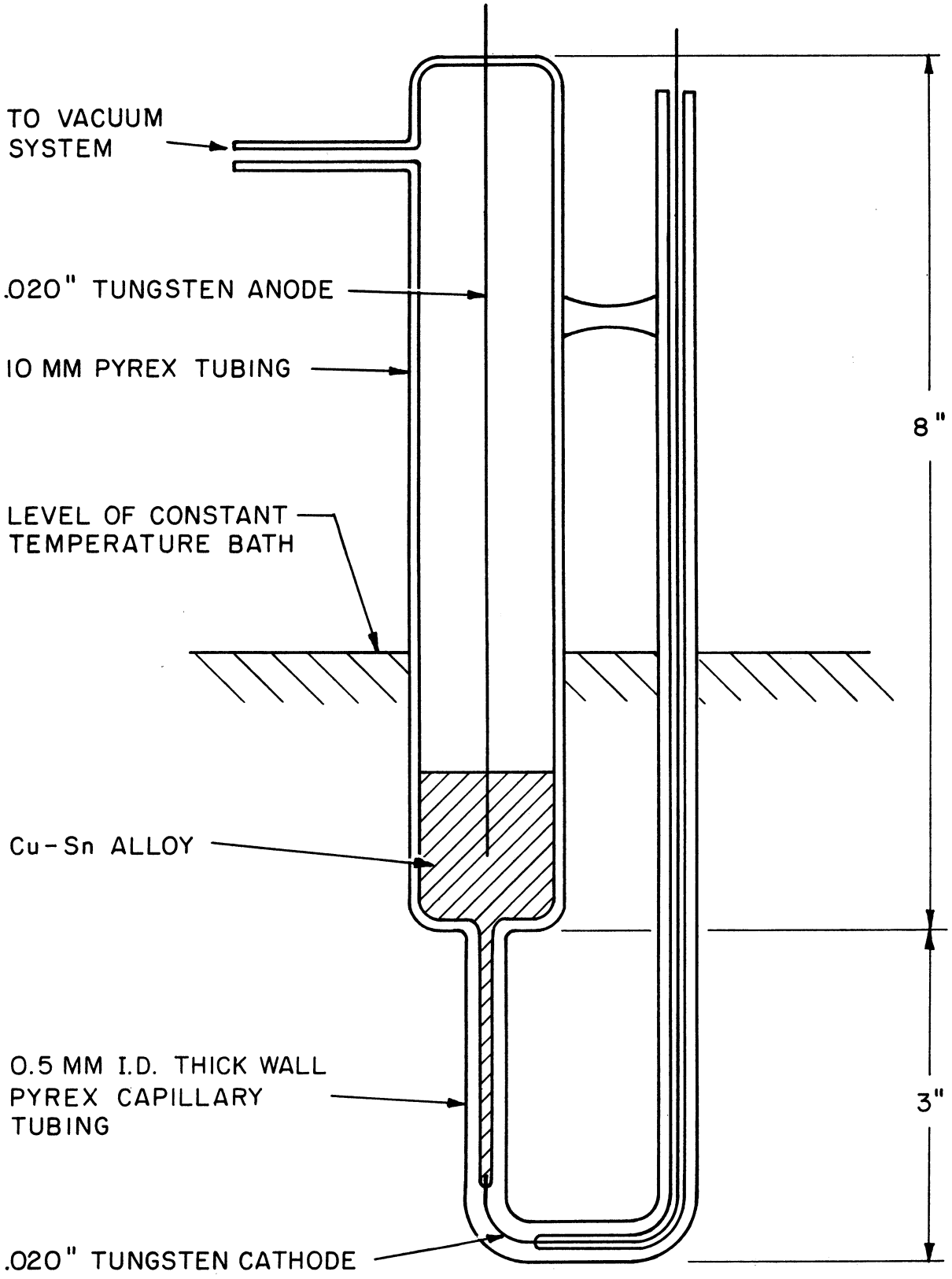

Figure 11. Diffusion Cell for Cu-Sn Runs

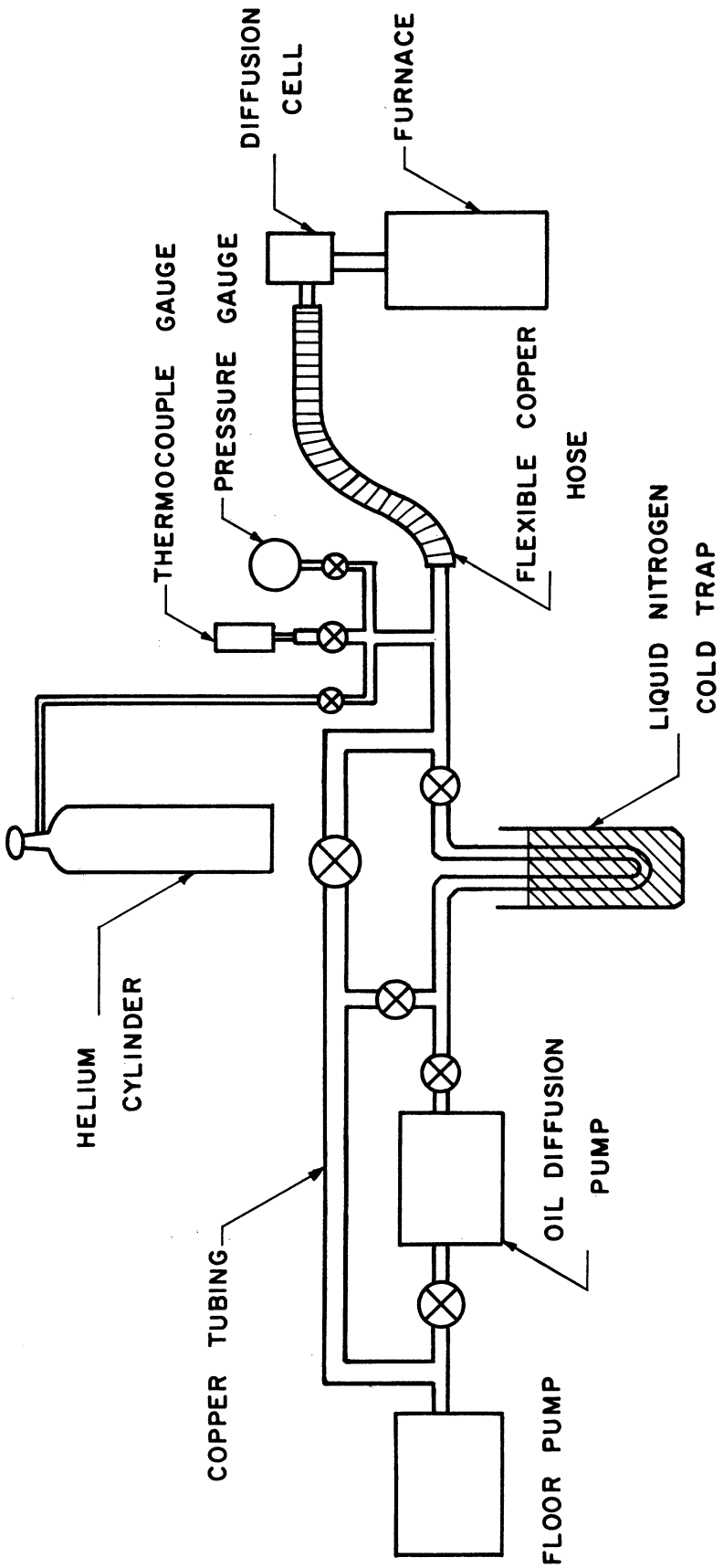

Figure 12. Vacuum System

direction that will not cause convection currents. For these experiments a Nobatron model E-28-10 power supply was used to supply the direct current. The ripple as measured on an oscilloscope was less than 1%.

After the current had been passed through the cell for the desired length of time, the cell was pulled up out of the bath. A blast of compressed air was played on the cell to hasten the cooling. This insured fast freezing of the alloy and minimized segregation. The capillary tubing was broken into four equal segments. The capillary segments and the reservoir were then chemically analyzed. See Appendix II-D for the analytical procedure.

Experimental Results on the Cu-Sn System. The experimental data are given in Table II. The tube segments were numbered consecutively starting with the cathode (the end of the capillary not connected to the reservoir). Run 2 failed after less than an hour and the segments were not analyzed. Run 9 was ruined during the analysis. The data for run 6, a blank run, and run 7 are presented graphically in Figures 13 and 14. It can be seen from Table II that in each run the Cu went to the anode. Run No. 6, the blank, shows the reverse trend, i.e., the concentration in the tube is higher than the reservoir concentration. This is undoubtedly due to the segregation. The first liquid alloy to freeze will be at the lower end of the diffusion tube. This will then be Cu rich, since Cu raises the liquidus line. (From Reference 21 the η phase of approximately 40 wt.% Cu is the first solid to precipitate from the alloys of greater than 0.7 wt% Cu.) Some of the runs, e.g., 1 and 3 show an increase in Cu concentration over that of the reservoir in the tube segment immediately adjacent to

TABLE II

Cu-Sn DATA

Run	Hours	°C	Amps.	Segment	Grams	Wt. % Cu
1	15	431	3.0	1	.04446	0.358
				2	.03530	0.411
				3	.03654	0.465
				4	.03283	0.488
				Res.	5.0968	0.429
3	48	427	3.5	1	.04376	0.242
				2	.03354	0.331
				3	.03834	0.446
				4	.03711	0.434
				Res.	6.4126	0.411
4	15	441	3.5	1	.06300	1.12
				2	.04084	1.30
				3	.04192	1.50
				4	.04050	1.49
				Res.	8.3829	1.46
5	15	427	3.5	1	.03451	1.10
				2	.03900	1.48
				3	.03946	1.53
				4	.03426	1.62
				Res.	8.1295	1.50
6	0	430	0	1	.03360	2.42
				2	.03643	2.36
				3	.03489	2.30
				4	.04335	2.13
				Res.	8.0773	2.00
7	48	427	3.0	1	.02799	0.96
				2	.03623	1.26
				3	.03746	1.70
				4	.04987	1.92
				Res.	6.0720	2.08
8	48	427	3.0	1	.05832	0.77
				2	.05697	0.93
				3	.05559	1.27
				4	.04450	1.56
				Res.	8.7300	1.47

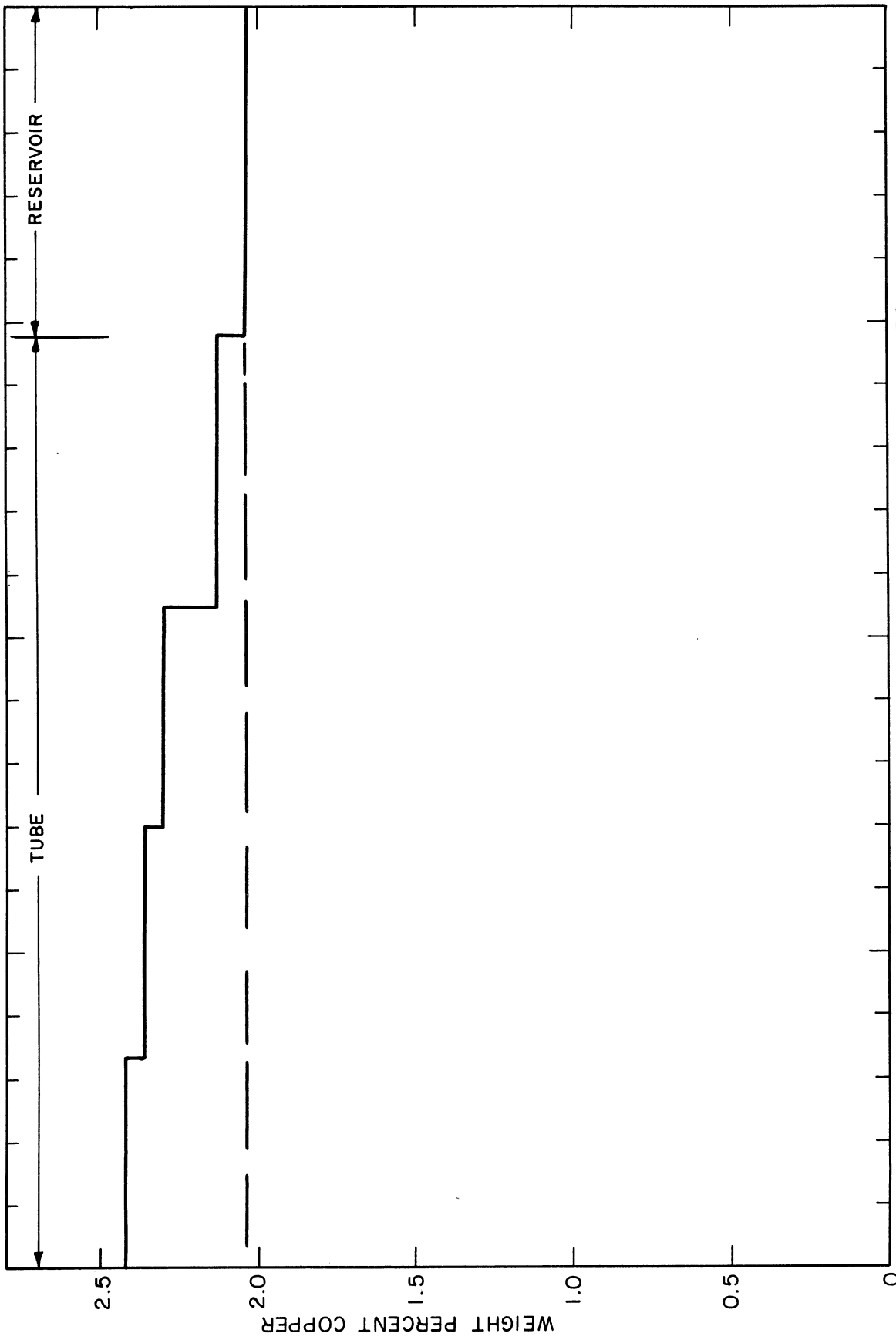

Figure 13. Cu-Sn Run No. 6, Blank, Dashed Line Shows Original Composition of Tube

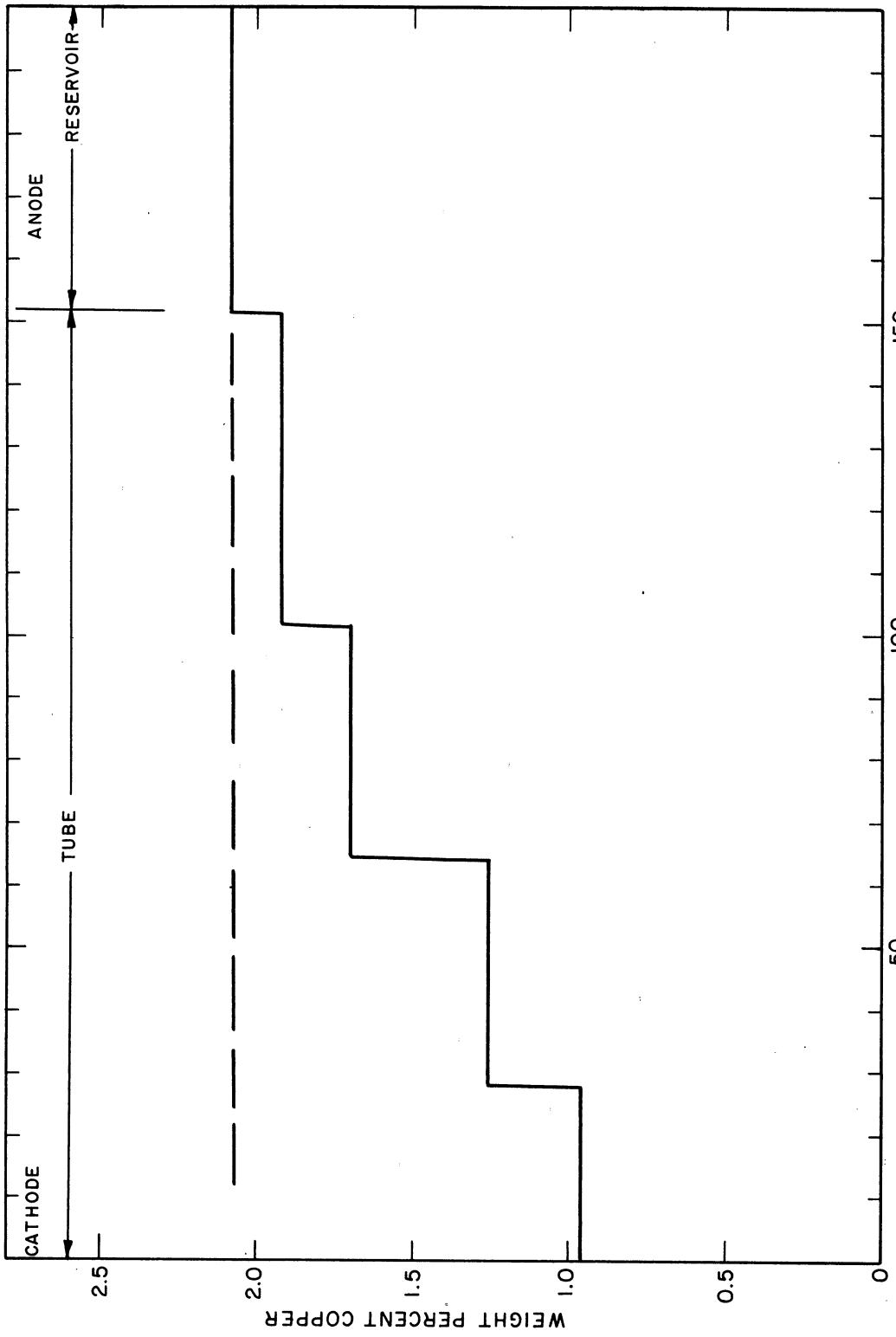

Figure 14. Cu-Sn Run No. 7, Dashed Line Shows Original Composition of Tube

the reservoir. This is also caused by segregation. Since the effect of the electric field works in the opposite direction of the segregation, there is no ambiguity in the interpretation of the results. Because of the segregation a quantitative measure of the mobility was not possible. Since one knows, however, that the segregation works against the effect of the electrical field, one can set a lower limit for the mobility from this data. This is 3.0×10^{-4} cm^2/sec volt. The reproducibility of these experiments may be checked by comparing runs 4 and 5.

Conclusions. The data is quite interesting from a qualitative standpoint. It shows that the Cu-Sn system is another one in which a reversal of migration direction takes place. This is on the basis of the data of Kreman and Gruber-Rehenburg[49] at 50 weight percent. In their work the Cu went to the cathode. No more conclusions can be drawn until it is determined exactly at which concentration this reversal of direction takes place. In this respect the data support conclusions of the resistivity increment correlation rather than the atomic mass correlation. However, this should be qualified by noting that once again the reversal follows the general rule noted earlier; in Cu rich alloys Cu goes to the cathode, while in Sn rich alloys the Sn goes to the cathode. The data of Roll and Motz[38] show that the liquid Cu-Sn resistivity isotherms have discontinuities at compositions corresponding to the intermetallic phases $Cu_{31}Sn_8$, Cu_3Sn, and Cu_8Sn_5.

D. Na-Hg System

Experimental Procedure. The experimental apparatus for the remainder of the experiments was modified in order to eliminate the segregation

that influenced the results on the Cu-Sn system. The diffusion cell is shown in Figure 15. The vacuum system shown in Figure 12 was used. The cell had three separate capillary tubes each with independent D.C. circuitry. This allowed three separate determinations of the mobility to be made from each experimental run. The cell was designed so that the capillary tubes could be moved vertically. At the completion of the run the capillary could be physically separated from the melt so that the alloy in the capillary did not solidify in contact with the reservoir, as in the case of the Bi alloys. Therefore segregation could not change the average capillary composition. It could, of course, influence the concentration distribution within the capillary, but this is of no consequence since only the average composition was used for calculating the mobility. The thin walls of the capillary tubes presented an additional advantage over the Cu-Sn apparatus. The temperature drop across the tube wall due to the transfer of I^2R heat out of the tube is smaller. The diameter of the tungsten electrode (.008") was chosen so that its temperature rise would be approximately the same as that of the capillary. If the electrode wire is too large it will remain cool and abstract heat from the capillary. This will cause a cold area at the top of the tube. The density gradient that is formed will be unstable and lead to convection. In the Cu-Sn apparatus the electrode was below the tube. Therefore a large (.020") wire was used since a cold spot at the bottom of the tube is stable.

The polarity of the capillary tubes was very carefully checked during all the runs. The polarity was determined by at least two laboratory D.C. voltmeters before each run. It was also determined at various times by the electrolysis of tap water.

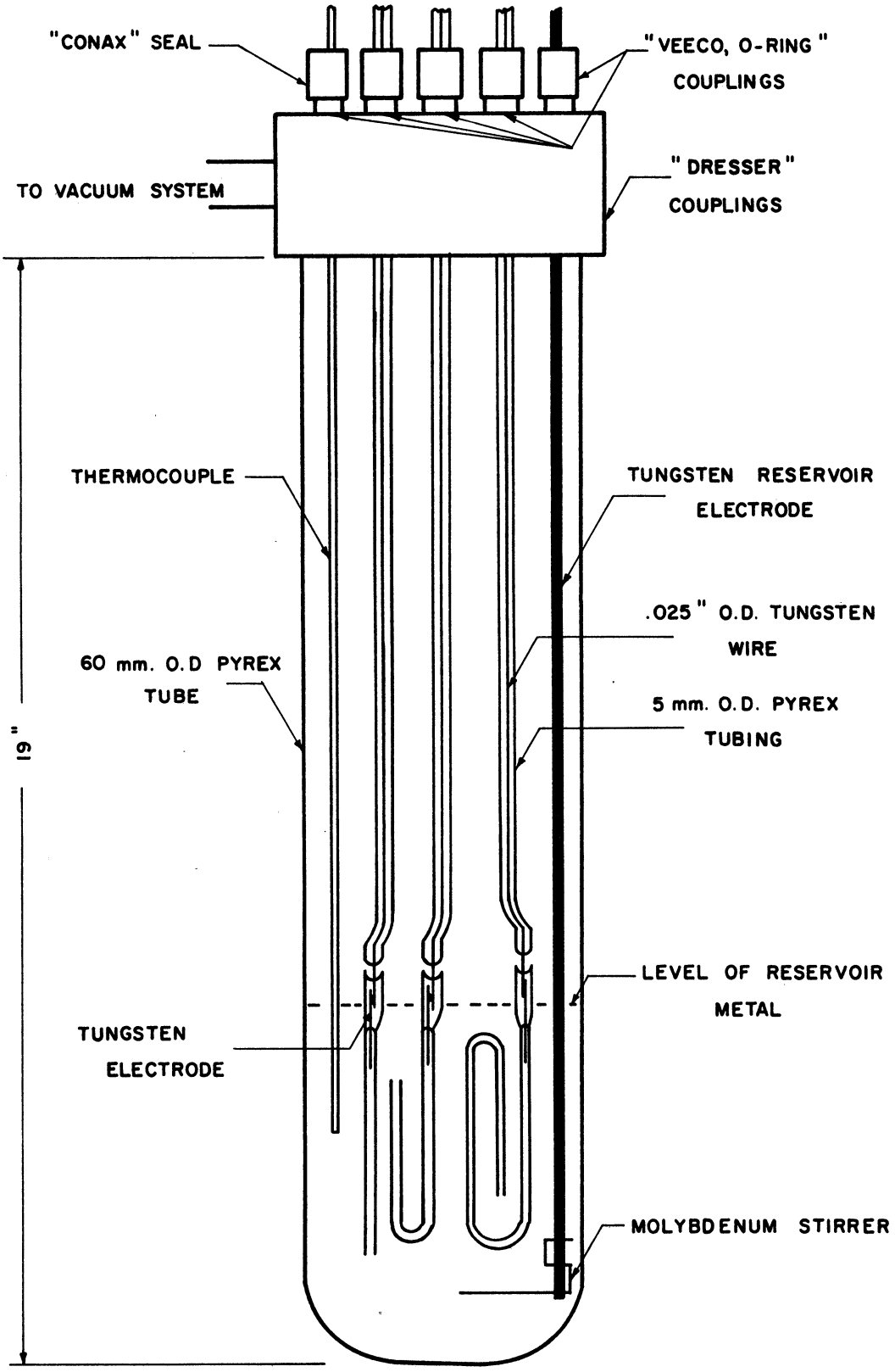

Figure 15. Diffusion Cell for Bi and Hg Systems
Showing the Three Types of Capillary Tubes

The heating of the runs was done with a 25" vertical "Hevi-Duty" tube furnace. Two types of temperature control were used. For some of the runs a Wheelco saturable core reactor was used, for others a Leeds and Northrup Micromax controller-recorder. The latter device controlled only about 1 ampere of the total heater current (normally 5 amperes). The temperature gradient in the reservoir was 0.8°C/cm; the top was hotter than the bottom.

A Nobatron rectifier model E-28-10 was used to supply the D.C. Its ripple was less than 1% as measured on an oscilloscope. Originally the direct current was measured with calibrated manganin shunts. In the latter stages of the work it became apparent that such accuracy was unwarranted. Ordinary uncalibrated ammeters were used for the remainder of the runs.

The Na amalgams* were made up in a dry box under thoroughly dried N_2. The procedure for making the amalgams and degassing them prior making a run is given in Appendix IV.

After the system was thoroughly degassed, the cell was cooled and re-evacuated. When a pressure of from 0.2 to 1.0 microns was obtained the tubes were lowered into the reservoir and He pressure applied. This procedure filled the tubes with the liquid metal. The cell and vacuum system were designed so that it would hold up to 45 psi absolute pressure. Running the experiments under positive pressure reduced the formation of bubbles within the tubes. These bubbles would grow large enough to form

* The Na metal was Mallinkrodt analytical reagent grade, 99.9% purity. The principal impurity is K. The Hg was from both Merck and Mallinckrodt, A.C.S. reagent grade.

an open circuit in the tube, ruining the run. (See Appendix IV). The temperature was raised to the desired level, and the direct current turned on through the tubes. After the desired length of time the current was turned off and the tubes raised from the reservoir.

Several extra tubes were attached to the run tube. These tubes were for the purpose of collecting samples of the reservoir alloy for analysis. This allowed the use of the same reservoir alloy for a number of runs. These blank tubes were identical to the run tubes and received exactly the same treatment throughout the experiment. The blank samples were approximately the same weight as the alloy in the run tubes. Three basic capillary shapes were utilized: straight, hairpin, and a double hairpin. They are shown in Figure 15. All runs after and including 27 had the double hairpin capillary; runs 1, 6, 23, 24, and 25 had hairpin capillaries. All of the remaining had straight capillaries.

Experimental Results on the Na-Hg System at Room Temperature and Test of the Accuracy of the Experimental Technique. The data from all of the completed Na-Hg runs are presented in Appendix II-A. The capillaries were given a number corresponding to the run and the capillary, i.e., A-19-1 signifies capillary tube 1 from amalgam run number 19. The rejection of certain data points for the Na-Hg and the Bi systems is explained in Appendix II-F.

The data taken at room temperature for the purpose of checking the absolute accuracy of the experimental technique are presented in Table III. In view of the standard deviations of the authors data, the excellent agreement of the average with Schwarz's value is certainly fortuitous. Clearly, however, the technique gives answers that are fundamentally correct.

The number of standard deviations in either direction from the mean necessary to give a confidence level of 95% was taken from Student's "t" distribution using n - 1 degrees of freedom, where n is the number of separate determinations of the mobility. It is necessary to use the "t" distribution rather than the normal distribution when the number of measurements is small, e.g., less than thirty. The "t" distribution corrects for the tendency of the calculated standard deviation to be too low when there are only a few samples.

TABLE III

ROOM TEMPERATURE Na-Hg DATA

Capillary	Observed Weight Percent Na	Temperature °C	Mobility x 10^4 cm^2/sec volt
A-1-1	.506	23	+1.52
A-3-2	.485	21	+1.19
A-28-1	.484	27	+1.19
A-28-3	.484	27	+0.95
A-31-1	.0976	35	+1.14
A-31-2	.0976	35	+1.40

Standard deviation of an individual measurement x 10^4	.202
Standard deviation of the average mobility x 10^4	.0902
Average mobility x 10^4 at the 95% confidence level	+ 1.23 $\pm$ .23
Mobility from Schwarz.[3]	1.19

For the purpose of calculating mobilities the resitivities reported by Müller[28] were used. The value 96.2 x 10^{-6} ohm-cm was used for the room temperature runs; at 334-342°C, 137 x 10^{-6} ohm-cm. The density of the amalgams was estimated from the density of pure Hg. The values used were 13.5 g/cm^3 at room temperature and 12.8 g/cm^3 at 334-342°C.

In Table III the data for the two different Na concentrations are treated together. There are two reasons for this. First, the two data points for the .0976 weight percent amalgam fall within the spread of the data at 0.5 weight percent Na. The scatter of the data is large enough so that no slight change in the mobility with concentration can be determined. Secondly, it has been shown by previous workers that the mobility is essentially constant up to a concentration of at least 1.0 weight percent Na.[2,3]

Experimental Results on the Na-Hg System at Elevated Temperatures. The data from the successful runs are shown in Table IV. The third and fourth columns give the original and final compositions of the capillary tube. The original composition is taken as the average of the blank tube analyses. The fifth column gives the percent confidence of the observed change in alloy composition. It was taken as 100 - P, where P is the percent chance that a blank tube from that particular run could have given an analysis as far from the mean as the capillary in question. Student's "t" distribution for n - 1 degrees of freedom was used, where n is the number of blank tubes used in the run.

The confidence level reported for the capillaries from run A-32 is the percentage chance that one blank tube of any three from that particular run would have an analysis as far from the mean as the tube through which current was passed. The low confidence levels reported for capillaries A-32-2 and A-32-3 do not mean that there is a large probability that the A.C. did affect the composition. For example two of the blank tubes from A-32 are as far from the mean composition of the blanks as capillary

TABLE IV

Na-Hg DATA

Capillary	Temp. °C	Original Wt. % Na	Final Wt. % Na	Confidence Level of Change, %	Capillary Polarity
A-1-1	23	.506	.534	95.5	+
A-3-1	21	.485	.503	85.0	+
A-3-2	21	.485	.528	92.0	+
A-19-1	26	.485	.464	99.2	-
A-19-2	26	.485	.469	98.5	-
A-19-3	26	.485	.433	99.7	-
A-28-1	27	.484	.539	> 99.9	+
A-28-3	27	.484	.520	> 99.9	+
A-31-1	35	.0976	.1058	> 99.9	+
A-31-2	35	.0976	.1028	99.5	+
A-31-3	35	.0976	.1132	> 99.9	+
A-32-1	35	.476	.477	> 99.9(a)	60 cycle A.C.
A-32-2	35	.476	.485	30.0(a)	60 cycle A.C.
A-32-3	35	.476	.487	45.0(a)	60 cycle A.C.
A-23-1	232	.486	.506	99.0	+
A-24-3	245	.474	.495	94.0	+
A-26-1	286	.488	.480	56.0(a)	+
A-25-1	342	.480	.439	> 99.9	+
A-27-1	344	.484	.538	> 99.9	-
A-27-2	343	.484	.532	> 99.9	-
A-27-3	344	.484	.512	> 99.9	-
A-29-1	338	.482	.514	99.6	-
A-29-2	338	.482	.521	99.7	-
A-30-1	334	.0968	.0897	99.5	+
A-30-2	334	.0968	.0934	98.0	+
A-30-3	334	.0968	.0929	98.5	+

(a) The confidence level is the percent chance that the observed composition came from the same population as the blank tubes.

A-32-2. For capillary A-26-1 the confidence level is the percent chance that the composition of any one blank tube lies as far from the mean as the capillary through which D.C. was passed.

From these data one can see that the predicted reversal of transference direction was indeed observed. The reversal is shown graphically in Figures 17 and 18. In Figure 17 the mobility is plotted versus temperature. The vertical bars indicate the spread between the maximum and minimum observed mobilities at that temperature. At 286°C, where no change was observed, the bar represents the estimated sensitivity of the measurements. One can see that somewhere around 290°C the mobility changes sign from plus to minus and then rapidly becomes more negative as the temperature is raised. A positive mobility means motion to the anode; negative, to the cathode. One must be cautious in attaching undue significance to the shape of the curve above 290°C since the magnitude of the mobility at 340° was estimated from only two of the capillaries listed in Table IX, i.e., A-25-1 and A-27-2. The other capillaries at that temperature were run for much longer periods of time and gave lower mobilities. Presumably this was caused by back diffusion.

In addition to the work on the 0.5 weight percent amalgams, experiments were done on an amalgam of .097 weight percent Na. Again the reversal of migration direction was found to occur. The data from Table IV and the data from Kremman's work, References 49 and 57, are shown in Figure 18. The sign (+ or -) within the marks indicates the direction of Na migration, i.e., a plus sign means that the Na migrates to the anode. A portion of the Na-Hg phase diagram[21] is also included.

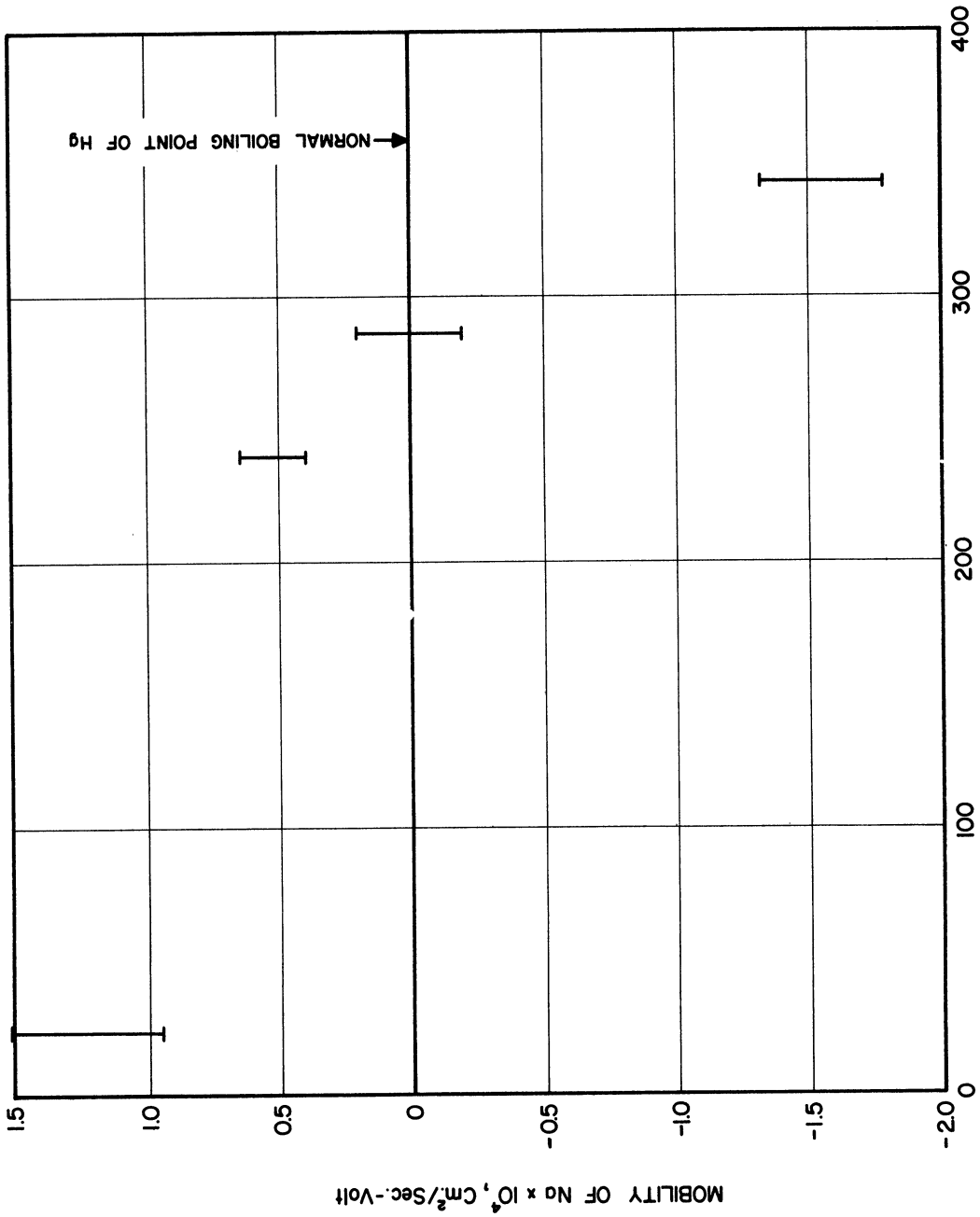

Figure 17. Mobility of Na in Hg versus Temperature

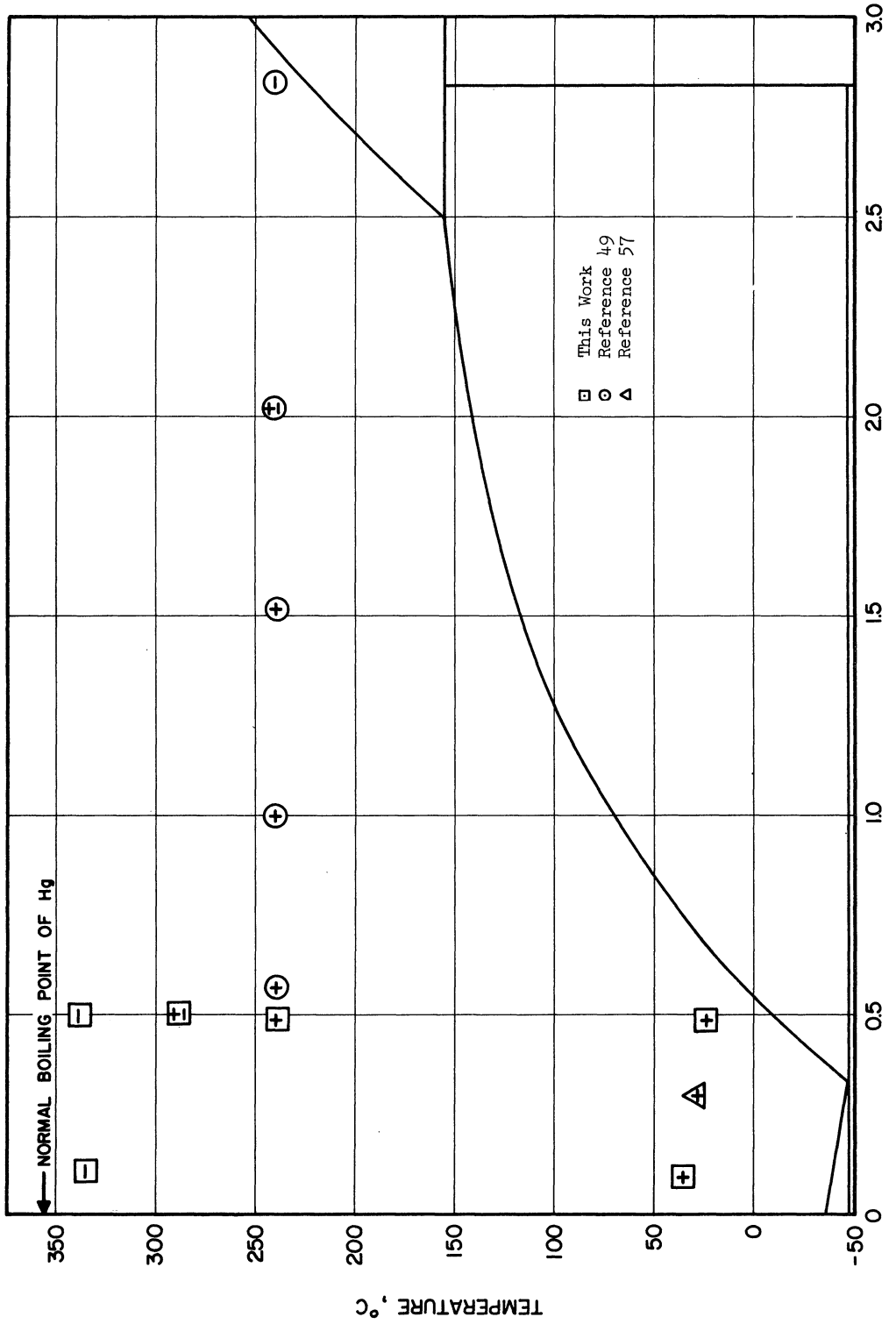

Figure 18. Direction of Transport of Na in Amalgams as a Function of Temperature and Composition.

In order to illustrate just how the original data looked, several examples are given in Appendix II-G.

Conclusions. Two important conclusions can be made based on the data on the Na-Hg system. First, the experimental technique developed by Mr. Verhoeven and the author gives mobilities of reasonable accuracy. This is concluded from the duplication of Schwarz's value of the mobility of Na in Hg at room temperature. It is important to note in this connection that the Na-Hg system is more difficult than many others. The mobility is fairly low, at least an order of magnitude lower than the highest one thus far determined. The concentration changes one observes are correspondingly much smaller than in other systems. Also, Na is present in almost any contaminant such as dust or dirt particles that may be introduced into the sample during the run or the analysis. Probably the worst offenders are small particles of Na_2O from the slight scum that forms on the amalgam during the run. Great care was taken in cleaning the tubes after the run and prior to analysis, but in one instance at least, tube A-1-1, this may have affected the results. Normally the total change in the amount of Na in the capillary tube was from 1/4 to 1/2 a milligram so any slight contamination would have a pronounced effect.

The second, and most important, conclusion is that at temperatures approaching the boiling point the Na concentrates at the cathode. This is very strong evidence supporting the hypothesis presented in Chapter III-B that the previously observed reversals with concentration are caused by some type of compound formation or association in the liquid alloy. There is a chance that the concentration at which a reversal occurs shifts to lower and lower Na compositions as the temperature is increased. At

340°C the reversal may still occur, but at a Na composition less than .097 weight percent Na. The author considers this rather unlikely. In the first place this concentration is less than .0075 atom fraction Na, well below the point where the first compound is formed -- $Na\text{-}Hg_4$ at .20 atom fraction Na. Secondly the plot of resistivity versus composition is smooth in the range from 0.0 to .03 atom fraction. There are no maxima, minima, or discontinuities. This indicates no unusual ordering effects in the liquid in this range.

E. Bi Systems

Experimental Procedure. The diffusion cell and capillary assembly for the Bi systems were essentially the same as for the Na-Hg system (Figure 15). The cell was made with two, rather than three, capillaries. This meant that it was possible to make two independent measurements of the mobility from each run. Weighed amounts of Bi and the alloying element* were placed in the large pyrex outer tube. The system was pumped down to about 10 microns of mercury pressure. The heating for these runs was provided by a 12" long "Hevi-Duty" tube furnace set in a vertical position about the outer pyrex tube. The cell was heated approximately two hours at about 50°C above the desired run temperature. Throughout this period the molten reservoir was agitated with the Mo stirrer attached to the thermocouple. This insured that the alloy composition was uniform and aided degassing. The temperature was then lowered to the desired

* The Bi was obtained from Belmont Smelting and Refining Works. It had a reported purity of 99.9986%. The alloying elements had the following purities: Cu, Baker and Adamson 99.98% shot; Mg, Dow Chemical Co. 99.98% vapor deposited; Zr, reactor grade, Hf free from Westinghouse; U, Mallinckrodt 99.97% reagent grade rod. The metals were used without further purification.

operating temperature. The capillary tubes were lowered into the reservoir and a positive absolute pressure of from 16 to 20 pounds per square inch of He was applied. This filled the tubes with the liquid alloy. After the D.C. was run for the desired length of time, the capillary tubes were raised out of the reservoir and the cell cooled.

Blank samples were taken of the reservoir exactly as with the Na-Hg system. These tubes underwent the same treatment as the run tubes. All of the samples were chemically analyzed and the mobility calculated from Equation (46).

The temperature was measured with a chromel-alumel couple placed in a type 430 stainless steel shield. This type of steel contains only Fe, C, and Cr. These elements are not soluble in liquid Bi. The temperature was controlled with a Leeds and Northrup Micromax controller recorder. The controller was an off-on type. It was wired so that it controlled only about 1 ampere of the total heater current (about 4 amperes). This procedure considerably reduced the oscillations about the operating temperature. The maximum temperature range throughout the course of the runs was normally $\pm$ 5 °C. The temperature of the reservoir metal was maintained hotter on the top than on the bottom in order to minimize convection. The gradient was about 0.7 °C per centimeter. The direct current was measured by calibrated manganin wire shunts. Manganin was used since its resistivity does not change measurably with changes in the ambient temperature. The shunts were calibrated with a Leeds and Northrup 0.1 ohm standard resistor. The current stayed constant within $\pm$ 1% in all of the runs. A Udylite rectifier model 2006-DU2 and the Nobatron model E-28-10

were used to supply the D.C. The output of the Udylite was filtered in a simple capacitance-inductance filter network so that its ripple was less than 2% as measured on an oscilloscope.

TABLE V

Cu-Bi DATA

Capillary	Observed Weight Percent Cu	Temperature °C	Mobility x 10^4 (a) cm^2/sec volt
30-1	.490	495	-1.50
30-2	.490	494	-1.45
33-2	.484	498	-1.86
37-1	.503	491	-1.75
37-2	.503	491	-1.41
38-1	.487	493	-2.08
38-2	.487	495	-2.22
48-1	.488	502	-2.32
48-2	.488	502	-2.02

Standard deviation of an individual measurement	.34
Standard deviation of the average mobility	.11
Average mobility at 95% confidence level	-1.85 $\pm$ .25

(a) A negative mobility means the Cu moves to the cathode.

Experimental Results on the Cu-Bi System. The raw d of the Cu-Bi runs are presented in Appendix II-B. Every run that was successfully completed is included. The capillaries were labeled by the number of the run and the number of the capillary. Thus, 33-1 signifies capillary 1 from run 33. The data that were used for the calculations of the mobility are presented in Table V and Figure 16. The reasons for throwing out certain of the data points are given for each such point in Appendix II-F. In Table V the second column is the initial observed (reservoir) composition of the alloy; it is the average composition obtained from

analysis of the blank tubes. The data in the Appendix along with the resistivity and density from another source[55] are sufficient for the calculation of the mobility. The values of resistivity and density for pure B_i were used. If these constants are measured in the future for these alloys, enough data is given in the tables so that the mobility may be recalculated. A positive mobility means motion of the solute to the anode, a negative mobility means motion to the cathode.

Of the nine samples used for the calculation of the average mobility, sample 30-1 of run 30 is most likely to have back diffusion errors. It has the shortest tube length and lowest current density, hence the lowest value of "s". It also was run for a relatively long time. Comparing the mobility from this tube with the mobility from the other tube of the same run, which was run for a much shorter time, one finds that they are essentially equal. The conclusion is then that there is no back diffusion. Both tubes from run 48 were not straight, but rather bent back upon themselves in the shape of a hairpin as shown in the center capillary in Figure 15. This should further limit convection if it occurs. While these tubes give mobilities somewhat higher than the average, this difference is not statistically significant. Run 38 (straight tubes) gave essentially the same mobilities as run 48. From this it is concluded that the shape of the capillary tube has no significant effect on the results. The two tubes from an individual run tended to give mobilities very close to one another. Note especially runs 30, 38, and 48. The agreement between the tubes of different runs was not nearly as good. No explanation of this is apparent to the author.

Experimental Results on the Mg-Bi System. The raw data for the Mg runs are presented in Appendix II-C. The results of the experiments are summarized in Table VI and Figure 16. Despite the scatter in the data it is obvious that the mobility of Mg in Bi is considerably greater than that of Cu. This difference is even more significant when one realizes that the Mg experiments were conducted at a temperature 150°C lower than the Cu experiments. The Mg reacted with the pyrex diffusion cell leaving a black deposit on the glass surfaces. This may be a source of some of the scatter, although the blank analyses were in all cases very close to the weighed-in value. It was necessary to perform the Mg runs at lower temperatures and concentrations than the Cu runs to alleviate the problem of reactivity. Run 44 was performed with a hairpin shaped capillary. For this run both of the mobilities are somewhat lower than the average, but do not differ by a significant amount. This lends further support to the conclusion that convection or the shape of the capillary are not influencing the results.

Experimental Results on the Zr-Bi System. Only three separate successful determinations of the mobility of Zr were performed. The data are summarized in Table VII. The raw data are given in Appendix II-D. It was difficult to get enough Zr in solution so that an accurate chemical analysis could be made. In addition, reactivity problems were encountered. For these reasons work was discontinued on this system after the direction of motion and a rough idea of the magnitude of the mobility were determined. The extremely poor confidence limits reported in Table VII for the mobility of Zr primarily reflect the fact that only three

determinations were made. One can say, however, that the value is roughly similar to that of Cu, and probably somewhat higher.

Experimental Results on the U-Bi System. Six runs were completed on the U-Bi system of which four are suitable for calculating a mobility. These runs are summarized in Table VIII. The same difficulties that interfered with the Zr experiments also were present in U-Bi system: namely, getting enough solute in solution for analysis and the reactivity of the alloy. The results, however, are better than those for Zr. With so few runs the agreement between them may be fortuitous. The average mobility was computed using all four of the good runs despite the fact that they were at different compositions and temperatures. The accuracy of the data is such that this is warranted.

Analytical Errors. The analytical procedures are given in Appendix III. The absolute accuracy of the analytical procedures may be estimated from Table IX. In columns 2 through 4 the number of blanks, the weighed-in reservoir concentration, observed concentration, and standard deviation of an individual determination of the concentration are given. For Cu and Mg the weighed-in and observed concentrations are very close to one another. For Zr and U the observed concentrations are considerably lower than those weighed-in. This is presumably caused by oxidation of the solute metal before it dissolved. A scum of oxide formed on the surface of the molten reservoir alloy during the time these solutes were dissolving. The effect is especially pronounced for Zr since it was present in such a small amount. This oxidation has no effect on the final results because the actual (observed) reservoir composition is used in the calculation of the mobility.

TABLE VI

Mg-Bi DATA

Capillary	Observed Weight Percent Mg	Temperature °C	Mobility x 10^4 [a] cm^2/sec volt
32-1	.503	348	-6.96
32-2	.503	352	-6.92
36-1	.500	343	-4.00
36-2	.500	343	-5.32
41-1	.530	344	-5.78
41-2	.530	344	-7.10
44-1	.494	344	-5.12
44-2	.494	344	-4.61

Standard deviation of an individual measurement	1.21
Standard deviation of the average mobility	.41
Average mobility x 10^4 at the 95% confidence level	5.78 $\pm$ .98

(a) A negative mobility means the Mg moves to the cathode.

TABLE VII

Zr-Bi DATA

Capillary	Observed Weight Percent Zr	Temperature °C	Mobility x 10^4 [a] cm^2/sec volt
U2-1	.0567	510	+1.43
U2-2	.0567	510	+3.14
U2-3	.0567	510	+3.25

Standard deviation of an individual measurement	1.02
Standard deviation of the average mobility	.59
Average mobility x 10^4 at 95% confidence level	+2.61 $\pm$ 2.54

(a) A positive mobility means the Zr moves to the anode.

TABLE VIII

U-Bi DATA

Capillary	Observed Weight Percent U	Temperature °C	Mobility x 10^4 [(a)] cm^2/sec volt
U-1-1	.310	510	+2.43
U-1-5	.310	510	+3.20
CB-1-1	.144	445	+2.31
CB-1-6	.144	445	+2.36

Standard deviation of an individual measurement	.42
Standard deviation of the average mobility	.21
Average mobility x 10^4 at 95% confidence level	$2.57 \pm .67$

(a) A positive mobility means the U moves towards the anode.

It is of interest to determine to what extent analytical errors influenced the uncertainty of the average mobility. Knowing the percentage composition change in the capillary, one can determine the error magnification factor from Figure 8. The standard deviation of an individual analysis is given in the last column of Table IX. It was computed by multiplying the standard deviation of the analysis times the factor from Figure 8 times the ratio of the average mobility to the average intial composition.

The estimated standard deviations of the mobility from analytical errors along--last column, Table IX--should be compared to the actual standard deviations of an individual determination of the mobility. It is evident that the analytical errors are a significant portion of the total scatter. In fact, for the Mg and U systems, it appears that most of the scatter can be attributed to analytical uncertainties. This

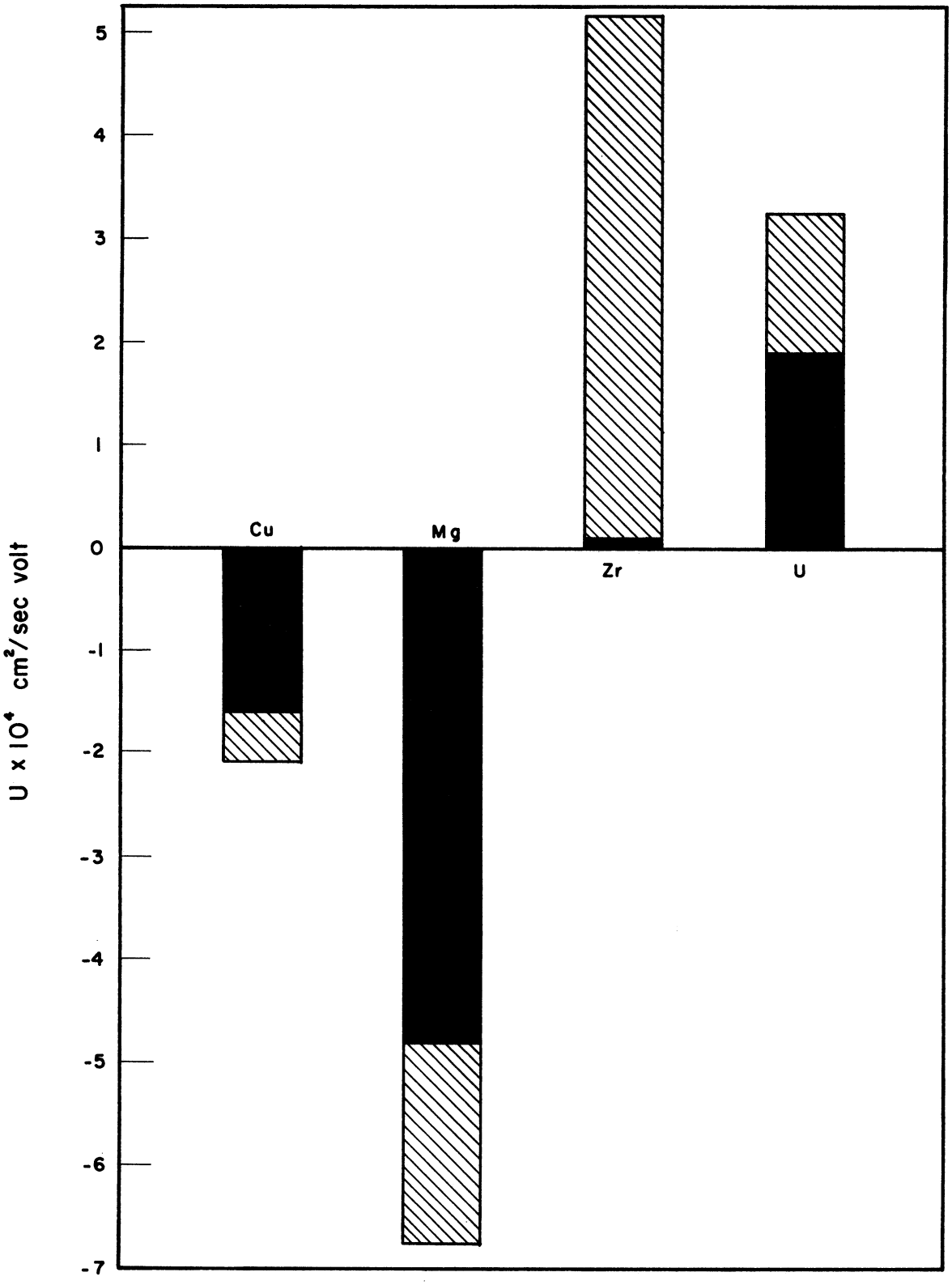

Figure 16. Mobilities in Bismuth, Showing Uncertainty at 95 Percent Confidence Level

TABLE IX

ANALYTICAL UNCERTAINTIES

Capillary	No. of Blanks	Weighed-in Composition	Observed Composition	Standard Deviation of Obs. Comp.	Percent Change of Cap. Comp.	Factor from Fig. 9	Standard Deviation of U x 10^4
30-1	4	.498 Cu	.490	.004	13.5	8.5	.126
30-2	4	.498	.490	.004	5.3	20.0	.296
33-2	4	.498	.484	.013	13.9	8.3	.400
37-1	8	.498	.503	.012	50.9	2.0	.088
37-2	8	.499	.503	.012	69.0	1.5	.066
38-1	7	.499	.487	.013	138.0	1.0	.048
38-2	7	.499	.487	.013	233.0	1.0	.048
48-1	8	.498	.488	.003	31.4	3.3	.036
48-2	8	.498	.488	.003	33.0	3.2	.035
32-1	5	.500 Mg	.503	.005	24.5	4.5	.26
32-2	5	.500	.503	.005	10.9	10.5	.61
36-1	6	.500	.500	.010	13.2	8.6	.99
36-2	6	.500	.500	.010	24.8	4.4	.51
41-1	6	.496	.530	.028	30.9	3.3	1.07
41-2	6	.496	.530	.028	57.0	1.8	.58
44-1	8	.496	.494	.014	24.9	4.4	.71
44-2	8	.496	.494	.014	33.9	3.2	.52
U-2-1	3	.0716 Zr	.0567	.0012	10.2	11.0	.61
U-2-2	3	.0716	.0567	.0012	34.4	3.1	.17
U-2-3	3	.0716	.0567	.0012	41.9	2.4	.13
U-1-1	3	.353 U	.310	.004	11.3	10.0	.33
U-1-5	3	.353	.310	.004	30.0	3.6	.12
CB-1-1	6	.184	.144	.006	20.8	5.1	.55
CB-1-6	6	.184	.144	.006	16.7	6.9	.74

points up the need for precise analytical methods and for experiments designed to obtain the maximum degree of concentration change in the capillary without introducing back diffusion. The latter may be realized by using much longer tubes with greater current densities.

Conclusions Based on Bi Data. Three conclusions can be made. First, there is further justification for the conclusion previously made that mobilities may be measured by the technique described in Reference 50. The present accuracy is only fair but can be significantly improved by modifying the procedure. Secondly, mobilities of solute atoms in molten Bi from 350°C to 500°C are the same order of magnitude as those in mercury at room temperature. This is consistent with the fact that diffusion coefficients in various liquid metals are approximately the same. Thirdly, three out of the four systems obey the mass correlations, i.e., the element with the smallest atomic weight moves towards the cathode. However, work done by Mr. John Verhoeven on Pd and Ni in Bi shows that both of these elements concentrate at the anode. The conclusion must be drawn that the atomic mass correlation is not as universal as it originally appeared. This conclusion may be qualified somewhat by the realization that Bi is a very unusual metal in many respects, e.g., it expands upon freezing, its resistivity is lower above the melting point than below, etc. Perhaps it is not surprising that the correlation is less satisfactory in bismuth systems. Another interesting fact comes to light as one also considers the previous data on Bi systems. The group I-B metals, Ag, Au, and Cu all go to the cathode; the group IV-A metals, Pb and Sn, also go to the cathode. The only ones to go to the anode, in

opposition to the correlation, are the transition metals, Fe (Reference 56) Zr, Ni, and Pd. With the exception of the Fe-C system, the above four systems are the only ones in which the transition elements have ever been studied. They may present a special case because of their small number of free electron.

Calculation of Diffusion Coefficient of Cu in Bi. In Chapter IV-B the possibility of determining diffusion coefficients from electrodiffusion experiments was discussed. The method was applied to runs 45 and 46 and capillary 33-1. The following diffusion coefficients were calculated: for tube 33-1, 6.5 x $10^{-5}cm^2/sec$; 45-1, 37 x $10^{-5}cm^2/sec$; 45-2, 22 x $10^{-5}cm^2/sec$; 46-1, 19 x $10^{-5}cm^2/sec$; 46-2, 17 x $10^{-5}cm^2/sec$. Data on similar systems would indicate that a D of about 5 x 10^{-5} should be expected. The large scatter and the high values given above indicate that convection probably affected the results. This given further support when one recognizes that runs 45 and 46 were ones in which the Cu was run out of the tube, creating an unstable density gradient. In tube 33-1 the solute was run into the tube. There is not enough data to state with any certainty that the higher values of the diffusion coefficients from runs 45 and 46 are actually caused by this effect, although this interpretation is plausible. Another source of convection may be the thermal gradients associated with the transfer of the joule heat from the capillary.

The electrodiffusion experiments were not designed with the intention of determining diffusion coefficients. The above results are presented solely to demonstrate that the method does give answers of approximately the correct order of magnitude. These results illustrate another application of the solution to the differential equation: namely, to determine if, and to what extent, convection does occur.

CHAPTER V

SUMMARY OF CONCLUSIONS

The most important result of this work was the work done on the Na-Hg system. Finding the predicted reversal of migration direction of Na in Hg at high temperatures lends strong support, not only to the reality of the atomic mass correlation, but also to the interpretation that the reversals of migration direction are caused by compounds or associations in the liquid metal. Very little can be said about the exact nature of these associations except that they appear to occur at compositions close to those where there are strong compound forming tendencies in the solid phase, and that they appear to break down at higher temperatures. The results are in agreement with many earlier works that also indicate compounds in the liquid state, e.g., resistivity measurements, thermodynamic data, and viscosity data.

By making important assumptions about the nature of the atom movements and the effect of electron friction, an equation is developed which gives a qualitative explanation of the empirically observed correlation. The proposed mechanism suggests that small, light, highly charged species should migrate to the cathode and that large, heavy, lightly charged species should move to the anode. This is in agreement with most of the observations.

The data on Cu-Bi, Mg-Bi, Zr-Bi, and U-Bi systems indicate that the mobilities of solute atoms in liquid Bi at 350 to 500°C are the same order of magnitude as the mobilities of solute atoms in Hg at room temperature. This behaviour is to be expected since the closely

related transport property, the ordinary diffusion coefficient, does not change remarkably from system to system when the measurements are made at approximately the same ΔT over the liquidus.

The data on the Bi systems and the Cu-Sn system also indicate that the atomic mass correlation is not quite as general as was originally believed. Several of these systems do not exhibit the predicted migration directions. The Cu-Sn system follows the resistivity increment correlation of another investigator. There are reasons to believe that these anomolous systems may be special cases.

A method of measuring mobilities at relatively high temperatures was developed with Mr. John Verhoeven as an integral part of the dissertation. The partial differential equation describing the diffusional processes was used to interpret the results of the experiments. The validity of the experimental technique was determined by duplicating the previously reported mobility of Na in Hg at room temperature.

APPENDIX I

PREVIOUS DATA

A. SUMMARY OF PREVIOUS ELECTRODIFFUSION EXPERIMENTS ON BINARY SYSTEMS[a]

Alloy	Temperature °C	Concentration wt %	Component migrating to cathode[b]
Ag-Al	900	50-80 Al	Al
Ag-Bi		30 Ag	Ag
Ag-Pb	1000	50	Ag
Ag-Sb			Ag
Ag-Sn		16 Ag	Ag
Al-Cu	1050	50	neither*
Al-Sn	800-1600		Al
Al-Au	700	9 Au	Al
Au-Bi	680	50	Au
Au-Pb	450	50	Au
Au-Sb	400	50	Au*
Bi-Cd		25-75	Cd
Bi-Pb	240-400		Pb
Bi-Sn	200,300	25-88	Sn
C -Fe	1000	2.5C	C
Ca-Hg	280	2 Ca	Ca
Cd-Hg	300	50	Cd
Cd-Pb	300		Cd
Cd-Sn	300	25-75	Cd
Cu-Sn	1000	50	Cu
Fe-P	1400	11 P	neither*
Hg-Li			Li
Na-Pb	370		Na(?)
Pb-Sn	350		Sn
Sb-Zn	500		Zn
Sn-Zn	400	50	Zn

(a) Data taken from Reference 2, page 34 except for the C-Fe system which came from Reference 13.

(b) Systems not correctly predicted by the atomic mass correlation are marked with an asterisk.

B. SUMMARY OF PREVIOUS ELECTRODIFFUSION EXPERIMENTS ON TERNARY SYSTEMS[a]

Alloy	Temperature °C	Concentration wt. %	Components migrating to cathode[b]
Be-Fe-Cu	1050	10 Be	Be, (Fe?)
Cu-Ag-Sn	1000		Cu, Ag
Cu-Sn-Bi	1000		Cu
Cu-Sn-Pb	1000	1 Pb	Cu
Cu-Zn-Pb	1000		Cu, Zn
Fe-Al-Sn	660		Fe, (Al?)
Na-Sn-Hg	240	1-5 Sn, 40 Na	Na, Sn

(a) All data taken from Reference 2, page 34.

(b) All systems correctly predicted by atomic mass correlation.

APPENDIX II

TABLES OF RAW DATA

A. Na-Hg RAW DATA

Capillary	Wt.%Na	Temp. °C	D.C. Amps[a]	Cap. I.D. cm.	Cap. Length cm.	Time Hours	Final Wt.% Na	Wt.of Cap. Metal, g.	$Ux10^4$ [b] $cm^2/sec\ volt$	Notes
A-1-1	.506	23 ± 1	+0.480	.05	7.6	48.0	0.534	0.2957	+1.52	Hairpin shaped capillary
A-3-1	.485	21 ± 1	+ .505	.05	3.8	24.2	.503	.1272	+ .864	
A-3-2	.485	21 ± 1	+ .476	.05	3.8	48.1	.528	.1443	+1.19	
A-6-2	.487	310 ± 1	+ .475	.05	3.8	7.7	.432	.1098		Hairpin shaped capillary
A-6-3	.487	310 ± 1	+ .445	.05	3.8	7.7	.491	.1043		
A-7-1	.487	337 ± 1	+ .785	.10	4.6	24.0	.479	.3668		
A-7-2	.487	337 ± 1	+ .747	.10	4.6	24.0	.474	.2888		
A-9-2	.487	340 ± 6	+1.03	.10	2.3	19.1	.474	.2312		Time is ± 0.3 hours
A-11-2	.509	334 ± 4	+ .524	.05	3.8	13.5	.354	.1457		Time is ± 3.5 hours
A-11-3	.509	334 ± 4	+1.02	.05	3.8	17.25	.355	.1658		
A-15-1	.505	336 ± 6	-2.0	.10	2.0	15.3	.306	.1315		Analysis obviously in error
A-15-2	.505	336 ± 6	-2.0	.10	2.0	15.3	.516	.1364		
A-15-3	.505	336 ± 6	-2.0	.10	2.0	9.3	.519	.1377		
A-17-1	.476	336 ± 4	-1.60	.10	3.8	22.75	.517	.2337		Time ± 0.5 hours
A-17-2	.476	336 ± 4	-1.74	.10	3.8	30.0	.474	.1816		
A-17-3	.476	336 ± 4	-1.70	.10	3.8	30.0	.489	.3344		
A-18-1	.487	239 ± 3	+2.01	.10	4.4	36.0	.488	.4316		
A-18-3	.487	239 ± 3	+1.93	.10	4.4	36.0	.490	.4572		
A-19-1	.485	26 ± 1	-1.99	.06	3.8	24.1	.464	.2151	+ .404	
A-19-2	.485	26 ± 1	-2.00	.06	3.8	24.1	.469	.1875	+ .274	
A-19-3	.485	26 ± 1	-1.96	.06	3.8	24.1	.433	.1885	+ .914	
A-20-1	.519	238 ± 2	+1.97	.06	3.8	50.1	.524	.1220		
A-20-2	.519	238 ± 2	+2.00	.06	3.8	50.1	.544	.0952		
A-20-3	.519	238 ± 2	+1.91	.06	3.8	50.1	.538	.0831		
A-22-1	1.49	240 ± 3	+1.99	.05	7.6	18.2	1.527	.1405		
A-22-2	1.49	240 ± 3	+2.02	.05	7.6	26.6	1.413	.1315		Time is ± 2 hours
A-22-3	1.49	240 ± 3	+1.89	.05	7.6	53.7	1.568	.1385		
A-23-1	.486	232 ± 3	+4.0	.075	15.2	27.0	.506	.9335		Hairpin shaped capillary
A-24-3	.474	245 ± 3	+3.4	.075	15.2	59.0	.495	.9814		Hairpin shaped capillary
A-25-1	.480	342 ± 4	+3.75	.075	15.2	19.0	.439	.9398	-1.79	Hairpin shaped capillary
A-26-1	.488	286 ± 2	+2.48	.075	15.2	49.75	.480	.8338		Time ± 1.75 hours
A-27-1	.484	344 ± 2	-3.09	.075	15.2	52.0	.538	.8643		Temperature at 265°C for 8 hours
A-27-2	.484	343 ± 2	-3.40	.075	15.2	31.0	.532	.8803	-1.32	
A-27-3	.484	344 ± 2	-2.53	.075	15.2	52.0	.512	1.2730		Temperature at 265°C for 8 hours
A-28-1	.484	27 ± 1	+3.95	.075	15.2	51.9	.539	1.0039	+1.19	
A-28-3	.484	27 ± 1	+3.85	.075	15.2	34.9	.520	.8044	+0.950	
A-29-1	.482	338 ± 6	-2.42	.075	15.2	48.8	.514	.8731	- .779	
A-29-2	.482	338 ± 6	-2.80	.075	15.2	48.8	.521	.8783	- .820	
A-30-1	.0968	334 ± 2	+2.44	.075	15.2	30.5	.0897	.8269	-1.30	
A-30-2	.0968	334 ± 2	+3.22	.075	15.2	30.5	.0934	.9398		
A-30-3	.0968	334 ± 2	+2.95	.075	15.2	30.5	.0929	1.0332		
A-31-1	.0976	35 ± 1	+3.22	.075	15.2	39.0	.1058	.7974	+1.14	
A-31-2	.0976	35 ± 1	+3.38	.075	15.2	19.8	.1025	.8836	+1.41	
A-31-3	.0976	35 ± 1	+3.15	.075	15.2	62.7	.1132	.8024	+1.40	
A-32-1	.476	36 ± 1	±3.17[c]	.075	15.2	45.0	.477	.9645		
A-32-2	.476	36 ± 1	±3.31[c]	.075	15.2	45.0	.485	.9707		
A-32-3	.476	36 ± 1	±2.97[c]	.075	15.2	45.0	.487	.9687		

a) The sign (+ or -) in front of the number of amperes indicates the polarity of the capillary tubes.

b) A positive mobility indicates the solute migrates to the anode, a negative mobility means motion to the cathode. The following values of the resistivity and density of the amalgams were used to calculate the mobility: at 21-35°C, $d = 13.5\ g/cm^3$, $\rho = 96.2 \times 10^{-6}$ ohm-cm; at 334-342°C, $d = 12.8\ g/cm^3$, $\rho = 137 \times 10^{-6}$ ohm-cm.

c) Sixty cycle alternating current was used for run A-32.

B. Cu-Bi RAW DATA

Capillary	Wt.%Cu	Temp. °C	D.C. Amps [a]	Cap. I.D. cm.	Cap. Length cm.	Time Hours	Final Wt.% Cu	Wt. of Cap. Metal, g.	Uxlo^4 [b] cm^2/sec volt	Notes
21	0.484	501 ± 8	+ 0.498	0.05	3.8	24.0	0.432	.0812	-1.48	The alloy was not stirred
23	.545	515 ± 4	+ .501	.05	3.8	48.0	.438	.0714	-1.17	"
25-1	.484	500 ± 2	+ .564	.05	3.8	47.7	.413	.0803	- .89	D.C. circuitry incorrect.
25-2	.484	500 ± 2	+ .497	.05	3.8	18.0	.396	.0579	-2.53	The D.C. amperes are not
26-1	.484	500 ± 4	- .565	.05	3.8	48.0	.522	.1246	- .88	certain.
26-2	.484	500 ± 3	- .498	.05	3.8	18.0	.527	.1062	-2.16	"
30-1	.490	495 ± 2	- 1.02	.05	3.8	24.0	.556	.1332	-1.50	
30-2	.490	494 ± 1	- .985	.05	3.8	9.0	.516	.1167	-1.45	
33-1	.484	498 ± 9	- 2.02	.10	4.1	48.1	.568	.2839	-1.04	The temperature dropped
33-2	.484	498 ± 9	- 2.01	.10	4.0	24.0	.551	.3184	-1.86	to 434°C for one half hour
37-1	.503	491 ± 3	- 2.09	.05	3.8	18.0	.759	.0635	-1.75	
37-2	.503	491 ± 3	- 2.08	.05	3.8	24.0	.850	.0500	-1.41	
38-1	.487	493 ± 6	- 2.06	.05	3.8	25.1	1.158	.0385	-2.08	The time is ± 0.3 hours
38-2	.487	495 ± 8	- 2.05	.05	3.8	36.0	1.625	.0344	-2.22	
45-1	.467	500 ± 5	+ 2.01	.05	5.18	15.0	.409	.0930	-1.12	Hairpin shaped capillary
45-2	.467	500 ± 5	+ 2.03	.05	5.16	26.0	.361	.1375	-1.20	Hairpin shaped capillary
46-1	.492	500 ± 5	+ 2.04	.048	5.13	15.0	.359	.0970	-1.73	Hairpin shaped capillary
46-2	.492	500 ± 5	+ 1.98	.05	5.17	26.0	.374	.1007	- .94	Hairpin shaped capillary
48-1	.488	502 ± 7	- 1.99	.046	5.1	8.75	.641	.0659	-2.32	Hairpin shaped capillary
48-2	.488	502 ± 7	- 1.98	.046	5.3	13.7	.649	.0822	-2.02	Hairpin shaped capillary

a) The sign in front of the current indicates the polarity of the capillary.

b) The values of density and resistivity were taken from reference 55. The values for pure Bi were used for all the Bi systems.

C. Mg-Bi RAW DATA

Capillary	Wt.%Mg	Temp. °C	D.C. Amps [a]	Cap. I.D. cm.	Cap. Length cm.	Time Hours	Final Wt.%Mg	Wt. of Cap. Metal, g.	Uxlo^4 cm^2/sec volt	Notes
27-1	2.005	498 ± 2	- .499	.05	-	21.0	2.36	.1343	-4.64	Severe wall reaction
27-2	2.005	499 ± 3	- .497	.05	-	49.2	4.09	.0805	-6.99	Severe wall reaction
29-1	.668	353 ± 3	- 1.03	.10	3.8	48.0	1.53	.2283	-12.50	
32-1	.503	348 ± 7	- 1.04	.10	3.8	23.1	.626	.3221	-6.96	
32-2	.503	352 ± 5	- 1.02	.10	3.8	10.5	.558	.3216	-6.92	
36-1	.500	343 ± 3	- 1.03	.10	4.6	36.0	.566	.3503	-4.00	
36-2	.500	343 ± 3	- 1.04	.10	4.6	36.0	.624	.3780	-5.32	
41-1	.530	344 ± 5	- 1.98	.075	6.50	18.2	.694	.3022	-5.78	
41-2	.530	344 ± 5	- 2.02	.079	6.36	29.8	.832	.3473	-7.10	
44-1	.494	344 ± 7	- 1.88	.071	6.50	11.8	.617	.2451	-5.12	Hairpin shaped capillary
44-2	.494	344 ± 7	- 2.00	.071	6.75	19.7	.661	.2521	-4.61	Hairpin shaped capillary

a) The sign in front of the current indicates the polarity of the capillary.

D. Zr-Bi RAW DATA

Capillary	Wt.%Zr	Temp. °C	D.C. Amps [a]	Cap. I.D. cm.	Cap. Length cm.	Time Hours	Final Wt.%Zr	Wt. of Cap. Metal, g.	Uxlo^4 cm^2/sec volt	Notes
28	.0181	446 ± 3	- .992	0.10	3.8	48.0	.0148	.3009	+2.32	Analysis doubtful
U2-1	.0567	510 ± 1	+ 1.96	.10	4.1	24.1	.0625	.3185	+1.43	
U2-2	.0567	510 ± 1	+ 1.98	.10	3.9	35.1	.0762	.3123	+3.14	
U2-3	.0567	510 ± 1	+ 1.88	.10	4.2	48.1	.0805	.3472	+3.25	

a) The sign in front of the current indicates the polarity of the capillary.

E. U-Bi RAW DATA

Capillary	Wt.% Uranium	Temp. °C	D.C. Amps [a]	Cap. I.D. cm.	Cap. Length cm.	Time Hours	Final Wt.% Uranium	Wt. of Cap. Metal, g.	Uxlo^4 cm^2/sec volt	Notes
U-1-1	0.310	510 ± 0.5	- 1.95	0.10	3.9	15.0	0.275	0.3100	+2.43	
U-1-3	.310	510 ± 0.5	- 1.99	.10	3.8	38.0	.211	(.1917)	+1.64	Some capillary alloy lost
U-1-5	.310	510 ± 0.5	- 1.89	.10	3.4	27.0	.217	.2694	+3.20	
CB-1-1	.144	445 ± 5	+ 2.00	.10	6.50	40.0	.174	.4300	+2.31	
CB-1-2	.144	445 ± 5	+ 2.00	.10	6.90	30.0	.149	.4032	+0.50	Some sample lost in analysis
CB-1-6	.144	445 ± 5	+ 1.99	.10	6.48	25.0	.168	.3433	+2.36	

a) The sign in front of the current indicates the polarity of the capillary.

F. REJECTION OF DATA

I. Na-Hg system Runs A-2, A-4, A-5, A-10, A-12, A-13, A-14, A-16, and A-21 are not included in the summary of raw data in Appendix II-A. The tubes from Run A-2 broke off and were lost in the reservoir; the Hg boiled out of the reservoir during Run A-4; the tubes from A-5 became so contaminated with dirt and scum they were not analyzed; Runs A-10 and A-13 were completed and analyzed, but the blank analyses were wildly innacurate, presumably from contamination; the diffusion cell blew up during Runs A-12 and A-16; every tube of Runs A-14 and A-21 failed because of bubbles. For every run there were originally three capillaries. The missing capillaries failed during the run for various reasons, in most cases from bubble formation.

Two runs performed at room temperature are not included in Table VIII. In A-19 the Na was run out of the tube rather than into it. The mobilities from this run are considerably lower than those calculated from all but one of the other room temperature runs. From Figures 9 and 10 it is evident that running the solute out of the tube gives a much greater possibility of introducing errors from ordinary diffusion. In addition, the density gradients arising from the change of concentration are unstable in this case, increasing the possibility of convection. Both of the above two factors, if present, will result in a lowering of the apparent, or observed, mobility. Since this is, in fact, what is observed, the author feels justified in disregarding this run. In capillary A-3-1 the change in the capillary concentration was too small for an accurate determination of the mobility.

The changes in the capillary concentration were not statistically significant in Runs A-6, A-7, A-9, A-17, A-18, and A-20. Of these runs the

tubes with the largest concentration changes were A-17-1 and A-20-2. The direction of their changes is in agreement with the results in Table IX. However, the percentage confidence that these changes are real and not just a chance fluctuation are only 88 and 80 percent respectively. For the remainder of these runs the confidence levels are much lower. The reason for the small changes in these tubes is not difficult to determine. Substituting logical values for U, V, and D it was found that the values of "s" for these runs ranged from .05 to 0.2; the values of dimensionless time τ were on the order of 0.1 to 0.3. From Figures 9 and 10 it is evident that only very small changes could be realized. As soon as the magnitude of "s" was significantly increased to approximately 0.75 there was no difficulty in observing concentration changes, i.e., all runs after and including A-23. The quantity "s" was increased by increasing the tube length and by using smaller diameter tubes and higher currents. Since there is the above theoretical reason backed by experimental observations that explains the lack of any effect in these runs, the author feels justified in disregarding them. In this connection it is interesting to note than Runs A-1, A-3, and A-19, which were performed at essentially the same conditions as the ones discussed above except that they were at room temperature, did give significant changes. This is easily explained. The ordinary diffusion coefficient, D, increases exponentially with temperature whereas the mobility, U_1, increases much more slowly. Since $s = U_1V/D$, the value of "s" will be considerably lower at high temperatures than at low temperatures for otherwise identical conditions.

Run A-11 performed at 335°C gave results agreeing with the high temperature results in Table IX. However the concentration changes in both tubes were so great as to arouse suspicion. Every now and then a tube would give anomalously low results. This may be caused by an impurity which suppresses the emission of the Na in the flame photometer. There is a possibility that this occurred in this case so even though the run agrees with the other data at that temperature it is disregarded.

Run A-15 showed this same effect in Tube 1. The other two tubes showed slight increases in concentration, in agreement with the data in Table IX. The whole run was thrown out however.

In Run A-22 an amalgam of 1.5 wt.% Na was used. The blank analyses showed so much scatter that the analyses of the run tubes must be considered doubtful. This amalgam is a two phase mixture at room temperature. It is possible the analytical scatter was caused by inhomogeneities in the alloy caused by insufficient stirring.

II. Cu-Bi system Runs 21,23,25, and 26 are disregarded for the reasons cited on the table. It is apparent that of the remaining runs, 45 and 46 give mobilities that are considerably lower than the average. These runs are the ones in which the Cu was run out of the tube. The same arguments presented for the amalgam Run A-19 apply here. The mobility calculated from capillary 33-1 is appreciably lower than the others. The long time of this run would tend to cause back diffusion. The larger tube diameter leads to an "s" value from two to four times lower than all the other tubes but 33-2. In addition, the larger the tube diameter the more likely convection is to occur. All of these effects would tend to give

an erroneously low mobility. It is felt that therefore Runs 45 and 46 and Tube 33-1 may be safely thrown out. The remaining nine capillaries must be used for the calculation of the mobility.

III. Mg-Bi system Run 27 and Tube 29-1 were thrown out of the calculation of the average mobility because they were run at different composition and temperatures than the others.

IV. Zr-Bi system Run 28 was disregarded on the advice of the chemist performing the analysis. He stated the results were very doubtful because of an error in the analytical procedure.

V. U-Bi system Capillary U1-3 and CB1-2 were disregarded for the reasons given on the table of raw data i.e. some of the alloy was lost from the tube of U1-3 and an analytical error in Run CB1-2 made the results erroneous.

G. EXAMPLES OF ORIGINAL Na-Hg DATA

The capillaries denoted by a number and the letter "B" are blank capillaries through which no current was passed. The abbreviation "ml" stands for the number of milliliters of 1% HNO_3 added to the amalgam in the capillary after the run was completed. (See Appendix III-E for the details of the analysis.) The abbreviation "ppm" stands for the observed Na concentration in parts per million in the dilute acid after the Na extraction was completed. "Sample weight" refers to the weight of the amalgam in the capillary in grams. The final column gives the composition of the tube in weight percent after the completion of the run.

RUN A-27

CAPILLARY POLARITY NEGATIVE; TEMPERATURE 344°C;
CAPILLARY 1, 3.09 AMPS FOR 52 HOURS; CAPILLARY 2, 3.4 AMPS.
FOR 31 HOURS; CAPILLARY 3, 2.53 AMPS FOR 52 HOURS.

Capillary	ml	ppm	Sample Weight	Wt.%Na
1	100	46.5	.8643	.538
2	100	46.8	.8803	.532
3	125	52.0	1.2730	.512
1B	100	47.0	.9699	.485
2B	100	48.1	.8710	.551(a)
3B	100	47.2	.9763	.484
4B	125	44.9	1.1625	.482
5B	125	46.3	1.1928	.485
6B	125	45.3	1.1691	.485

(a) This blank is obviously in error. It may be rejected by applying Chauvenet's criterion for the rejection of data points lying sufficiently far from the mean.

RUN A-28

CAPILLARY POLARITY POSITIVE; TEMPERATURE 27°C;
CAPILLARY 1, 3.95 AMPS FOR 51.9 HOURS; CAPILLARY 2, 3.85
AMPS FOR 34.9 HOURS.

Capillary	ml	ppm	Sample Weight	Wt.%Na
1	100	54.1	1.0039	.539
2	75	55.7	.8044	.520
1B	100	48.3	.9939	.486
2B	100	48.1	.9968	.483
3B	100	48.6	1.0047	.484
4B	100	46.3	.9463	.489
5B	100	52.9	1.1086	.477
6B	100	48.8	1.0012	.487

RUN A-29

CAPILLARY POLARITY MINUS, TEMPERATURE 338°C;
CAPILLARY 1, 2.42 AMPS FOR 48.75 HOURS; CAPILLARY 2, 2.80 AMPS FOR 48.75 HOURS

Capillary	ml	ppm	Sample Weight	Wt.%Na
1	100	44.9	.8731	.514
2	100	45.7	.8783	.521
1B	100	43.4	.8938	.485
3B	100	43.7	.9279	.471
4B	100	44.9	.9201	.487
5B	75	45.3	.7015	.484
6B	100	44.6	.9281	.481

RUN A-30

CAPILLARY POLARITY POSITIVE; TEMPERATURE 334°C; CAPILLARY 1,
2.44 AMPS FOR 30.5 HOURS; CAPILLARY 2, 3.22 AMPS FOR 30.5 HOURS;
CAPILLARY 3, 2.95 AMPS FOR 30.5 HOURS

Capillary	ml	ppm	Sample Weight	Wt.%Na
1	20	37.1	.8269	.0897
2	20	43.9	.9398	.0934
3	20	48.0	1.0332	.0929
1B	20	40.6	.8452	.0961
2B	20	40.7	.8389	.0970
3B	15	47.0	.7385	.0955
4B	20	40.8	.8396	.0972
5B	20	41.1	.8363	.0983

RUN A-31

CAPILLARY POLARITY POSITIVE; TEMPERATURE 37°C; CAPILLARY 1, 3.22 AMPS FOR 39 HOURS; CAPILLARY 2, 3.38 AMPS FOR 19.8 HOURS; CAPILLARY 3, 3.15 AMPS FOR 62.7 HOURS

Capillary	ml	ppm	Sample Weight	Wt.%Na
1	20	42.2	.7974	.1058
2	20	45.3	.8836	.1025
3	20	45.4	.8024	.1132
1B	20	41.2	.8515	.0968
2B	20	42.8	.8728	.0981
3B	20	42.1	.8725	.0965
4B	15	45.7	.6964	.0984
5B	20	42.0	.8480	.0991
6B	20	42.2	.8701	.0970

RUN A-32

60 CYCLE ALTERNATING CURRENT; TEMPERATURE 35°C; CAPILLARY 1, 3.17 AMPS FOR 45 HOURS; CAPILLARY 2, 3.31 AMPS FOR 45 HOURS; CAPILLARY 3, 2.97 AMPS FOR 45 HOURS.

Capillary	ml	ppm	Sample Weight	Wt.%Na
1	100	46.0	.9645	.477
2	100	47.1	.9707	.485
3	100	47.2	.9687	.488
1B	100	48.7	1.0213	.477
2B	100	53.3	1.1357	.469
3B	100	50.6	1.0468	.484
4B	100	52.4	1.0980	.478
5B	100	51.9	1.1009	.472
6B	100	44.5	.9229	.482

APPENDIX III

ANALYTICAL PROCEDURES

A. SPECTROPHOTOMETRIC DETERMINATION OF URANIUM IN BISMUTH

I. INTRODUCTION

Uranium is determined spectrophotometrically at 412 mμ and 390 mμ as the dibenzoylmethane-uranium complex. The applicable range is 50 to 120 μg of uranium; up to 300 mg of bismuth can be tolerated. This method has been used for samples containing 99 percent bismuth and 1000 ppm uranium with respect to bismuth.

The bismuth is complexed with diaminocyclohexane tetraacetic acid (DCTA), and the uranium is complexed with dibenzoylmethane. The dibenzoylmethane-uranium complex is extracted into amyl acetate, and the absorbance of the resulting organic layer is measured at two wavelengths.

II. APPARATUS

Spectrophotometer, Beckman Model DU with tungsten lamp and blue-sensitive cell. Absorption cells, 1 cm. path length, corex or quartz (pyrex cells also seem to be satisfactory).

III. REAGENTS

1. Nitric acid, concentrated, reagent grade
2. Ammonium hydroxide, 5 M
3. Hydrochloric acid, 3 M
4. Saturated ammonium chloride solution
5. Bromcresol green indicator solution, 0.04 percent
6. Dibenzoylmethane solution, one percent in ethanol (absolute or 95 percent).
7. Amyl acetate, reagent grade. The isoamyl acetate was the only amyl acetate available in a reagent grade; consequently, it was used since the original reference did not specify which ester was used.

8. Diaminocyclohexane tetraacetic acid (DCTA) solution: 100 g. is dissolved in 300 ml of 5 M NaOH; after dissolution the pH is adjusted to 5.2 with HCl and NaOH; finally the solution is diluted to 500 ml.

IV. PREPARATION OF SAMPLES

1. Weigh the bismuth sample and dissolve in concentrated nitric acid.

2. Transfer to a volumetric flask and dilute to the mark with water. This dilution should be such that an aliquot no larger than 10 ml will be required for an analysis.

V. PROCEDURE

1. Withdraw an aliquot (no more than 10 ml) containing 50 to 100 μgms. of uranium and no more than 300 mg of bismuth. Transfer to a 60-ml separatory funnel. (See Note 1).

2. Add water to bring volume up to 10 ml.

3. Add 5 ml of the DCTA solution (see Note 2).

4. Add three drops of the bromcresol green indicator solution.

5. Add dropwise ammonium hydroxide, 5 M, and/or hydrochloric acid, 3 M, until the solution just turns from blue to yellow.

6. Add 5 ml of saturated ammonium chloride solution.

7. Add water to make the volume about 20 ml (see Note 3).

8. Add 1.00 ml (pipet) of dibenzoylmethane solution while rotating the funnel (see Note 4).

9. Immediately add from an eye dropper 12 drops of 5 M ammonium hydroxide.

10. Add 10.00 ml (pipet) of amyl acetate.

11. Shake the contents of the funnel thoroughly and allow the two layers to separate (see Note 5). Centrifuge for one minute.

12. Pipet enough of the organic layer (top layer) into the absorption cell to fill it.

13. Measure the absorbance at 412 mμ and at 390 mμ against a blank which has been prepared in the same manner as the sample using water instead of a uranium containing sample (see Notes 6 and 7).

VI. NOTES AND PRECAUTIONS

1. A 10-ml aliquot is maximum because the final volume of the aqueous layer is 20 ml, and 10 ml of reagents must be added.

2. Five ml of DCTA will keep in solution about 300 mg of bismuth. If a precipitate does occur, add more DCTA.

3. The diluted solution should be clear at this point; if not, probably insufficient DCTA was added.

4. After the addition of dibenzoylmethane, the solution will be turbid and a small amount of precipitate will be present. Keep the dibenzoylmethane in ethanol solution tightly stoppered to prevent volatilization.

5. The two layers should be clear now with the aqueous layer colored blue and organic layer yellow. The intensity of the yellow color will be determined by the amount of uranium present.

6. Unless one has tightly stoppered absorption cells, it will be necessary to work rapidly during the photometry because of the volatility of amyl acetate.

7. It has been found that soapy water followed by thorough rinsing with water and a final rinse with acetone will clean the absorption cells very nicely.

VII. CALCULATIONS

The concentration of uranium is read from a calibration curve of absorbance versus uranium concentration which is best prepared from a series of standard uranium solutions. These solutions should be treated in the same manner as the sample and their absorbances read at the two wavelengths.

$$\% \text{ U} = \frac{\mu\text{g of U read from calibration curve}}{1000 \times \text{sample wt. in mg}} \times \frac{\text{dilution volume}}{\text{aliquot volume}} \times 100$$

$$\text{ppm U} = \frac{\mu\text{g of U} \times 10^6}{1000 \times \text{sample wt. in mg}} \times \frac{\text{dilution volume}}{\text{aliquot volume}}$$

The concentration of the uranium as read from the 412 mμ curve should agree with that read from the 390 mμ curve. The two readings taken together should show if any interference is present. The ratio of absorbances A(412mμ): A(390 mμ), is constant at 1.9 to 2.0 over the range studied (50 to 120 μg U).

VIII. REFERENCES

(1) H. L. Finston, Brookhaven National Laboratory, private communication.

(2) J. H. Yoe, F. Will III, and R. A. Black, Anal. Chem. 25, 1200 (1953).

B. DETERMINATION OF MAGNESIUM IN BISMUTH ALLOYS

I. INTRODUCTION

Magnesium is determined titrimetrically employing versene (ethylenedinitrilo) tetraacetic acid disodium salt, as the titrant and Eriochrome-black-T as the indicator[1]. Magnesium forms a wine-red complex with the indicator that changes to a deep blue color at the end-point upon titration with versene.

II. INTERFERENCES

1. Uranium interference is removed by complexation of the uranyl ion with carbonate. $(UO_2(CO_3)_3^{-4})^2$.

2. Zirconium interference is removed by precipitation as a hydroxide.

3. Bismuth interference is removed by precipitation as a mixture of BiOCl and $Bi(OH)_3$. The presence of BiOCl promotes the formation of a granular precipitate, thereby minimizing absorption and occlusion.

III. APPARATUS

Beckman pH meter; Buchner type funnels with fritted disc (medium porosity).

IV. REAGENTS

1. Hydrochloric acid - 2N

2. Eriochrome-black-T indicator. Dissolve 0.2 grams of the indicator in 50 ml of methanol, reagent grade, containing two grams of hydroxylamine hydrochloride.

3. Standard magnesium solution. Dissolve six grams of magnesium, reagent grade, in dilute hydrochloric acid and dilute to one liter. Dilute a portion of stock solution 1:100 to obtain a final solution containing 0.06 mg Mg/ml.

4. Versene (ethylenodinitrito) tetraacetric acid disodium salt standard solution. Dissolve four grams of the component in one liter of water. A portion diluted 1:10 will yield a titer of approximately 0.027 mg Mg/ml. Solution is standardized accurately against standard Mg solution, containing approximately 600 mg Bi/ml.

5. Bismuth stock solution was prepared by dissolving high purity bismuth (15.2471 grams) in nitric acid, (concentrated) and diluting with water, yielding 30.49 mg Bi/ml.

6. Buffer. Dissolve 67.5 grams of ammonium chloride in 200 ml of distilled water, add 570 ml of concentrated ammonium hydroxide, dilute to one liter. Final pH is 10.

7. Sodium hydroxide - 0.5N.

8. Sodium Carbonate solution. Dissolve ten grams of sodium carbonate in water and dilute to 100 ml.

V. PREPARATION OF SAMPLES

1. Weigh the sample, transfer the weighed sample to a beaker, add sufficient water to cover the sample and add concentrated nitric acid.

2. Following dissolution, heat samples to near boiling in order to expel dissolved nitrogen oxides. Cool, transfer to a suitable size volumetric flask and dilute to mark with water. Dilution should be such that a five to ten ml aliquot will be required for analysis.

VI. PROCEDURE

1. Remove an aliquot portion of sample 5-10 ml containing approximately 0.5-1 mg Mg and transfer to a beaker.

2. Add 5 ml of 2N hydrochloric acid.

3. Add sodium hydroxide 0.5N slowly, with stirring, until the mixture attains a pH of 2, as measured by a pH meter, then add 2 ml of sodium carbonate solution (0.1 gm/ml) and resume addition of sodium hydroxide until the mixture attains a pH of 9.

4. Allow the precipitate formed to stand five to ten minutes.

5. Filter thru a fritted disc funnel (medium porosity).

6. Transfer filtrate to a 500 ml erlenmeyer flask.

7. Add 2.5 ml of buffer solution (pH 10).

8. Add 20 drops of Eriochrome-black-T indicator solution.

9. Titrate with standard versene solution until solution changes from wine-red color to a deep blue (see Note 2).

VII. CALCULATIONS

$$\% \text{ Mg} = \frac{(\text{ml versene})\ (\text{titer})\ (\text{dilution ml})\ (100)}{(\text{wt. gms. sample})\ (\text{aliquot})\ (103)}$$

VIII. NOTES

(1) Standardization of the versene solution against a magnesium solution containing a large excess of bismuth compensates for these quantities of bismuth which may not be completely removed through precipitation.

(2) Near the end-point the solution will appear blue with a red tinge, care must be taken to assure the complete absence of red at the end-point.

IX. REFERENCES

(1) Charlot and Bezier, Quantitative Inorganic Analysis, (John Wiley and Sons, Inc., N.Y., 1957) p. 471.

(2) H. Willard and H. Diehl, Advanced Quantitative Analysis, (d. van Nostrand Company, Inc., N.Y., 1943) p. 364.

C. SPECTROPHOTOMETRIC DETERMINATION OF ZIRCONIUM IN BISMUTH ALLOYS

I. INTRODUCTION

The spectrophotometric method for the determination of zirconium reported by Flaschka and Farah[1] has been applied to the analysis of bismuth alloys. Minor modifications were made in the preparation of the blank[2]. The absorbancy of a zirconium-pyrocathecol violet complex is measured at 620 mμ in a solution buffered at a pH of 5.2. The optimum concentration range of zirconium is 3μg to 50μg. A large number of interfering ions are effectively masked by versene.

II. INTERFERENCES

Cations: The alkali metals, ammonium, alkaline earths, Mn, Fe^{+3}, Al, La As^{+4}, Ce^{+3}, Zn, Cd, Hg^{+2}, Cu, Ni, Co, Pb, Bi, Mo, Y, W, As^{+3}, Tl, and Ag do not interfere when present in a molar ratio of less than 3000:1 to zirconium. U, Y, Ti, Cr, and Th in limited amounts do not interfere. Uranium interferes when encountered in concentrations greater than 100 times the molar concentration of zirconium. The uranium may be eliminated as an interference by complexing with ascorbic acid. Sb, Sn, Hg and oxidizing agents interfere. In and Ga may be present up to a 500:1 molar ratio to zirconium.

Anions: ($^{+}_{-}$) Cl, Br, $SO_4^{=}$, ClO_4^{-} do not interfere. Complexing anions such as citrate, oxalate, tartrate, phosphate and F^{-} interfere.

III. APPARATUS

Beckman Quartz Spectrophotometer with tungsten lamp and blue sensitive filter; absorption cells, Beckman pH meter.

IV. REAGENTS

1. Versene (ethylenedinitrilo) tetraacetic acid disodium salt, 0.25M, (93 gms. 1 liter). Dissolution of the versene is best accomplished by warming the mixture to 40°C.

2. Nitric acid, concentrated, reagent grade.

3. Methyl red, 0.05 percent aqueous solution, prepared by adding 7.4 ml of 1/20 N NaOH/100 mg indicator.

4. Pyrocathecol Violet, 0.001M aqueous solution, (0.386 gm/liter).

5. Buffer solution. The solution is prepared by dissolving sodium acetate (27 gms) in approximately 700 ml of water and adding glacial acetic acid until a pH of 5.2 is attained as measured by a Beckman pH meter.

6. NH_4OH - 5M

7. HCl - 2N

V. PREPARATION OF SAMPLE

1. Weigh the sample and transfer to a beaker. Add sufficient water to cover the sample and add concentrated nitric acid (see Note 1).

2. Following dissolution, heat the samples to near boiling in order to expel dissolved nitrogen oxides. Cool, transfer to a suitable size volumetric flask and dilute to the mark with water. Dilution should be such that an aliquot no larger than 10 ml will be required.

VI. PROCEDURE

1. Add 5 ml of versene (0.25M), sufficient to complex 260 mg Bi, to a 25 ml volumetric flask (see Note 2).

2. Remove an aliquot portion of sample (not more than 10 ml) and transfer to volumetric flask containing the versene (see Note 3).

3. Add one drop of methyl red (0.05 percent), neutralize the mixture to yellow with NH_4OH(5M) and bring back to red with HCl(2N).

4. Add at least 3 ml of buffer solution.

5. Add 2 ml of Pyrocathecol Violet (0.001M), using a pipette or burette.

6. Fill the flask to mark with buffer, mix well. Allow to stand 15 minutes.

7. Transfer a portion to absorption cell and measure the absorbancy at 620 mμ against a reagent blank containing 3.5 ml of Bi stock solution.

VII. PREPARATION OF CALIBRATION CURVE

1. The stock solution of $ZrOCl_2.8H_2O$, 0.3568 gms/1 liter is equivalent to 101 μg Zr/ml. The solution is prepared by dissolving the salt in 0.5 liter of water containing 100 ml conc. HCl and diluting to 1 liter. Portions of this stock solution are diluted according to needs.

2. Bismuth stock solution is prepared by dissolving high purity purity bismuth in concentrated nitric acid and diluting with water. 15.2471 gm. Bi/.51 yields a stock solution containing 30.49 mg Bi/ml.

3. To a 25 ml volumetric flask containing 5 ml of versene (0.25M) add from 3 μg Zr to 50 μg Zr and 3.5 ml of bismuth stock solution. Prepare a blank containing all reagents and 3.5 ml of bismuth stock solution. Follow the procedure outlined above and measure the absorbancy at 620 mμ against the reagent blank.

VIII. CALCULATIONS

$$\% \text{ Zr} = \frac{(\mu\text{g Zr})\ (100)\ (\text{dilution ml})}{(\text{gms. Sample})\ (10^6)\ (\text{ml aliquot})}$$

IX. NOTES

1. Final solution must be at least 2N HNO_3 to prevent hydrolysis.

2. More versene must be added if the amount of bismuth in the aliquot taken contains greater than 260 mg bismuth or if a sufficient quantity of other ions are present that use versene.

3. A precipitate may appear at this time. Upon neutralization with NH_4OH it will redissolve. The precipitate is probably acidified versene.

4. In preparing the calibration curve it is essential that the versene be added before adding zirconium and bismuth in order to prevent precipitation of BiOCl.

5. The procedure reported by Flasckha and Farah cites the preparation of blank by dividing the solution containing zirconium into two parts. To one part is added NH_4F to complex the zirconium. However, the preparation of the reagent blank as described above was found to give reproducible and accurate results and to be appreciably more rapid.

6. Rinse all glassware with 2N HCl, in order to insure complete removal of zirconium and bismuth.

X. REFERENCES

(1). H. Flaschka and M. V. Farah, Z. Anal. Chem. 152, 401(1956).

(2) J. Young, J. French and J. White, Anal Chem. 30, 43, 422 (1958).

D. SPECTROSCOPIC DETERMINATION OF COPPER IN BISMUTH AND TIN ALLOYS

Copper in Bismuth

I. INTRODUCTION

The spectrophotometric method for the determination of copper reported by G. Frederick Smith and W. H. McCurdy, Jr.[1] and Y. Yshihara and Y. Taguchi[2] was successfully applied to the determination of copper in the presence of uranium and large quantities of bismuth.

Copper is extracted from an aqueous solution of pH 5-6 as a neocuproine complex with isoamyl alcohol and measured at 454 mμ. Beer's law is obeyed over the range of 0.15 to 10.6 ppm copper in isoamyl alcohol. The method is quite selective for copper and may be used in the presence of many cations and anions. A minor modification of the original procedure was made in order to more rapidly determine the pH of the aqueous phase prior to extraction.

II. INTERFERENCES

Smith reported that no cation other than the cuprous ion formed a colored complex that was extractable under the conditions employed. The chloride, sulfate, nitrate, perchlorate, tartrate, citrate and acetate anions do not interfere. Many other anions that either react with hydroxylamine or give a yellow colored solution may be eliminated by employing suitable conditions. The following cations were found to produce no detectable interference:

Cation	Weight Ratio Cation: Cu^{+1}
Bi^{+3}	28,000: 1
UO_2^{+2}	234: 1

III. APPARATUS

Beckman DU Quartz Spectrophotometer with tungsten lamp.

IV. REAGENTS

1. Concentrated nitric acid.
2. p - Bromocresol Green, 0.04 percent aqueous solution.
3. Ammonium hydroxide - 5 M.
4. Hydrochloric acid - 1 M.
5. Hydroxylamine hydrochloride, 30 percent, aqueous solution.
6. Sodium citrate, 30 percent, aqueous solution.
7. Neo - cuproine, 0.1 percent ethanol - water solution (1.9 by volume).
8. Isoamyl alcohol (Reagent Grade). (See Note 3).

V. PROCEDURE

1. Dissolve the bismuth alloy in concentrated nitric acid. Heat to expel nitrogen oxides, cool and dilute to volume.
2. Transfer an aliquot of sample containing 5 to 75 μg copper to a 60 ml separatory funnel.
3. Add 10 ml hydroxylamine hydrochloride (30 percent).
4. Add 2 ml of sodium citrate (30 percent).
5. Add 2 drops of p-Bromocresol Green.
6. Add ammonium hydroxide (5M) and/or hydrochloric acid (1M) till the solution changes from a blue to a green-yellow color.
7. Add 8 ml of sodium citrate.
8. Add 2 ml of neo-cuproine solution (0.1 percent) with mixing.
9. Make up to a volume of 30 ml with distilled water.
10. Add 10 ml of isoamyl alcohol and shake for 20 seconds. Allow the phases to separate.

11. Remove a portion of the organic phase and measure the absorbancy at 454 mμ against a reagent blank.

VI. CALIBRATION CURVE

A calibration curve was prepared from a stock solution of copper (99.9 percent) in 1N nitric acid. Amounts of bismuth up to 47,860 μg and uranium up to 400 μg were added to 1.71 μg copper without any noticeable interference.

VII. NOTES

1. The complex contains a molar ratio of copper to neo-cuproine of 1:2 with copper present as the cuprous (Cu^{+1}) ion.

2. p-Bromocresol green indicator (pH 3-5) was introduced for determining the pH of the aqueous phase prior to extraction. The indicator exhibited an absorbancy of 0.010/1 drop at 454 mμ, a sufficiently low value to permit its use in the determination.

3. This solvent exhibits a nauseating odor and should be used in a hood.

4. Addition of sodium citrate prevents hydrolysis and precipitation of heavy metals during the subsequent neutralization operation.

5. Exactly 2 drops of indicator is used in both blank and sample (see Note 1).

6. Complex formation, for all practical purposes, occurs instantaneously.

7. Smith[1] performed two extractions. However, it was found in this laboratory that one 10 ml extraction was sufficient to remove the copper complex. The use of a single extraction significantly decreased the time required to perform the analysis.

Copper in Tin

Except for the dissolution of the sample the procedure is identical for that of Cu in Bi.

DISSOLUTION PROCEDURE

1. Dissolve the alloy in a mixture of 6N HCl and 6N HNO_3 in a ratio of 20:1 by volume.

2. Transfer an aliquot of sample containing 5 to 75 µg Cu to a 60 ml separatory funnel.

3. The remainder of the procedure is identical to the procedure for Bi alloys.

NOTES

1. The calibration curve used is that determined for Cu-Bi. Its validity was verified by preparing artificial mixtures of Cu and Sn, dissolving, and determining the amount of Cu present.

REFERENCES

(1) G. F. Smith and W. H. McCurdy, Jr., Anal. Chem., 24, 371 (1952).

(2) Y. Yshira and Y. Taguchi, Japan Analyst, 6, 588 (1957).

E. FLAME PHOTOMETRIC DETERMINATION OF SODIUM IN MERCURY

I. INTRODUCTION

Sodium is determined flame photometrically at 589 mμ. The sodium is dissolved from the amalgams with dilute HNO_3. The emission in a hydrogen-oxygen flame is compared with the emission of previously prepared standard solutions.

II. APPARATUS

Beckman Model DU Spectrophotometer with flame photometer attachment and Deeminac ion exchange demineralizer.

III. REAGENTS

1. Dilute HNO_3, one percent by volume in deionized water.
2. Reagent grade $NaNO_3$.
3. De-ionized water.

IV. PROCEDURE

1. Place the capillary tube containing the amalgam into a weighed polyethylene bottle and reweigh to determine the weight of the amalgam and the tube.
2. Pipette sufficient dilute HNO_3 into the bottle so that the final concentration of sodium will be close to 50 ppm.
3. Let the tightly capped bottles stand for not less than two days. The bottles are periodically shaken during this period.
4. Compare the emission of the unknown solution with the emission of the standards made up from the $NaNO_3$ and deionized water.
5. Add sufficient concentrated HNO_3 to the polyethylene bottle to dissolve the mercury, leaving the glass capillary.
6. Wash the glass in the bottle twice with deionized water and twice with acetone.

7. Let opened bottle set overnight to completely dry.

8. Weigh bottle plus glass.

9. Empty glass from bottle and reweigh empty bottle.

V. NOTES AND PRECAUTIONS

1. Extreme care must be taken to avoid dust and other sodium containing contaminates.

2. The standard solution were made up by diluting a stock solution of sodium made from $NaNO_3$ and deionized water.

3. There was a standard solution every 5 ppm in the range from 20 to 100 ppm.

4. Most of the work was carried out at about 50 ppm. In this region the transmission reading on the spectrophotometer varies linearly with concentration.

5. Typical instrument settings were: Oxygen pressure, 10 psig; Hydrogen pressure, 3 psig; slit width, 0.1 mm; sensitivity, 0.1 switch setting and knob fully clockwise.

6. The small amount of acid in the samples does not change the reading. This was determined experimentally by the author and also by Collins and Polkinhorne[1].

VI. CALCULATIONS

The concentration of the unknown is determined with a linear, graphical interpolation between the standard solutions that lie on either side. The standard solutions are run at the same time as the unknown. It is not possible to use a standard curve since the flame characteristics vary from day to day.

$$\% \text{ Na} = \frac{(\text{ppm Na in extract}) \times (\text{ml of extract}) \times 10^{-4}}{(\text{wt. glass + amalgam}) - (\text{wt. glass})}$$

VII. REFERENCES

(1) G. C. Collins and H. Polkinhorne, Analyst 77, 430 (1952).

APPENDIX IV

PREPARATION AND DEGASSING OF AMALGAMS

A. Preparation

The amalgams were made up in a dry box under N_2. Oil pumped, extra dry N_2 was further dried by passing it through successive columns of silica gel and anhydrous $Mn(ClO_4)_2$ before it was continuously purged through the box. The dew point within the dry box was reduced further by placing open pans of P_2O_5 about. Freshly cut surfaces of Na metal would slowly cloud over in this atmosphere, but the thickness of the hydroxide layer was negligible even after an hour. Dry polyethylene bottles were weighed outside the dry box and then brought inside through an airlock. The airlock was successively evacuated and filled with dry N_2 three times before it was opened to the inside of the dry box. The Na metal was cut into small pieces and placed in the polyethylene bottles which were then tightly capped and brought outside to be reweighed. The amount of Hg necessary to make the desired composition was then weighed out. The Na and Hg were brought back into the dry box. Because the heats of formation of the amalgams are strongly negative it was necessary to form the amalgam in a pyrex beaker. The Na would dissolve in the Hg almost instantly, leaving a light scum on the surface. The amalgams were stored in the dry box in capped polyethylene bottles until they were used.

The amalgam was poured in air into the large outer pyrex tube immediately before the run was to start. The amalgams were quite unreactive after their formation and could be exposed to the air for short

periods of time with negligible scum formation. The apparatus was then assembled and degassing started.

B. Degassing

It was necessary to thoroughly degas the amalgam before starting the run. Otherwise, small bubbles would nucleate in the capillary tubes. These would increase in size rapidly and cut off the direct current. A great number of the total tubes failed in this manner. The most effective method found for degassing was to first pump on the system with the floor pump while heating the amalgam. The mercury would boil at about 170°C, condense in the top of the cell above the furnace and run back into the reservoir. This was continued for at least an hour. Then the gas was bled into the furnace and the temperature raised to about 30 to 50°C above the operating temperature. The pressure was adjusted so that the amalgam was just below its boiling point. The system was kept at this state for several days. Every few hours the amalgam was stirred in order to dislodge the bubbles that had nucleated on the walls of the large tube. After several days, no more bubbles would form on the tube.

The effect of the bubbles was especially severe for small capillary tubes. It was not possible to use tubes smaller than .030" I.D. The bubbles had a tendency to nucleate at the very end of the capillary, next to the reservoir. To alleviate this, the end of the tubes were flared out and fire-polished. The growth of the bubbles appeared to be autocatalytic. The failure of a tube may have proceeded as follows. Once a bubble formed on the wall of the tube it cut down the cross sectional area of the tube at that point. The increase

in current density created a hot spot, which expanded the bubble further. This process continued very rapidly; the tube would become open circuited almost without warning.

Bubble formation was considerably less severe with the other systems. For this reason it seems most likely that the Na is responsible. The Na will form hydrogen from any residual moisture in the diffusion cell. The rapid growth of the bubbles would be aided by the large diffusion coefficient of hydrogen.

APPENDIX V

MISCELLANEOUS

A. Efficiency of Electrolysis of Alloys.

Suppose the transport of mass in an electric field were reversible. The work necessary to transport one electrical equivalent (one Faraday) of material will then be

$$dW_r = F\, dV$$

where W_r is the reversible work required, F is 96,500 coulombs, and V the voltage. Integrating, one has for the reversible work necessary to transport one equivalent through a potential difference of V volts

$$W_r = FV$$

Now assume that electronic conduction is present. One can define a quantity equal to the number of total electrical equivalents (Faradays) that must be passed through the metal to transport one equivalent of solute. This number is designated by 1/n. One then has for the irreversible case

$$dW_{irr} = \left(\frac{1}{n}\right) F\, dV$$

We can see that under this definition "n" is simply the transport number of the solute atoms. Again integrating we find

$$W_{irr} = \left(\frac{1}{n}\right) FV$$

The percent efficiency is simply

$$\text{percent eff.} = 100 \left(\frac{W_r}{W_{irr}}\right)$$

or

$$\text{percent eff.} = 100\ n$$

Typical values of n/x range from 10^{-4} to 10^{-3} where x is the mole fraction (reference 3). For concentrations from .01 to .10 mole fraction the value of n will be in the range from 1×10^{-6} to 1×10^{-4}. The efficiency will therefore be of the order of .01 to .0001 percent.

B. The Interrelation Between Electrodiffusion and the Diffusion Potential

The entropy dissipation function $T\sigma$ for an irreversible process may be written as the product of fluxes and forces.

$$T\sigma = \sum J_i X_i \tag{1}$$

where T is temperature, σ is the rate of production of entropy in the system per unit volume; the J_i, fluxes (per unit area per unit time) of a quantity such as heat, mass, or electricity; the X_i are generalized "forces" such as temperature or voltage gradients. In general, irreversible processes can be described by linear relationships between the forces and fluxes.

$$J_i = \sum_j L_{ij} X_j \tag{2}$$

The Onsager reciprocity relations state that when J_i and X_i are chosen to satisfy Equation (1) the phenomenological coefficients L_{ij} of Equation (2) are symmetrical.

$$L_{ij} = L_{ji} \tag{3}$$

For the present case there are two fluxes and two forces. The fluxes are J_1, the flow of solute atoms in moles/cm^2 sec and j_2 the flow of electricity in amperes/cm^2. (There is only one independent flow of mass in a binary system.) When the "forces" are chosen as $\frac{\partial \mu_i}{\partial z}$ and E, Equation (1) is satisfied

$$T\sigma = J_1 \left(\frac{\partial \mu_1}{\partial z}\right) + j_2 E \tag{4}$$

Here $\frac{\partial \mu_i}{\partial z}$ is the gradient of chemical potential, and E the electrical field strength in volts/cm. It will be assumed there are no viscous effects or chemical reactions taking place. For the one dimensional case Equation (2) become

$$J_1 = L_{11} \left(\frac{\partial \mu_1}{\partial z}\right) + L_{12} E \tag{5}$$

$$j_2 = L_{21} \left(\frac{\partial \mu_1}{\partial z}\right) + L_{22} E \tag{6}$$

Now the diffusion potential is simply the derivative $\left(\frac{dV}{dx_1}\right)$ when $j_2 = 0$, where V is voltage and x_1 is the mole fraction of the solute. Setting $j_2 = 0$ in Equation (6) one has

$$\left(\frac{\partial \mu_1}{\partial z}\right) = - \left(\frac{L_{22}}{L_{21}}\right) E \quad , \text{for } j_2 = 0 \tag{7}$$

Writing Equation (5) for the case of constant composition one has

$$J_1 = L_{12} E \tag{8}$$

The definition of the mobility is simply

$$J_1 = U_1 N_1 E \tag{9}$$

Using Equation (3) one has from (8) and (9)

$$L_{21} = U_1 N_1 \tag{10}$$

At constant composition Equation (6) reduces to

$$j_2 = L_{22} E \tag{11}$$

Comparing with Ohm's Law

$$j_2 = \frac{E}{\rho} \tag{12}$$

one obtains

$$L_{22} = \frac{1}{\rho} \tag{13}$$

Substituting (10) and (13) into (7) one finds

$$\left(\frac{\partial \mu_1}{\partial z}\right) = - \frac{E}{\rho U_1 N_1} \tag{14}$$

Re-arranging and using the fact that $dV = E\, dz$

$$dV = - \rho\, U_1 N_1\, d\mu_1 \tag{15}$$

It now remains to compute $d\mu_1$ in terms of x_1. To do this use the definition of the chemical potential at constant temperature.

$$d\mu_1 = RT\, d \ln x_1 \gamma_1 \tag{16}$$

where γ_1 is an activity coefficient.

$$d\mu_1 = RT\, [d \ln x_1 + d \ln \gamma_1] \tag{17}$$

Rearranging

$$d\mu_1 = \left(\frac{RT}{x_1}\right) \left[1 + \frac{d \ln \gamma_1}{d \ln x_1}\right] dx_1 \tag{18}$$

Substituting Equation (18) into Equation (15) one obtains the desired result

$$\left(\frac{dV}{dx_1}\right) = - \frac{\rho\, U_1 N_1 RT}{x_1} \left[1 + \frac{d \ln \gamma_1}{d \ln x_1}\right] \quad , \text{for } j_2 = 0 \tag{19}$$

For an ideal solution this reduces to

$$\left(\frac{dV}{dx_1}\right) = - \rho\, U_1 N_o RT \quad , \text{for } j_2 = 0 \tag{20}$$

where N_o is the molar density of the solution. If one uses the relation between the mobility and the transport number as defined in part A of this appendix

$$n = U_1 N_1 F \rho \tag{21}$$

one obtains the following formula

$$\frac{dV}{dN_1} = - \frac{nRT}{N_1 F} \tag{22}$$

Here the fact that $N_1 = N_o x_1$ was used. Equation (22) is identical with the equation Schwarz used for the calculation of diffusion potentials (reference 3, page 40). Schwarz's method of derivation was not correct even though he obtained the correct answer. This is similar to the situation where Kelvin (58) derived the correct expression for the thermoelectric effect even though he used admittedly incorrect assumptions. Helmholtz (59) was the first to obtain the correct expression for the diffusion potential. He also used classical, equilibrium thermodynamics which is not correct in view of the extreme irreversibility of the process. The above proof is presented with no claims of originality. It is reported here because the author is not aware of any development in literature specifically for electrodiffusion in alloys. The proof follows very closely the lines laid down by Miller (60) for the diffusion potential of ionic salts in a neutral solvent and his treatment of thermoelectricity.

Since the Onsager reciprocity relations were used in the derivation of Equation (19) they may be tested by a direct measurement of the mobility U_1 and a measurement of $\frac{dV}{dx_1}$ at $j_2 = 0$. Mangelsdorf (4) verified the validity of the reciprocity relations in electrodiffusion using Schwarz's (3) diffusion potential data.

LITERATURE

1. J. C. Angus, E. E. Hucke, and D. V. Ragone, The Effect of an Electric Field on the Segregation of Solute Atoms at a Freezing Interface, Paper presented to the A.I.M.E. International Symposium on the Physical Chemistry of Process Metallurgy, Pittsburgh, April 1959.

2. G. N. Lewis, E. Q. Adams, and E. H. Lanman, J.A.C.S., 37, 2656 (1915)

3. K. Schwarz, Elektrolytische Wanderung in flussigen and festen Metallen. (J. A. Barth, Leipzig, 1940)

4. P. Mangelsdorf Jr., J. Chem. Phys., 30, 1170 (1959)

5. S. I. Drakin and A. K. Maltsev, J. Phys. Chem. (USSR), 31, 2036 (1957)

6. S. I. Drakin, Izvest. Sektora. Fiz. Khim. Anal. (USSR), 20, 341 (1950)

7. E. Haeffner, Nature, 172, 775 (1953)

8. G. Nief and E. Roth, C. R. Acad. Sci., Paris, 239, 162 (1954)

9. V. A. Lunden, C. Reutersward and A. Lodding, Z. Naturforschg., 10a, 924 (1955)

10. F. Skaupy, Z. physik. Chem., 58, 560 (1907)

11. F. Skaupy, Physik. Z., 21, 597 (1920)

12. F. Skaupy, Z. Physik, 3, 178 (1920)

13. F. Skaupy, Z. Elektrochem., 35, 862 (1929)

14. M. A. Rabkin, Journal of Applied Chemistry (USSR), 30, 832 (1957)

15. C. Wagner, Z. physik. Chem., B15, 347 (1932)

16. C. Wagner, Z. physik. Chem., A164, 231 (1933)

17. K. Schwarz, Z. physik. Chem., A164, 223 (1933)

18. S. I. Drakin, J. Phys. Chem. (USSR), 27, 1586 (1953)

19. B. Baranovski, J. Phys. Chem. (USSR), 28, 1676 (1954)

20. P. Mangelsdorf Jr., J. Chem. Phys., 33, 1151 (1960)

21. M. Hansen, Constitution of Binary Alloys. (McGraw Hill Co., N.Y. 1958)

22. O. Kubaschewski and J. A. Catterall, Thermochemical Data of Alloys. (Pergamon Press, London and N. Y., 1956)

23. R. L. McKisson and L. A. Bromley, J.A.C.S., 73, 314 (1951)

24. F. Sauerwald and W. Teske, Z. anorg. Chem., 210, 247 (1933)

25. K. Banerjee, Indian Journal of Physics, 3, 399 (1929)

26. N. S. Gingrich and R. E. Henderson, J. Chem. Phys., 20, 1117 (1952)

27. B. R. Orton, B. A. Shaw, and G. I. Williams, Acta. Met., 8, 177, (1960)

28. P. Müller, Die elektrische Leitfahigkeit der Metallegierungen im flussigen Zustande, Doctor's dissertation, Royal Technical High School at Aachen (1911)

29. K. Bornemann and P. Müller, Metallurgie, 7, 396 (1910)

30. K. Bornemann and G. von Rauschenplat, Metallurgie, 9, 473, 504 (1912)

31. R. Kremman, M. Pestemer and H. Schreiner, Rec. trav. chim., 51, 557 (1932)

32. C. T. Ewing, J. A. Grand, and R. R. Miller, J.A.C.S., 73, 1168 (1951)

33. M. von Wogau, Ann. Physik (4), 23, 345 (1907)

34. S. Barrat, Trans. Faraday Soc., 25, 878 (1929).

35. A. Röder and W. Morawitz, Z. Elektrochem., 60, 431 (1956)

36. A. Knappwost, Z. physik Chem. (Frankfurt), 21, 358 (1959)

37. A. Roll and H. Motz, Z. Metallk., 48, 435 (1957)

38. N. F. Mott and H. Jones, The Theory of the Properties of Metals and Alloys. (Dover Publications, New York, 1958)

39. L. S. Darken, Trans. A.I.M.E., 175, 184 (1948)

40. J. E. Reynolds, B. L. Averbach, and M. Cohen, Acta Met., 5, 29 (1957)

41. H. W. Schadler and R. E. Grace, Trans. A.I.M.E., 215 559 (1959)

42. E. Riecke, Ann. d. Phys. u. Chem., 66, 353 and 545 (1898)

43. P. Drude, Ann. d. Physik., 7, 687 (1902)

44. H. A. Lorentz, Theory of Electrons (B. G. Teubner, Leipzig, 1909)

45. J. C. Angus, J. V. Verhoeven and E. E. Hucke, Electric Mobilities in Molten Alloys. Paper presented to the A.I.M.E. International Symposium on the Physical Chemistry of Process Metallurgy, Pittsburgh, April, 1959.

46. P. Mangelsdorf Jr., Private communication.

47. K. P. McCarty and E. A. Mason, The Kirkendall Effect in Gaseous Diffusion, Report No. 1MP-OSR-13 of the University of Maryland Institute of Molecular Physics, September 11, 1959.

48. R. Kremann and R. Gruber-Rehenburg, Monat. Chem., 45, 311 (1925)

49. R. Kremann, A. Vogrin and H. Scheibel, Monat. Chem., 57, 323 (1931)

50. J. D. Verhoeven, J. C. Angus, W. D. Bouwsma, and E. E. Hucke. The Determination of Electrical Mobilities in Molten Alloys. The University of Michigan Research Institute Report No. 2917-1-T, August 1960.

51. M. Mason and W. Weaver, Phys. Rev., 23, 412 (1924)

52. R. Furth, Z. Physik, 40, 351 (1926)

53. R. Furth, Z. Physik, 45, 83 (1927)

54. S. R. DeGroot, L'effect Soret (Thesis, Amsterdam, 1945)

55. R. N. Lyon et al., Liquid Metals Handbook (U.S. Gov. Printing Office, Washington 25, D. C., 1952)

56. J. R. Weeks, Private communication, Brookhaven National Laboratory (1959)

57. R. Kremann, F. Bauer, A. Vogrin and H. Scheibel, Monat Chem., 56, 35 (1930)

58. W. Thompson, Proc. Roy. Soc. (Edinburgh) 3, 225 (1854)

59. H. von Helmholtz, Ann. Phys. 3, 201 (1878)

60. D. G. Miller, Thermodynamics of Irreversible Processes: The Experimental Verification of the Onsager Reciprocity Relations. University of California Radiation Laboratory Report UCRL-5644-T, July 30, 1959